Proceedings of

BARN 92

Biological Applications of Relativistic Nuclei

Clermont-Ferrand, october 14-15-16, 1992

Edited by J.P. ALARD and J.C. MONTRET

LABORATOIRE DE PHYSIQUE CORPUSCULAIRE

UNIVERSITE BLAISE PASCAL IN2P3 CNRS

63177 AUBIERE CEDEX

PCCF RI 9308

Proceedings of

BARN 92

Biological Applications of Relativistic Nuclei

Clermont-Ferrand, october 14-15-16, 1992

Edited by J.P. ALARD and J.C. MONTRET

LABORATOIRE DE PHYSIQUE CORPUSCULAIRE

UNIVERSITE BLAISE PASCAL IN2P3 CNRS

63177 AUBIERE CEDEX

PCCF RI 9308

ORGANIZING COMMITTEE

J.P. ALARD (LPC-IN2P3, Clermont)
J.J. BARD (C.J.P., Clermont)
R. BIMBOT (IPN, Orsay)
N. BRETEAU (CHR, Orléans)
P. CHAUVEL (CAL, Nice)
P. GOURMELON (Fontenay-aux-Roses)
J.L. HABRAND (IGR, Paris)
G. KRAFT (GSI, Darmstadt)
J.P. LONGEQUEUE (IN2P3, Paris)
G. MEYNIEL (INSERM, Clermont)
J.C. MONTRET (LPC-IN2P3, Clermont)
J.C. ROSENWALD (I.C., Paris)
R. ROZAN (C.J.P., Clermont)
W. SCHIMMERLING (USRA/NASA)
A. VEYRE (INSERM, Clermont)
A. WAMBERSIE (Louvain).

BARN 92

Oct. 14-15-16th, 1992

PLANNING OF THE WORKSHOP

WEDNESDAY 14 (a.m)

Chairman : J.C. MONTRET

8 h 30 - Welcome to Participants
and Introduction to the Workshop

9 h 00 - **J. CUGNON**
"Description of heavy ion reactions"

9 h 30 - **J.P. ALARD**
"Nuclear fragmentation and applications to biology and space physics"

10 h 00 - **I. SCHALL**
"Nuclear fragmentation of high energy light ion beams in water"

10 h 10 - **F. CUCCINOTA**
"Nuclear fragmentation models and uncertainties in cosmic ray transport and radiobiology studies"

10 h 20 - 10 h 35 : **DISCUSSION**

10 h 35 - 11 h 00 : **COFFEE BREAK**

11 h 00 - **J. CASTRO**
" Role of charged particle therapy in radiation oncology"

11 h 30 - **J. GUEULETTE**
"Radiobiological prerequisites for cancer therapy with heavy ion beams"

11 h 40 - **J.P. PIGNOL**
"Some progress in boron neutron capture therapy"

11 h 50 - 12 h 10 : **DISCUSSION**

12 h 15 - 14 h 00 - **LUNCH**

WEDNESDAY 14 (p.m.)

Chairman : P. CHAUVEL

14 h 00 - **R. BIMBOT**
"Heavy ion accelerators and radioactive beams for biomedical applications"

14 h 20 - **D.B. ISABELLE**
"Irradiation facilities for radiotherapy using protons, neutrons or pions"

14 h 40 - **J.C. ROSENWALD**
"Particle beams for conformal therapy"

15 h 10 - **W. ENGHARDT**
"Positron emission tomography for dose localization and beam monitoring in light ion tumour therapy"

15 h 20 - **T. KOHNO**
"Present status of Himac"

15 h 30 - **T. KANAI**
"What is the best particle for the heavy ion radiation therapy ?"

15 h 40 - **T. KANAI**
"Pre-therapeutic bio-physical experiments fort Himac project"

15 h 50 - 16 h 05 - **DISCUSSION**

16 h 05 - 16 h 20 - **COFFEE BREAK**

16 h 20 - **P. SIGMUND**
"Current problems in particle stopping"

16 h 50 - **V. MICHALIK**
"Spatial aspects of light ion tracks"

17 h 00 - **J. MEDIN**
"Development of a Monte Carlo code for the simulation of therapeutic protons"

17 h 10 - **M. KRAMER**
"Heavy ion track structure calculations"

17 h 20 - 17 h 35 - **DISCUSSION**

18 h 00 - RECEPTION AT THE TOWN-HALL

THURSDAY 15 (a.m.)

Chairman : R. ROZAN

9 h 00 - **W. SCHIMMERLING**
"The problems of radiations in space"

9 h 30 - **J. MILLER**
"Nuclear fragmentation and the space radiation problem"

9 h 40 - **S.B. CURTIS**
"Risk from relativistic heavy ions on manned space missions"

9 h 50 - **G. PERBAL**
"Plant development in space"

10 h 00 - **L. JUST**
"Interactions of 1.3 GeV/nucl. Kr nuclei in emulsions"

10 h 10 - 10 h 25 - **DISCUSSION**

10 h 25 - 10 h 40 - **COFFEE BREAK**

10 h 40 - **G. KRAFT**
"Biological action of heavy charged particles"

11 h 10 - **D.E. WATT**
"Assessment of the indirect component of radiation action by relativistic nuclei"

11 h 20 - **R. CHERUBINI**
"Comparison between cross section of deuterons and protons for cell inactivation and mutation induction"

11 h 30 - **J.L. PONCY**
"Biological effects of ^{20}Ne ion irradiation on tumoral and healthy rodent cells"

11 h 40 - **A. COURDI**
"Radiation response of human tumour cell lines to heavy charged particles"

THURSDAY 15 (a.m.)

11 h 50 - **L. SABATIER**
"Chromosome instability induced by heavy ions in human fibroblasts"

12 h 00 - **B. LARSSON**
"Towards prediction of radiation response in individual patients"

12 h 10 - **A. COURDI**
"Relative biological effectiveness of 65 MeV protons at beam entrance and at the spread-out Bragg peak"

12 h 20 - **DISCUSSION**

12 h 50 - **LUNCH**

THURSDAY 15 (p.m.)

TOUR OF THE REGION

Le Mont Dore
Puy de Sancy
Orcival
Cordès

Banquet at Orcival

FRIDAY 16

Chairman : J. CASTRO

9 h 00 - **R. ROZAN, G. KANTOR**
"Protons and neutrons versus X or Gamma Rays external radiotherapy : alternative options ?"

9 h 30 - **N. BRETEAU, A. WAMBERSIE**
"Neutron therapy from radiobiological expectation to clinical reality"

10 h 00 - **P. CHAUVEL**
"Clinical indications for protontherapy"

10 h 30 - 10 h 50 - **DISCUSSION**

10 h 50- 11 h 10 - **COFFEE BREAK**

11 h 10 - **M.F. LOMANOV**
"Inverse problem in light ion therapy"

11 h 20 - **N. BRASSART**
"Optimisation of the protontherapy beam line in Nice"

11 h 30 - **P. CHAUVEL**
"A protontherapy cooperative group for uveal melanomas : the SERAG"

11 h 40 - **R. CHERUBINI**
"Status report of Laboratori Nazionali di Legnars radiotherapy project"

11 h 50 - **P. CHAUVEL**
"How to organize a possible future for protontherapy, considering the present constraints on health politics"

12 h 00 - **L. SCHWARTZ**
"A new design for a proton linear accelerator"

12 h 10 - **G. KRAFT**
"Status of the therapy project at GSI"

12 h 20 - 12 h 40 - **DISCUSSION**

12 h 50 - **LUNCH**

14 h 00 - 15 h 30 - ***ROUND TABLE AND CONCLUSIONS.***

PREFACE

The Workshop "Biological Applications of Relativistic Nuclei" has been hold in october 1992 in Clermont-Ferrand.

Several accelerators in the world deliver beams of relativistic particles (protons and heavy ions) with energies ranging from 100 to 2000 A.MeV. An intense research activity is devoted with these beams in the field of nuclear physics, namely for the study of the properties of highly excited nuclear matter and its equation of state. On the other hand, interesting applications of these beams can be developped in radiobiology and biomedicine. In particular, those high LET radiations can deposit a high dose at the end of their range in the irradiated matter, and can be used for interesting improvements in radiotherapy. Indeed, classical methods of radiotherapy, using X, γ rays, electrons and neutrons have been treated in the workshop, since the different methods are complementary. On the other hand, heavy ion interactions in matter are of fundamental importance for the preparation of the future missions in space (evaluation of risks for astronauts and implications for the realization of the spacecrafts).

Another interesting point is the work in the field of radiobiology, where research on biological response of cells or subcellar objects has been extended now to more molecular levels (DNA) and other systems as cellular membran.

Finally, all those problems has stimulated physicists to study the interaction of high LET ions with matter, especially in two directions: First, nuclear fragmentation reactions, which cause a modification of the structure of beams and an alteration of the Bragg peak, with important consequences for therapy; fragmentation reactions of nuclei up to iron have also a great interest in space physics. Secondly, emission of electrons in heavy ion -atom collisions are now measured. The understanding of the formation of tracks is in progress. An important theoretical activity is now developped in parallel with these two aspects.

We note that dedicated accelerators are now ready or in project for therapy applications: Nice, Orsay in France, The Himac project in Japan, Loma Linda in USA, Villingen in Switzerland etc... We also note the great role of the Bevalac in the near past years. Now, experiments at GSI are in progress for the preparation of therapy activities.

Finally this workshop is an example of a pluridisciplinary meeting which permitted discussions between physicists, radiobiologists, physicians. It also proves (if necessary) that fundamental research in the field of particles and nuclei has interesting and motivating aspects for practical applications. I hope that similar meetings will be organized and developped in the future. This workshop has been supported by IN2P3/Laboratoire de Physique Corpusculaire, the French Physical Society, University Blaise Pascal of Clermont-Ferrand and Centre Jean Perrin. Support has been also obtained from the Ministere des Affaires Etrangeres of France, The Commissariat a l'energie Atomique (Fontenay aux Roses) , the Companies Philips and General Electric, the local authorities : Conseil General d'Auvergne, Conseil Regional and Ville de Clermont-Ferrand.

All of them are gratefully acknowledged for their help. Finally I wish to thank the organizing comittee, people who have participated to the organization of the workshop, and all the members of my group in Clermont for their help, especially during the sessions.

J.P. Alard

DESCRIPTION OF HEAVY ION REACTIONS[1]

Joseph CUGNON
University of Liège
Institute of Physics B.5
Sart Tilman
B-4000 Liège 1
(Belgium)

The nuclear reactions between nuclei (or heavy ions) play an important role in heavy ion transport in materials, be them of biological or spatial interest : as a matter of fact, the probability of having a nuclear reaction along the total path of an incoming ion is non negligible (~ 0.3 for a ^{12}C ion of 200 MeV/u in water) and the specific ionisation along this path is influenced by these reactions [1,2].

The various reaction mechanisms encountered in the energy domain extending from 10 MeV/u and 2 GeV/u are depicted schematically in fig. 1, where E_{lab} is the energy per nucleon of the incident projectile and b , the impact parameter of the collision. At low energy and in central collisions (small b), a compound nucleus (complete fusion, CF) is formed, which recoils with the momentum of the projectile and evaporates a few slow neutrons. In deep inelastic collisions (DIC) occurring in peripheral collisions (large b), the projectile sticks to the target for a while and eventually escapes, emerging at angles smaller than the grazing angle. The relative motion is considerably damped leading to mass and charge exchange between the two partners and to their internal excitation, which is followed by neutron emission.

At high energy and large b , the projectile barely touches the target but receives sufficient energy (but no momentum) to break into pieces which travel at very small angle, with roughly the incident velocity (this is the fragmentation (F) process). For small b's, there is a geometrical separation of the system. The part of the projectile which is not intercepted by the target continues undisturbed. Similarly, the part of the target which is not intercepted by the projectile remains almost at rest. There is a complete stopping between the two parts that intercept each other, leading to a very excited system which explodes in nucleons and very light particles. This process is referred to as the participant-spectators (PS) regime.

In the intermediate energy regime, at large impact parameters, one goes continuously from the DIC, where nucleons are exchanged between the two partners, to the massive transfer (MT), where a piece of the projectile is transferred to the projectile, while the rest continues almost undisturbed, and to the fragmentation regime. At low impact parameter, one goes continuously from CF, to incomplete fusion (F), in which only one part of the projectile participates to the

[1]Work supported by contract SPPS-IT/SC/29

fusion process, whereas the rest leads to copious light particle emission, to multifragmentation (MF), in which the fused system decays by emission of several intermediate mass ($3 \leq Z \leq 20$) fragments, and finally to the PS regime. In all this series of processes, there is always formation of a fused system, but its decay properties vary with excitation energy, leading to the various kinds of reactions.

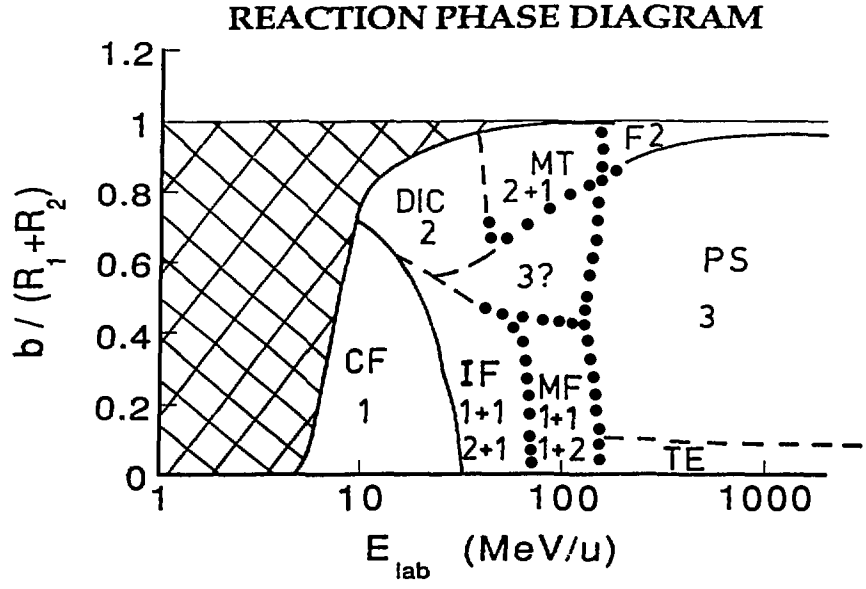

Reaction "phase diagram" giving the various reaction mechanisms and their location in the incident projectile energy per nucleon (E_{lab}) - impact parameter (b) plane. Nuclear reactions are absent in the shaded area. The meaning of the abbreviations is given in the text. The figures in each zone indicate the number of primary fragments. The separations indicated by dotted lines are known with some uncertainty. Those indicated by dots correspond to presumably smooth transitions. See text for detail.

These reaction mechanisms are reasonably well understood theoretically in terms of mean field effects, dominant at low energy, and nucleon-nucleon collisions, dominant at high energy [3, 4]. The theoretical models handling these two dynamical aspects predict a smooth variation of the relative importance of these two effects throughout the plane of Fig. 1. What distinguishes the various mechanisms is in fact the number and the relative size of the "primary" fragments, i.e. the clusters present at the end of the collision process itself and prior to any fragmentation or evaporation processes. The numbers of the primary fragment is indicated in Fig. 1. For instance, the CF leads to a single primary fragment and the PS corresponds to three primary fragments. When two numbers are given with a plus sign in between, the first one refers to the number of large fragments and the second to the number of small fragments. For instance, the IF produces sometimes

one large and one small, and sometimes two large and one small primary fragments.

More details on the reaction mechanism can be found in refs. [3, 5, 6]. We here want to emphasize the classification based on the number of primary fragments and the continuous aspects of the dynamics : fused system formed at any energy, smooth variation of mean field and collision effects.

Whatever the mechanism is, fragments are basically emitted in the forward direction for energies of biological interest. The study of transport properties inside material thus requires mainly the knowledge of fragment yields. The theory of heavy ion reactions yield predictions which are reasonably reliable for the general flow of nucleons in phase space, but not so much for the production of a specific nuclear species. Briefly speaking, theoretical models can tell that so many nucleons are emitted in a given angle-energy interval, but they cannot tell reliably whether these nucleons are free or whether they form one or two clusters. Absolute measurements are thus eagerly needed. The theoretical models are however useful for neutron production, whose cross section has received so far few attention from the experimental side.

References

[1] J. Miller, this workshop
[2] F. Cuccinota, this workshop
[3] J. Cugnon, in "Heavy Ion Collisions", ed. by P. Bonche et al., Plenum Press, New York, 1986, p. 209
[4] J. Cugnon, in "The Nuclear Equation of State, Part A", ed. by W. Greiner et al., Plenum Press, New York, 1989, p. 257
[5] B. Borderie, M.F. Rivet and L. Tassan-Got, Ann.Phys.Fr. **15** (1990) 287
[6] D. Guerreau, Proc. of the International School of Physics Enrico Fermi Course CXII, ed. by C. Détraz et al., NHPC, Amsterdam, 1991, p. 37

NUCLEAR FRAGMENTATION AND APPLICATIONS TO BIOLOGY AND SPACE PHYSICS

J.P. ALARD
for the Diogene Collaboration (Saturne)
and the FOPI Collaboration (GSI-Darmstadt)

Laboratoire de Physique Corpusculaire
IN2P3/CNRS, Université Blaise Pascal,
63177-AUBIERE CEDEX (France)

Relativistic Heavy Ion Collisions (RHIC) offers the opportunity to study nuclear matter in extreme conditions of density and temperature. The Equation of State of Nuclear matter is of fundamental importance, both for Nuclear Physics and Astrophysics. On the other hand, RHIC present a great interest in the field of Radiobiology, Medicine and Space, since Relativistic heavy ions undergo in matter both electromagnetic interactions, with the well known characteristics of high LET particles, and nuclear interactions which result principally in the fragmentation of the projectile and target nuclei.

The major part of the collisions are in fact due to Electromagnetic interactions (ionisation, multiple scattering, electronic capture...) which result in the well known Bragg distribution, showing that a great part of the dose is delivered at the end of the range, and thus in a small volume. This permits interesting applications for the radiotherapy of localized lesions.

On the other hand, fragmentation reactions correspond to the complete destruction of the projectile/target system, and result in a modification of the structure of the incident beam. Furthermore, it appears that most of the nuclear collisions are peripheral ones, and that the fragmentation of the projectile remnant is the most important component. As a result, fragments are emitted near the direction of the incident beam, with velocities peaked around the incident velocity. We can observe a distortion of the Bragg curve, which must be taken into account when we want to make use of fast high LET ions for radiotherapy, especially if the irradiated zone is localized near a radiosensitive organ.

Finally, fragmentation reactions of fast heavy ions occur during the long space manned missions, due to the interactions of cosmic rays (Carbon, Nitrogen, Oxygen, Iron nuclei) with the matter of spacecrafts and with the body of astronauts. The very poor information about fragmentation cross sections for these light nuclei make difficult the precise evaluation of radiation risks for the crews.

So it appears that measurements of fragmentation cross sections of light nuclei on various targets are of fundamental importance, both for biological and space applications.

Now, we give a brief description of two experimental setups which permit the realization of fragmentation experiments. Although such experiments are devoted to Physics, we will show that some of the results are interesting for other applications.

The DIOGENE experiment(1)(Clermont Saclay Strasbourg collaboration) consists of a cylindrical time projection chamber (TPC) permitting identification of particles and light fragments (up to $Z = 6$) emitted in the angular range 25 to 140 degrees. The detection of forward emitted fragments is obtained by a "Plastic wall" covering the angular range 0-6

degrees, and detecting fragments with charges up to Z=8.

Several target/projectile combinations have been used (α + C, Cu, Pb; Ne + NaF, Nb, Pb and Ar + Ca, Nb, Pb) at several incident energies (200, 400, 600, 800 A.MeV). Experiments have been performed between 1982 and 1988.

The FOPI Experiment(2)(collaboration: Bucharest, Budapest, Clermont, GSI Darmstadt, Heidelberg, Mainz, Moscow, Rossendorf, Strasbourg, Warsaw, Zagreb) consists of two parts: -The Phase I part permits the analysis of fragments of charge up to Z = 20, emitted in the angular range 1 to 30 degrees. This part of the setup is running now at GSI; first experiments have been done using Au + Au collisions between 100 and 800 A.MeV.

The "Phase II" part includes a central TPC permitting the analysis of light particles (pions, protons and fragments up to α particles). It is completed by a drift chamber called "Helitron" permitting the determination of the mass of fragments in the angular range $5 - 30^0$, using a magnetic field given by a solenoid around the TPC. The whole detector is completed by barrels of scintillators and Cerenkov counters.

As an example, fig 1 gives the charge distribution given by the FOPI detector for Au+Au collisions at 150 A.MeV; fig 2 gives an example of momentum spectrum in Ne + C collisions (Diogene) showing that impulsions are peaked at beam momentum, and that a part of the fragments are emitted with velocities above the beam velocity. This aspect has been verified for all others projectile target systems. both for Diogene data and Darmstadt data. It confirms the important role of the fragmentation of the projectile in interactions of heavy ions with matter(3).

On the other hand, these results have been used in a crude simulation of nuclear interactions of a 400 A.MeV Neon beam both in water and lead. Fig 3 shows an example of the spatial dispersion, due to nuclear interactions, of a Ne beam through matter.

Finally we can conclude that fragmentation reactions leads to a modification of the composition of the beam, of its spatial extension, and to an alteration of the Bragg peak (high range tail). These last points are of fundamental importance, namely for space (evaluation of risk) and medicine (radiotherapy with high LET particles). We must now perform dedicated experiments, using light ions (from He to Fe), with appropriate targets, and a measurement of absolute production cross sections of fragments. In addition, development of fragmentation codes giving a good description of inclusive data are needed, providing event by event simulations, and permitting 3D computations of nuclear interactions of relativistic heavy ions in matter. Such calculations are now in progress at the LPC Clermont and use the "Freesco" code as a microscopic model for the description of elementary nuclear collisions.

References

(1)J.P.ALARD et al, Nucl. Instr. and Methods, A261(1987)379.
(2)A.GOBBI et al, Nucl. Instr. and Methods, to be published.
(3)P.MOREL, Thesis, Clermont-Ferrand, Fev. 1992.

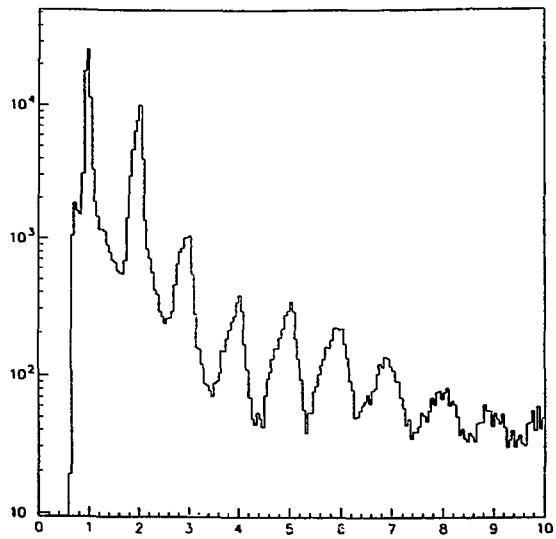

FIG 1

Au + Au (150 A. MeV)
Charge distribution

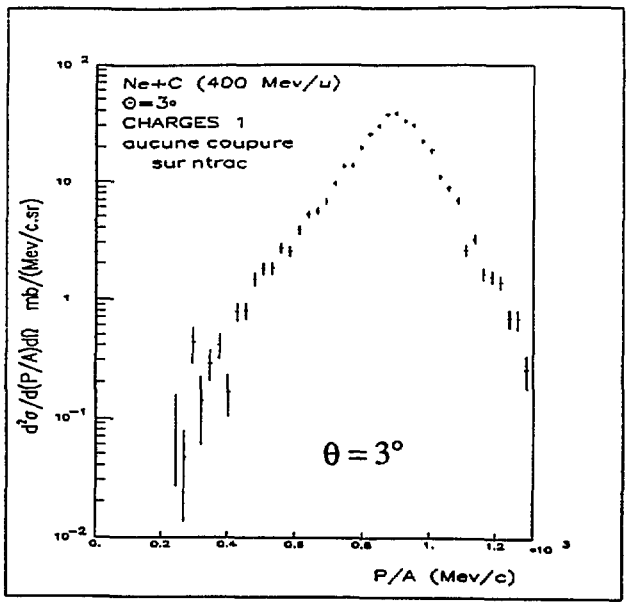

FIG 2

Ne + C (400 A.MeV)
Momentum spectrum of
one-charged fragments

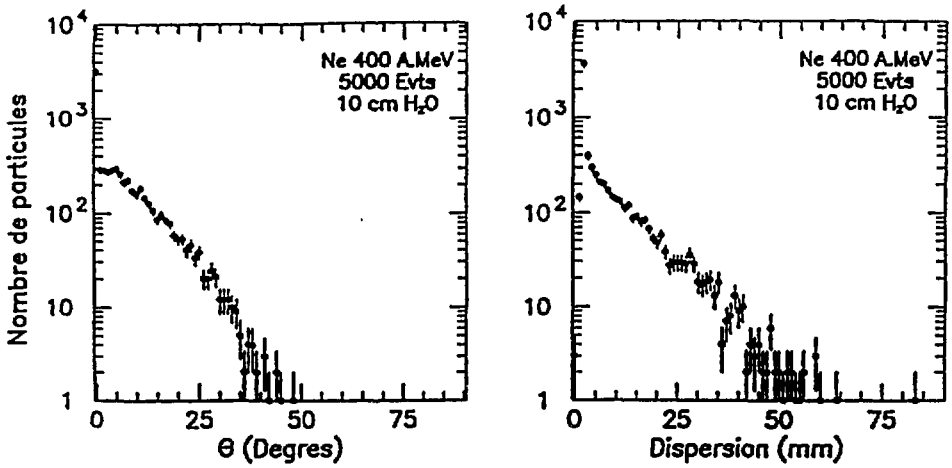

FIG 3

Spatial dispersion of a Ne beam in water
(nuclear interactions only)

Nuclear fragmentation of high-energy light-ion beams in water

I. Schall[*], *D. Schardt*[*], *H. Geissel*[*], *G. Kraft*[*], *A. Magel*[*], *M.F. Mohar*[*], *G.Münzenberg*[*], *F. Nickel*[*], *C. Scheidenberger*[*], *W.Schwab*[*], *E. Kankeleit*[**], *A. Fukumura*[***]

[*] *GSI, Postfach 110552, D-6100 Darmstadt, Germany*
[**] *Technische Hochschule, Schloßgartenstraße 9, D-6100 Darmstadt, Germany*
[***] *NIRS, 9-1, Anagawa 4-chome, Inage-ku, Chiba-shi, 263, Japan*

Introduction

Light-ion beams with energies of a few hundred MeV/u offer favorable conditions for the treatment of deep-seated tumors because of their depth-dose characteristics combined with an increased biological efficiency (RBE) and a reduced or vanishing oxygen effect in the Bragg peak region. Although the biological efficiency increases with atomic number, some limitations are given due to the nuclear fragmentation along the beam path. The built-up of lower-Z projectile fragments reduces the biological effect in the target volume and causes a dose distribution behind the Bragg maximum of the primary beam. Therefore, light-ion beams ranging between carbon(Z=6) and neon(Z=10) are favorable candidates for tumor therapy.
So far, only a few sets of experimental data on fragmentation of light ions in water (as a tissue equivalent) are available from BEVALAC experiments [1,2,3]. At GSI we started such investigations by nuclear fragmentation of a 400 MeV/u ^{20}Ne-beam in a thick water target at the heavy ion synchrotron(SIS). [4]. Recently, we have carried out an experiment where we studied favorable therapy beams simultaneously.

Comparative measurements with ^{10}B, ^{12}C, ^{14}N, ^{16}O beams

In order to compare the projectile fragmentation of favorable therapy beams under identical experimental conditions we performed an experiment at the projectile fragment separator FRS (Fig.1).

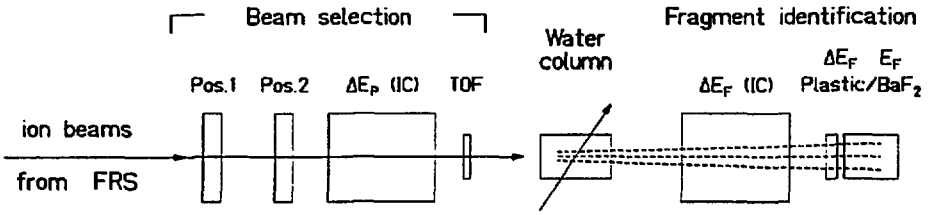

Fig1.: Experimental setup at the final focus of the Fragment Separator FRS.

Secondary beams of ^{10}B, ^{12}C, ^{14}N, ^{16}O were produced from a primary ^{18}O beam (702 MeV/u and 340 MeV/u) hitting a 1 g/cm^2 thick beryllium target and all ions having A/Z=2 were separated in flight by magnetic rigidity analysis. At the final focus of the separator the individual beam particles were selected by ΔE, time-of-flight, and position sensitive detectors before hitting a water column of variable length (Fig.2). Behind the water target the Z-distribution of projectile fragments was measured via their energy loss ΔE_F in a large position sensitive ionisation chamber and a scintillator telescope.

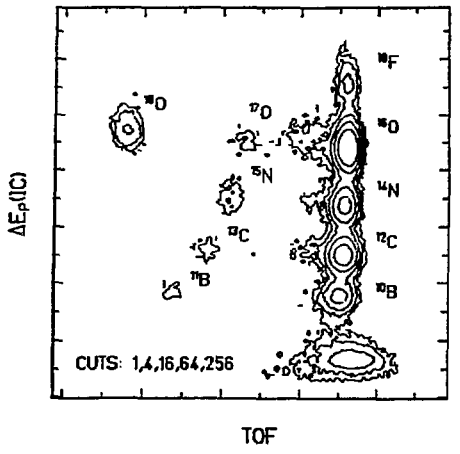

Fig2.: Fragments produced by the projectile fragmentation of 702 MeV/u ^{18}O, reaching the final focus plane for an A/Z=2 setting of the FRS.

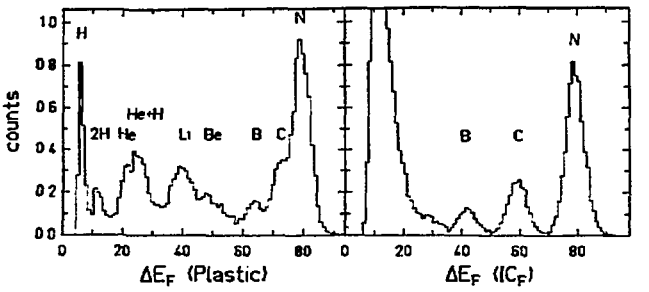

Fig.3: Fragmentation of ^{14}N at a projectile energy of 682 MeV/u. The Z-distribution is measured at a water depth of 25.5cm. The atomic numbers of the heavier fragments are clearly identified in the ionisation chamber signal (right hand side) whereas the lighter particles are better identified in the scintillator spectra (left hand side).

In figure 3, the element distribution of 682 MeV/u ^{14}N particles after passing 22.5cm of water is shown. Fragments with higher Z are clearly identified in the ionisation chamber whereas lower Z-particles are better identified in the plastic scintillator spectrum. For all relevant therapy beams we obtained the beam composition down to Z=1 at various penetration depths. The measurements also include beam attenuation for ^{10}B, ^{12}C, ^{14}N, ^{16}O, ^{18}O and also a number of radioactive isotopes. The complete analysis is still in progress. As an example in Fig.4 the attenuation of the primary ^{14}N ions is shown as function of the penetration depth. The loss of ^{14}N ions is obtained as the ratio of the Z=7 peak distribution measured with the ionisation chambers before and after the water column. The measured mean free path for the charge changing reaction is λ=199(1) mm. For the comparison with models or parametrisations of the total cross section one has to take into account a small contribution of other nitrogen istopes produced in the water target. The parametrisation of the total cross section of Kox et al.[5] give a value of 184 mm. These first results show that the FRS provides excellent conditions for studying the fragmentation of light-ion therapy beams.

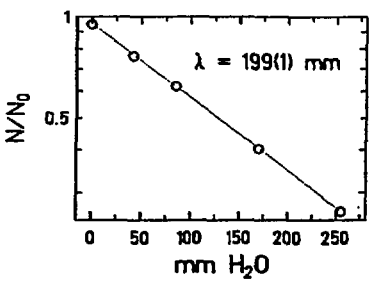

Fig4.: Relative attenuation of primary ^{14}N-particles as a function of penetration depth in water.

1) W.Schimmerling et al., Radiat. Res. 120,36 (1989)
2) H.D. Maccabee, Radiat Res. 54,495 (1973); H.D. Maccabee and M.A. Ritter, Radiat. Res.60, 409 (1974),
3) J. Llacer et al., Med. Phys. 11,266 (1984)
4) I. Schall et al.,IVth Workshop on Heavy Charged Particles in Medicine and Biology, GSI-Report 91-29, Sept.1991, A4
5) S. Kox et al., Phys. Rev. C35,1678(1987)

NUCLEAR FRAGMENTATION MODELS AND UNCERTAINTIES IN COSMIC RAY TRANSPORT AND RADIOBIOLOGY STUDIES

Francis A. Cucinotta, John W. Wilson, Lawrence W. Townsend, and Judy L. Shinn
NASA Langley Research Center
Mail Stop 493
Hampton, VA 23681-0001

The biological effects of relativistic nuclei are of interest because of their potential hazards to astronauts during spaceflight and for possible radiotherapy treatment for cancer patients. Nuclear fragmentation alters the composition of relativistic ion beams as they pass through tissue or other shielding materials, providing a mixed radiation field and complicating the understanding of biological effects. For high energy proton beams, production of high linear energy transfer (LET) secondaries in tissue is responsible for the increase in relative biological effectiveness (RBE) above unity and is observed to reach values above two for some endpoints at low doses [1]. In survival studies along the Bragg curve, fragmentation effects cause moderately charged beams to alter their shoulders as they progress through the plateau region. Higher charged beams, which are normally exponential, also undergo a change in their slope [2]. The description of the transport process, including the complications of mixed radiation fields, is accurately described by the Boltzmann equation [3]; however, the accuracy of the solution is largely dependent on the nuclear fragmentation cross sections.

For the study of transport processes in radiobiology, track-structure models are required in order to consider the lateral extension of an ions track due to secondary electrons. The Katz parametric formalism for the action cross section [4] has been used in a linear kinetics model to provide a description of dose-rate and cell cycle effects [5]. The mutation rate at the HGPRT locus has been modeled using data for human lung [6] and skin [7] fibroblasts in the kinetics model. As a test of the importance of fragmentation parameters on prediction of biological effects during spaceflight, the physical bounds on the fragmentation process have been considered [8] and are used to evaluate the uncertainty in mutation rates in deep space. Here the upper bound considers only the removal of one nucleon in each fragmentation event, while the lower bound considers the complete dissociation of the projectile nucleus in the event. Results with the present model of cosmic ray transport [3] indicate mutation rates of about 5×10^{-6}/year for nominal shields and an uncertainty larger than 50 percent for shields with depths greater than 20 g/cm^2 from the

fragmentation parameters alone. Fragments produced with the greatest mass are much more effective in producing mutations and also control the growth of lighter particles which become important for thick shields.

The dominance of peripheral events in nuclear fragmentation and the importance of the heavy fragments in biological studies indicates that models of this process will be very useful. Traditionally, the abrasion-ablation models [9] have been the most successful and are quite convenient for application, since they require only the one-body density, energy dependent, two-body amplitudes and a standard evaporation code. One of the drawbacks of these models is that the excitation energy of the pre-fragment that results from abrasion is not determined by the model and is treated in an ad hoc fashion. Recent progress in the modeling of light ion breakup suggests that the abrasion step can be re-formulated in terms of many body response functions and the distribution in excitation energies found as a function of the number of abraded nucleons [10].

REFERENCES

1. F. A. Cucinotta; R. Katz; J. W. Wilson; L. W. Townsend; J. L. Shinn; and F. Hajnal: Radiat. Res. 127, 130 (1991).
2. R. Katz; F. A. Cucinotta; J. W. Wilson; and J. L. Shinn: NASA TP 3235 (1992).
3. J. W. Wilson, et al.: NASA RP 1257 (1991).
4. R. Katz; B. Ackerson; M. Homayonfar; and S. C. Scharma: Radiat. Res. 47, 401 (1971).
5. J. W. Wilson; F. A. Cucinotta; and J. L. Shinn: NATO Adv. Study Institute (1991).
6. R. Cox and W. K. Masson: Int. J. Radia. Biol. 36, 149 (1979).
7. K. Tsuboi; T. C. Yang; and D. J. Chen: Radiat. Res. 129, 171 (1992).
8. L. W. Townsend; F. A. Cucinotta; J. L. Shinn; and J. W. Wilson: NASA TM 4386 (1992).
9. L. W. Townsend; J. W. Wilson; F. A. Cucinotta; and J. W. Norbury: Phys. Rev. C 34, 1491 (1986).
10. F. A. Cucinotta; L. W. Townsend; and J. W. Wilson: Phys. Rev. C 46, ___ (1992).

THE ROLE OF CHARGED PARTICLE THERAPY IN RADIATION ONCOLOGY

Joseph R. Castro, M.D.

University of California Lawrence Berkeley Laboratory
Berkeley, CA 94720

Supported by NIH-NCI CA 19138 and DOE Contract DE-AC03-76SF00098.

PROTON AND HELIUM ION STUDIES

Accumulating evidence from several centers has shown the clinical potential of protons and helium ions in the treatment of selected human cancers (2,3,4,6). Despite the limitations of the laboratory based accelerators utilized for these trials, the potential for improved local control and survival has been demonstrated in the treatment of tumors in critical locations such as the skull base, juxtaspinal area, eye, paranasal sinus, nasopharynx, liver, soft tissue, bone and pelvis.

The use of protons and helium ions in treatment of uveal melanoma has now been accomplished in over 2000 patients with a high rate of local control (97%), retention of the eye in 85% and preservation of useful vision in about 50% of patients (5,7). Long term follow-up has shown survival comparable to enucleation, although about 20% of patients eventually manifest distant spread of tumor. A search for improved treatment techniques, and reduction of complications by lowering the tumor dose is underway.

Over 150 patients have been irradiated at UCLBL for unresectable or residual chordoma or chondrosarcoma of the skull base or spine using helium or neon ions. The local control and survival have been significantly improved compared to previous historical results using photon irradiation. This is in consequence to the improved dose localization of charged particles with their ability to deliver 10-30% more dose to the tumor while maintaining the same or lesser dose to adjacent normal structures. For lesions of the skull base or cervical spine, we have mainly utilized helium ions delivering a mean dose of 67 Gray-equivalent. The crude local control rate is 65% (61 of 94 pts) with a followup period ranging from 4 to 175 months, median of 38 months. The 5 year survival and local control rates calculated by Kaplan-Maier technique are 70% and 63%, respectively. Five-year local control is better for chondrosarcoma (70%) than for chordoma (58%), and in the skull base (68%) than in the cervical spine (50%). A previous evaluation at LBL has shown a higher rate of local control for small lesions (less than 20 cc), and for those treated at time

of initial diagnosis, rather than post recurrence (1). Serious complications have been encountered at about the 10-15% level. Critical tissues are cranial nerves, brain stem, spinal cord and temporal lobes of the brain. Helium ion therapy has also been used successfully at LBL in treating tumors of different histology (such as unresectable meningioma or sarcoma) in the skull base, paranasal sinuses, juxtaspinal area, retroperitoneal space, soft tissue and bones.

Hospital based proton facilities are now in operation or being planned in a number of countries. The advent of such flexible gantry-equipped clinical facilities will permit improved beam delivery techniques, and coupled with better treatment planning, a larger percentage patients requiring radiation treatment will benefit from this therapy.

HEAVY ION STUDIES

At UCLBL, exploration of neon ion therapy has been carried out. Heavy ion beams exemplify both dose distribution and improved biological potential secondary to their high-LET deposition. Their biological advantages include overcoming resistance to low-LET irradiation, especially in tumors with slow growth kinetics which permit repair of low-LET irradiation. Clinical data using heavy ions such as carbon, neon and silicon have been slower to acquire due to the limited resources at UCLBL, but suggest potentially valuable application in tumors resistant to conventional low-LET radiotherapy. Salivary gland, paranasal sinus, nasopharynx, biliary tract, soft tissue, bone and prostate tumors have been treated in Phase I trials with promise of improved local control (8,9). Local control rates have ranged from 44% for biliary tract tumors to 90% for locally advanced prostate gland tumors. Particular promise has been apparent in retroperitoneal soft tissue sarcoma, a site which is poorly controlled by low-LET photon therapy and in adenocarcinoma of salivary gland and biliary tract origin.

Most of these Phase I-II patients had unresectable or residual large volume disease, and received varying doses of high-LET irradiation as treatment techniques were developed. Considering the difficulties of performing a valid trial under these circumstances, the fact that promising results were obtained in several tumor sites is itself exciting. Optimized use of heavy ions with improved treatment planning, better beam delivery techniques and individualized patient selection will lead to further clinical gains. The goal is to determine in advance of their therapy which patients require high-LET beams so preselected and planned treatment can be given. The role of heavy charged particles in radiation oncology in the next century is promising but its optimal use will require further research.

REFERENCES

1. Berson, A.M., Castro, J.R., Petti, P., Phillips, T.L., Gauger, G.E., Gutin, P., Collier, J.M., Henderson, S.D. and Baken, K.: Charged Particle Irradiation Of Chordoma and Chondrosarcoma Of The Base Of Skull and Cervical Spine: The Lawrence Berkeley Laboratory Experience. Int. J. Radiation Oncology Biology Physics 5-3:559-565, September 1988.

2. Castro, J.R. and Reimers, M.M.: Charged Particle Radiotherapy Of Selected Tumors In The Head and Neck. Int J Rad Onc Biol Phys 14-4:711-720, April, 1988.

3. Castro, J.R., Petti, P.L., Daftari, I.K., Collier, J.M., Renner, T., Ludewigt, B., Chu, W., Pitluck, S., Fleming, T., Alonso, J. and Blakely, E.: Clinical Gain From Improved Beam Delivery Systems. Radiation and Environmental Physics (1992) 31:233-240.

4. Castro, J.R., Collier, J.M., Petti, P.L., Nowakowski, V., Chen G.T.Y., Lyman, J.T., Linstadt, D.E., Gauger, G., Gutin, P., Decker, M., Phillips, T.L., and Kari Baken, R.T.: Charged Particle Radiotherapy For Lesions Encircling The Brain Stem Or Spinal Cord. Int J. Radiation Oncology Biol Phys 17-3:477-484, Sept. 1989.

5. Char, D.H., Castro, J.R., Kroll, S., Irvine, A.R., Quivey, J.M. and Stone, R.D.: Five Year Follow-up of Helium Ion Therapy for Uveal Melanoma. Archives of Ophthalmology Vol. 108, Feb.1990.

6. Feehan, P., Castro, J.R., Phillips, T.L., Petti, P.L., Collier, J.M. , Daftari, I. and Fu, K.: Recurrent Locally Advanced Nasopharyngeal Carcinoma Treated With Heavy Charged Particle Irradiation. Int J Rad Onc Biol Phys. Vol. 23, No. 4, pps.881-884, 1992.

7. Linstadt, D., Castro, J., Decker, M., Quivey, J., Char, D. and Phillips, T.: Long-term Results of Helium Ion Radiotherapy for Uveal Melanoma. Int. J. Rad Onc Biol Phys. Vol. 19, Sept. 1990.

8. Linstadt, D., Castro, J. and Phillips, T.: Results of the Phase I-II Neon Trial at Lawrence Berkeley Laboratory. Int J Rad Onc Biol Phys 20:761-769, April 1991.

9. Nowakowski, V., Castro, J.R., Petti, P.L., Collier, J.M., Daftari, I., Ahn, D., Gauger, G., Gutin, P., Linstadt, D. and Phillips, T.L.: Charged Particle Radiotherapy of Paraspinal Tumors. Int. J. Rad. Onc. Biol. Phys. Vol. 22, pp. 295-303, 1991.

RADIOBIOLOGICAL PREREQUISITES FOR CANCER THERAPY WITH HEAVY IONS

J. Gueulette and A. Wambersie
Université Catholique de Louvain, Cliniques Universitaires St-Luc,
1200 Brussels, Belgium.

Control of primary tumour remains one of the main challenges in the treatment of cancer and, in that respect, the introduction of new types of ionizing radiations is a promizing approach in radiotherapy. **As far as protons or helium ions are concerned**, they aim at improving the physical selectivity of the irradiation and no benefit has to be expected from their radiobiological properties since they stay in the field of low-LET radiations. Their clinical advantage has been demonstrated for several tumour types (uveal melanomas, chordomas or chondrosarcomas of the base of the skull, etc.). **As far as neutrons are concerned** (the most widely high-LET radiation used in therapy), radiobiological data suggest that the reduction of OER, the reduction of the influence of cycle phase, etc. could bring a benefit in some situations. Their clinical advantage have been demonstrated for several slowly growing and well differenciated tumours, but the need for patient selection is clearly apparent.

Heavy ions combine the advantage of a high physical selectivity (comparable to that of protons) with the high-LET advantages in the treatment of some type of tumours. However, since the proposed ions (carbon, neon, argon...) cover a (very) high LET range, their clinical application raises some specific problems.

As can be seen on Figure 1, heavy ions cover a higher LET range than neutrons, where the RBE variations for different biological systems are very steep and about falling in the "overkilling" region. As a consequence, the *amplitude* ***and*** *the direction* of the radiobiological differential effect brought by heavy ions (e.g. the alteration of the relative intrinsic radiosensitivity from cell line to cell line) is likely to rapidly vary according to the actual LET of the beam and might be quite different than for neutrons. It means that the high LET advantage of heavy ions does not necessarily implicate the same type of tumour as those disclosed through the clinical experience with neutrons, even if the reduction of OER remains a general potential benefit. In this respect, the selection of patients who would beneficiate from heavy ions remains one of the most important points, which emphasizes the need for the development of appropriate "predictive assays".

The second problem is related to the obtainment of the **full** potential therapeutic benefit of heavy ions and to the safety of their application. In this respect one knows that the LET and, consequently, the RBE of heavy ions increases all the way from the entrance of the beam in tissue to the end of the (spread out) Bragg peak. If the fact that RBE in the initial plateau is lower than in the spread out Bragg peak is an additional advantage of the good dose distribution of heavy ions (Figure 2), the increase of RBE in the peak requires to be very attentive to the obtainment of an "iso-survival" region where the biological effect remains constant over the whole target volume. Therefore, it is needed that RBE variation in the spread out Bragg

peak is carefully studied (choice of the biological system ?), making it possible to design the spreading out system yielding the suitable dose distribution. In this respect it is worth remembering that if a given dose would leave on average one surviving cell in a tumour, a 20 % underdosage in one tenth of the tumour would bring the average number of surviving cells to four, corresponding to a fall of the cure probability from 37% down to 2 % !

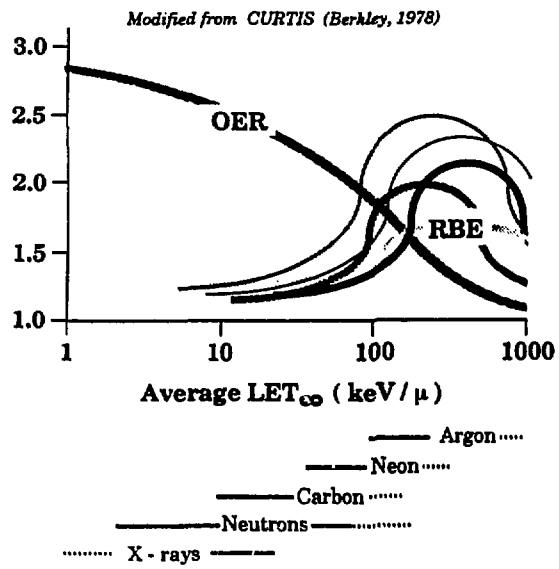

Figure 1 : OER and RBE variation as a function of LET for different hypothetical biological systems. This highly schematic figure is based on the fact that most of the available biological data indicate that RBEs exhibit their maximum values around LET = 100 keV/ μm. The LET range cover by different particles is shown on the bottom of the figure (*redrawn from Curtis, Berkeley, 1978*)

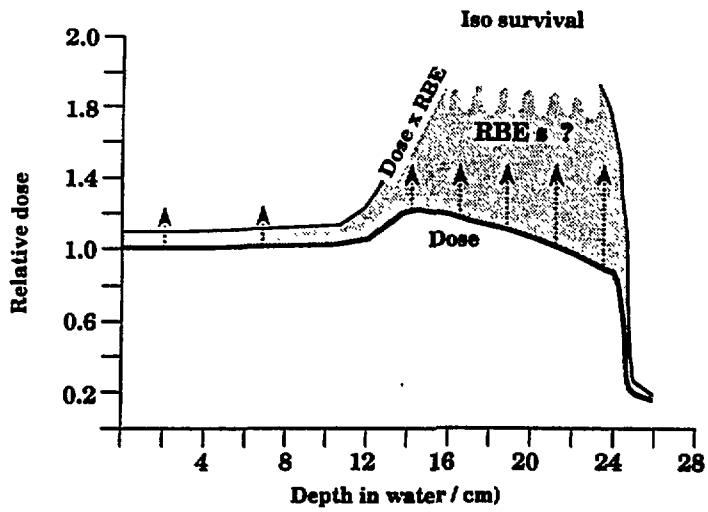

Figure 2 : Relative dose as a function of depth in water for a modified carbon beam (Bragg peak spread out over approx. 12 cm). The high RBE values in the peak enhance the advantage of the good dose distribution but raises the problem of the obtainment of a suitable iso-survival region *(redrawn from E.Hall, 1981)*.

SOME PROGRESS IN BORON NEUTRON CAPTURE THERAPY

J.P.PIGNOL[1], J.C.ABBE[2], J.SAHEL[3], L.MEYER[3], R.BELKHOU[2], N.DAYMARD[2], R.MASSARELLI[2], G.METHLIN[1]

1- Centre Paul STRAUSS, STRASBOURG
2- Centre de Recherches Nucléaires, STRASBOURG
3- Clinique d'Ophtalmologie, Hospices Civils de STRASBOURG

BASIC PRINCIPLES

In 1936 LOCKER first suggested to use the 10B(n,a)7Li capture reaction to treat cancer. The idea was to introduce selectively boron into tumoral cells, and to irradiate the tissue with thermal neutrons. Separately these two elements have small effects, but the capture, with a very high reaction cross section (3838 barns), produces two high LET particles: one alpha with an energy of 1.47 MeV and one lithium ion carrying 0.85 MeV. The ranges of these particles in biological tissues, 8µm and 5µm, are close to the tumoral cell diameter (1, 2).

A first therapeutic attempt was made in the 50's, with the medical nuclear reactor of Brookhaven and Boston, to treat high grade glioblastoma using PCB boric acid and intraoperative thermal neutron irradiation. This trial failed as it did not show any advantages above conventional treatment, and anatomopathologic studies have shown high skin, normal brain and vessels radiation induced damages. The precise data analysis have shown that if no boron was detected macroscopicaly in normal brain, the compound used had a tumor to blood ratio of 0.5; as a consequence the microcirculation has received the highest radiation dose. In addition the thermal neutron flux is halved each 1.8 cm, and decreased by a decade at 6-7cm.

More tumor selective coumpounds, BoroSulfHydryl (BSH) and ^{10}BoroPhenylAlanine (BPA), have been used in the japanese trials. With BSH, on a series of 116 cases of various cerebral tumors including 38 high grade glioblastomas, HATANAKA has obtained very good results in term of survey : 58% at 5 years for grade III-IV within 6 cm from the brain surface. MISHIMA and al have shown complete tumor regression on 12 cases of primary or metastatic malignant melanoma (1).

With these clinical results and the progress in beam design , in coumpound chemistry and especially in microdosimetry, a new lease of life began for this therapy.

Reactors, accelerators or radioisotopes like ^{152}californium (2.6 years, 3.8 n/fission) may be used to provide enough neutrons, a total fluence of 10^{12}-10^{13} n/cm^2 being required. These neutrons are moderated either to thermal energy as in the japanese experience, or filtered to epithermal as suggested by R.FAIRCHILD to treat deeper tumors, the tissues acting as moderators (1, 2).

EDGE WITH RELATIVISTIC NUCLEI

Three arguments plead for close collaboration between relativistic nuclei and BNCT:

1- Neutron sources : reactors and radioactives sources produce fast neutrons and energetics gammas (around 2MeV) requiring moderation and filtering, and they raise severe radioprotection problems. Accelerators are the best alternative for hospital implantation (1, 2). Two options can be considered:

* low energy projectile on light target, like the 7Li(p,n)7Be reaction,
* high energy projectiles on heavy target, such copper, producing neutrons by spallation.

In addition, it may be attractive to find new applications to high technology and very expensive particles medical accelerators.

2- Microdosimetry : Microdosimetric data could be advantageously shared. As the LET varies all along the trajectory of relativistic nuclei, the radiobiological effect change. The same problem is hardly debated in BNCT for the RBE value associated to every components resulting from neutron irradiation.

3- Tumors selection: These new radiation techniques bring the hope to treat conservatively radioresistant tumors, usually out of any therapeutic ressources: the use of high LET particles permits to kill cells with high DNA dammages repair, with oxygene depletion and non dividing cells. If relativistic nuclei allow to irradiate a target volume with high accuracy and deep tumors, BNCT allows to treat larger area increasing the probability to reach boronated micrometastasis.

BNCT OF UVEAL MELANOMA

With less than 0.2% of all malignancies, uveal melanoma is rare. Yet, this tumor represents 80% of all ocular tumors, and the survival rates for patients treated with a conservative technique fall from 65% at five years to 46% at 15 years (3).

Two therapeutic approaches are usefull for posterior uveal melanomas under 10mm thickness and 15mm diameter: relativistic nuclei or brachytherapie.

However, some cases cannot benefit of these conservative scheme and they raise therapeutic problems : ocular melanoma with extraocular extension (13% of all the cases), including those rowing up along the optic nerve, splitted under conjunctival melanoma and metastatic melanoma which is to this date almost incurable. They open a wide field for new therapeutic approaches including BNCT.

Along these views, an animal model of uveal melanoma has been done with *human malignant cells*. A suspension of 2.10^6 cell/100µl of OM461 cell line (gratefully from Pr.D.M.ALBERT, Massachusetts Eye and Ear Infirmary, Boston) has been injected in the anterior chamber of an immunosupressed New Zealand rabbit weighting 3kg500. 15 days latter, as the tumor is well seen to the naked eye, the biodistribution of BPA (90mg/kg) have been mapped using the alpha-autoradiography technique (4). The picture infra shows the ^{10}boron distribution in the eye. The tumor show a selective, although heterogenous, uptake of BPA. This picture is not representative of the best tumor/normal tissue ratio which could be expected because the dose of 90mg/kg of BPA is lower than that used by CODERRE in his animal studies (150-600 mg/kg) or in proposed clinical trials (2g/kg). Yet it is representative of the 10boron uptake of an human tumor grown in an animal model.

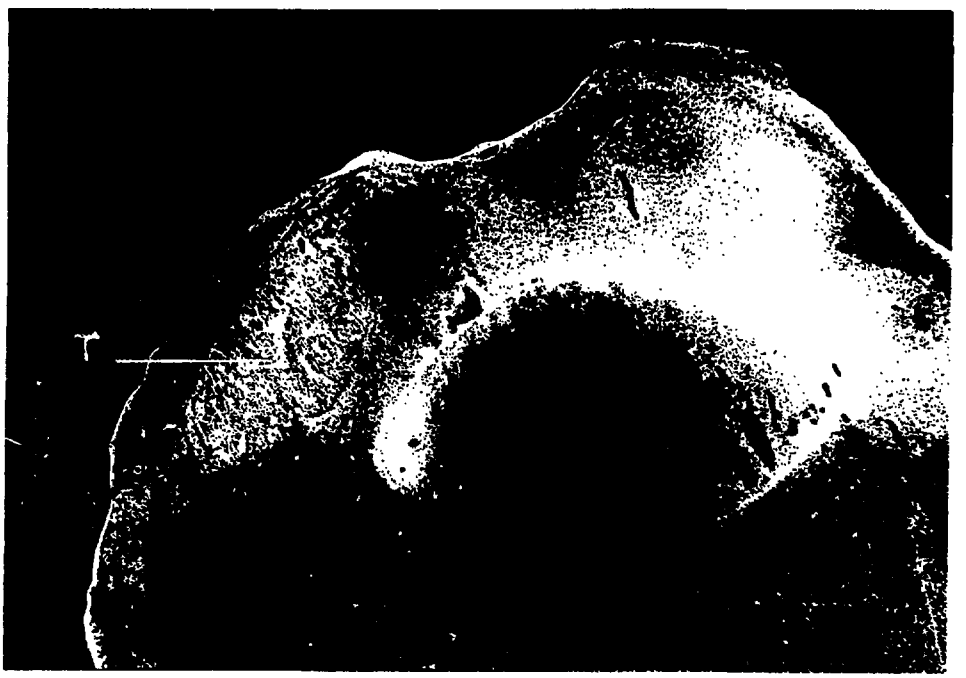

Aknowledgments : This work has been supported by the Ligue Contre le Cancer.
Thanks are due MrSTAMPFLER and MrSENS from the Reacteur Universitaire de Strasbourg, for neutron irradiations.

BIBLIOGRAPHY

1-R.F.BARTH, A.H.SOLOWAY, R.FAIRCHILD-Cancer Research, 50:4, 1061-70 (1990)
2-L.DEWIT, R.MOSS, D.GABEL-Eur.J.Cancer, 26:8, 912-14 (1990)
3-D.M.ALBERT, J.D.EARLE, J.SAHEL-In"Cancer principles and practice of oncology", Vol.2, J.B.LIPPINCOTT Comp., Philadelphia, 1989.
4-J.A.CODERRE, J.D.GLASS, R.FAIRCHILD, U.ROY, I.FAND-Cancer Research, 47, 6377-83(1987)

HEAVY ION ACCELERATORS AND RADIOACTIVE BEAMS FOR BIOMEDICAL APPLICATIONS

R. BIMBOT
Institut de Physique Nucléaire, 91406 - Orsay Cedex, France

Introduction

While protontherapy is developing, with the recent starting of the Loma Linda accelerator in California, and of the two French Centers at Nice and Orsay[1], radiotherapy using heavy ions from C to Si (generally referred to as light ion therapy) is still in its early stage. The only machine on which treatments were ever performed is the Berkeley Bevalac, an accelerator designed for fundamental research in Physics, and the only machine dedicated to medicine is being built in Chiba, Japan. If one excepts the CERN accelerators which produce ultrarelativistic heavy ion beams, two facilities in Europe, the Saturne national accelerator in Saclay (France) and the GSI-Synchrotron SIS in Darmstadt (Germany) are able to deliver heavy ion beams with ranges exceeding 25 cm in water. These machines are presented in this paper, together with less energetic ones which are, or can be used for pretherapeutic biomedical studies. The production of radioactive beams of positron emitters, which are powerful tools for combining light ion therapy with a precise localization of the dose deposition is briefly discussed at the end of this talk.

1. Medium energy heavy ion accelerators

This section is devoted to machines producing beams in the energy range 20-150 MeV/u. Such energies are not sufficient to perform radiotherapy of deeply seated tumors. However, they are quite suitable for studying radiation effects on cells in the Bragg peak region. This presentation will mainly focus on two european machines, UNILAC at Darmstadt and GANIL at Caen.

Originally designed to accelerate all heavy ions up to 10 MeV/u, and recently upgraded to 20 MeV/u, the **UNILAC**[2] is composed of two linear sections (Wideröe and Alvarez) followed by a series of single resonators. An intermediate stripping at 1.4 MeV/u takes place at the exit of the Wideröe section. Up to 1989, beams were thus available both at 1.4 MeV/u. in the stripperhall and at variable energies between 2 MeV/u and the maximum energy in the main experimental hall. The stripperhall was closed in 1989 to install a new injection line. From 1975 to now, biomedical experiments have been performed at GSI over the whole energy range and a significant part of the present knowledge in this domain is due to this extensive work[3].

In operation since 1983, the **GANIL** French national heavy ion facility is made of two conventional sector cyclotrons with a small compact cyclotron acting as injector[4]. The maximum beam energy is 100 MeV/u for light projectiles (C to Ne). Two beam lines are currently used for biomedical research. One of them is equipped with a sweeping magnet which distributes the beam over a broad area (5 x 100 cm^2) ; the other one is composed of an achromatic spectrometer (LISE) which is particularly suitable for research in beam dosimetry, fragmentation, radioactive beam production and biomedical research. A coordinated program covering these domains has been initiated and is presently developing. Part of the results obtained will be presented by J.L. Poncy[5].

Let us mention two other medium energy machines which are the **MSU** supraconducting cyclotron K1200 and the **RIKEN** Facility, a conventional sector cyclotron with two possible injectors, a linear accelerator, or a cyclotron. Both the MSU and RIKEN machines are

equipped with spectrometers adapted to radioactive beam production. At RIKEN, a biomedical program is being pursued, in close connexion with the Chiba project.

2. High energy machines

The very first biology experiments using GeV/u heavy ion beams were performed in 1971 using the Princeton Synchrotron beams[6,7], but the major biomedical experiments, and the unique heavy ion radiotherapy program been realised at Berkeley[9] on the **Bevalac Accelerator**, which combines a linear injector (SUPERHILAC) at 8.5 MeV/u and a 2 GeV/u synchrotron. This machine has produced heavy ion beams since 1974, and biomedical research started at the same period using three dedicated beam lines. These lines were located inside the Bevalac Biomedical Facility, an area specially designed for radiotherapy, radiobiology, radiology and radiological physics[10].

The **Saturne French national facility** is a combination of two synchrotrons, the MIMAS injector, which acts also as a storage ring in order to increase the intensity delivered by the ion source DIONE, and the Saturne accelerator which delivers heavy ion beams up to 1.2 GeV/u and proton beams between 100 MeV/u and 2.9 GeV/u. Although these beams are well adapted to biomedical research and treatment, no significant program has been realised up to now in this domain. Note also that the Saturne experimental area as equipped with several spectrometers ; one of them (SPES IV) is suitable for radioactive beam production. However, the intensities available for primary beams would make it difficult to exploit the secondary beams for biomedical studies.

The **GSI synchrotron SIS** for which the UNILAC machine acts as an injector and which is coupled to the ESR storage ring has been completed in 1990[11]. It delivers light ion beams up to 2 GeV/u. A biomedical experimental area exists and is now equipped with a fast magnetic deflection system which has been developed for medical applications[13]. Physics and biology experiments using the SIS beams are currently running. Several contributions to this workshop concern these topics[14].

A significant step towards light ion therapy has been made with the project **HIMAC** of the National Institute of Radiological Science which is under construction at Chiba, Japan[15]. Approved in 1987, this facility is expected to complete in 1993. Dedicated to medicine, it is made of a linear injector and two superimposed synchrotrons which deliver He to Si beams from 100 to 800 MeV/u through horizontal and vertical beam lines. The status of this medical center will be presented at this meeting by T. Kohno[16].

Several other medical heavy ion machines have been proposed in the world. Let us mention the LIBRA project[9] and the Biomedical Heavy Ion Center at LBL[18] in USA, the GSI-Heidelberg proposal for a 480 MeV/u synchrotron[19] and the EULIMA project for either a superconducting cyclotron or a synchrotron delivering 400 MeV/u Ne ions[20,21]. None of these projects has yet been approved.

3. Radioactive beams

Radioactive beams of positron emitters may be produced through fragmentation of high energy heavy ion beams ; note that they can also be obtained by direct acceleration of radioactive nuclei, as proposed in ref. [22]. Such beams may be very useful either for diagnostic or for treatment if the irradiation is combined with positron emission tomography[23,10]. A recent review of the question is presented in ref.[24].

The separation and transmission of secondary radioactive beams, produced in a thick target, requires the existence of an achromatic beam line (or spectrometer). Most of the machines mentioned in this talk are equipped with such devices, and produce currently such beams. At Berkeley, first diagnostic experiments have been realised with ^{19}Ne beams[25], at

MSU, localization experiments of ^{18}F ions implanted in a phantom have been performed using a 3 dimension PET camera[26], at GSI, a localization counter has been developed for a precise determination of the range end point of β^+ emitters[27], at Chiba, an experimental area is being built for application of radiaoctive beams, and in the EULIMA proposal based on a supraconducting cyclotron the production of such beams was one of the strong points[28].

Indeed, the intensities presently available on high energy machines, are not sufficient for direct treatment with radioactive beams. Efforts should be made in this direction, to increase again the precision and security of heavy ion radiotherapy.

References

1. D.B. Isabelle, this meeting.
2. N. Angert and C. Schmelzer, Kerntechnik **19** (1977) 57.
3. See for example G. Kraft, Nucl. Sci. Appl. **3** (1987) 1.
4. J. Fermé et al and other contributions in Proc. 9th Int. Conf. on Cyclotrons and their Applications, Caen (France) 7-10 sept. 1981, G. Gendreau edr. Ed. Phys. Fr., p. 3..
5. J.L. Poncy et al, this meeting.
6. M.G. White et al, Science **174** (1971) 1121.
7. P.W. Todd et al, Science **174** (1971) 1127.
8. P. Chauvel and A. Wambersie, Proc. EULIMA Workshop on the potential value of light ion beam therapy, Nice, 3-5 nov. 1988, Report EUR.12165 EN (1989).
9. C.A. Tobias et al, in ref. 8 ; J.R. Castro, this meeting.
10. C.A. Tobias, Rad. Research **103** (1985) 1.
11. P. Kienle, Proc. of the Workshop on Experiments and Experimental Facilities at SIS/ESR, Darmstadt (RFA) 30/3-1/4/1987, Report GSI 87-7, p. 1.
12. G. Kraft, Extended Abstracts - Fourth Workshop on heavy charged particles in Biology and Medicine (sept. 1991), report GSI-91-29.
13. T. Haberer et al, in ref. 12, p. G2.
14. W. Enghardt, this meeting ; G. Kraft, this meeting ; I. Schall, this meeting.
15. K. Kawachi et al, in ref. 12, p. K6.
16. T. Kohno, this meeting.
17. P. Marin and P. Mandrillon, Proc. 2nd EPAC Conference, Nice (1990), Ed. Frontières.
18. J.R. Castro, in ref. 17, p. S56.
19. D. Bohne, in ref. 12, p. F1.
20. P. Mandrillon, in ref. 17, p. S4.
21. P. Mandrillon et al, in ref. 8, p. 419.
22. G. Berger et al, in ref. 17, p. S118.
23. J.R. Alonso et al, IEEE Trans. Nucl. Sci. **NS26** (1979) 3003.
24. R. Bimbot, Proc. 2nd Int. Conf. on Radioactive Nuclear Beams, Louvain la Neuve, Belgique, 19-21 août 1991, Th. Delbar Ed., Adam Hilger Bristol, p. 409.
25. A. Chatterjee and J. Llacer, Proc. 1st Int. Conf. on Radioactive Nuclear Beams, ed. by W.D. Myers, J.M. Nitschke and E.B. Norman, World Scientific (1990) 404.
26. D. Litzenberg et al, Proc. 2nd Int. Conf. on Radioactive Nucl. Beams, Louvain la Neuve, Belgique, 19-21 août 1991, Th. Delbar Ed., Adam Hilger Bristol, p. 423.
27. W. Enghardt, this meeting.
28. R. Bimbot, in ref. 8, p. 443.

IRRADIATION FACILITIES FOR RADIOTHERAPY USING PROTONS, NEUTRONS OR PIONS

D.B. ISABELLE
C.E.R.I.-C.N.R.S., 3A , rue de la Férollerie
45071 ORLEANS CEDEX 2 (France)

For the last twenty years, radiotherapeuts in collaboration with physicists have been testing the use of charged particules and of neutrons to cure cancer tumors. Such particles are advantageous either due to their well defined range in matter allowing an accurate energy deposition at the tumor localization, or to their better radiobiological efficiencies. As shown in many papers at this conference, high energy heavy ions will be the most efficient killers. But the accelerators delivering few hundred MeV per nucleon ions are very expensive. They are described in the companion's paper by R. Bimbot. We will limit our presentation to accelerators for proton-, neutron- or piontherapy (1).

For all these applications a proton accelerator is needed and it is interesting to figure out the energy scale:

- for neutrontherapy one needs proton (or deuteron) with an energy of 60 to 70 MeV,
- for protontherapy, protons with variable energy from 70 to 250 MeV protons are needed,
- for piontherapy, the production of a pion beam implies the use of 500 to 600 MeV protons.

Up to very recently, the accelerators used for such therapeutic treatment were, old machines originaly designed for fundamental research in nuclear physics. They are cyclotrons, synchrocyclotrons, synchrotrons and proton linac. The main problem encountered to transform these machines for patient irradiation has been the design and construction of the beam handling systems. We will consider here briefly the three types of new radiotherapies and show the evolution of the technology. Due to the lack of space, we will not go in any details, but refer the readers to the appropriate litterature.

Let us first consider the case of piontherapy. It was first suggested by Fowler and Perkins (2). Some RBE measurements were performed in the sixties at Berkeley, Brookhaven and CERN. Finally patient irradiation facilities were installed at LAMPF (Los Alamos, USA) and SIN (Villigen, CH). The largest experience was obtained in this last laboratory (3). It shows that for some types of tumors negative pions have a good efficiency. But to obtain a proper pion intensity on the target a very elaborated beam handling system with many irradiation channels is needed. So the cost of such equipment associated to the cost of running a high energy accelerator is not compensated by a real improvement in survival rates. So the facilities are or will be closed in the near future.

The proton therapy was initiated in 1961 at the cyclotron laboratory at Harvard University (USA). The importance of proton therapy for the treatment of eye melanomae has been demonstrated there, as more than 5 000 patients have been treated. Other nuclear physics accelerators were adapted to proton therapy in Russia (Leningrad and Dubna), in Switzerland (PSI at Villigen) in Japan and more recently, the Orsay synchrocyclotron (France).

To reach tumors at various depths the proton energy must be varied. It can be achieved with a variable energy accelerator. But the delay needed for an energy change is in general relatively long and it seems preferable to use a fixed proton energy beam and to degrade its energy using a variable thickness absorber. The beam scanning over the tumor cross section can be achieved either with a beam scatterer or by magnetic sweeping of the proton beam. All details about conformal therapy will be found in the paper by J.C. Rosenwald in these proceedings.

A second problem to be analysed is the use of a continuously isocentric beam transport system, called a gantry. In the first treatment facilities, there were no gantry. The beam is kept horizontal and the patient being seated on a rotating chair can be properly aligned. This is also the case for the Nice medical cyclotron (65 MeV) which started operation in 1992 (4). But the large medicaly dedicated accelerators, such as the 250 MeV synchrotron at Loma Linda (California) or the 200 MeV cyclotron at PSI Villigen (CH) or the CYCLONE 230 project of IBA are or will be equiped with an isocentric gantry. Such beam handling system are very large and heavy due to the magnetic rigidity of the high energy protons. The solution proposed by Jongen from IBA (5) is shown in Fig. 1. The 90° bending magnet can be rotated to sweep the beam in a plane perpendicular to the drawing plane, while the next to last magnet sweeps the beam in the plane of the figure, a similar gantry has been proposed by E. Pedroni at PSI. Another solution is the so-called "corkscrew gantry" designed at Loma Linda (6). Instead of being deflected in one plane the beam is first bent by 90° to be brought in a plane perpendicular to the beam axis. Then two 135° bends bring the beam focus to the isocentric point (Fig. 2). The last solution has the advantage to be twice lighter than the classical one, and also to need less building space allowing an easier floor design.

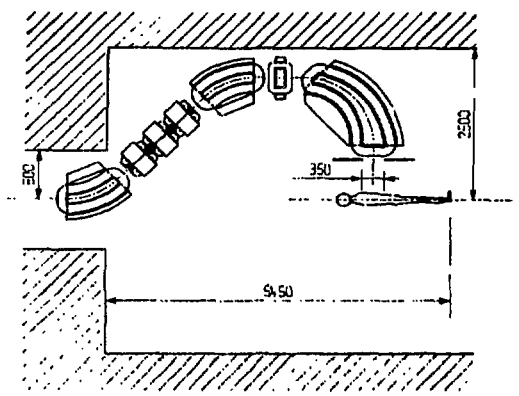

Fig. 1. IBA isocentric gantry scheme

Finally, there is a project for a 200 MeV isochronous superconducting cyclotron studied by H. Bloser and his collaborators to be installed at the Ontario Cancer Institute (7). The weight of this machine is such that it could be mounted on a gantry allowing isocentric irradiation in two treatment rooms. One may guess that in the near future medicaly dedicated cyclotrons with isocentric gantry will be installed around the world. To be complete, we must mention that apart from cyclotron or synchrotron based projects, a new type of proton linac has been proposed (see contributed paper by D. Tronc to this conference).

High energy neutrons are also used with some success for cancer therapy (see N. Breteau's contribution in these proceedings). To produce high energy neutrons one uses nuclear reaction such as d(t,n)α or (p,xn) and (d,xn). The neutron generator using the (t,n) reaction induced by deuterons produces nearly monoenergetic 14 MeV neutron beam, but the

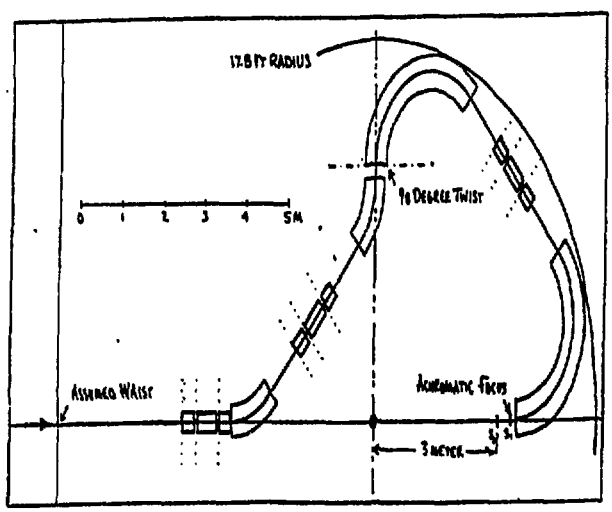

Fig.2. Developed view of the corkscrew gantry of Loma Linda

beam intensity is too low and treatment time are not realistic. So most neutron beam actually in operation are produced using Be targets irradiated with protons or deuterons. The neutron energy spectrum extends from zero to the particle energy and presents a maximum at about 1/3 of the proton energy or 1/2 of the deuteron energy. The proper proton energy for neutrontherapy is 65 to 70 MeV. The neutron beam intensity as well the exact shape of the energy spectra depends on the incident particle energy and target thickness. Then to be able to compare the biological effects of various neutron beams it is important to perform microdosimetric intercomparison studies of the different high energy neutron therapy beams (8).

A second problem with therapeutic neutron beams has to do with the beam collimator. As they have no electrical charge, neutrons have a very long range in matter. Neutron collimators are built with a complex assembly of iron and hydrogenated material, eventually loaded with boron to absorb neutrons. Then such collimators are very heavy, and cumbersome to manipulate. Additional absorbers are also needed to obtain the proper beam localisation on the patient. Multileaves iron collimators have been developped in particular at Louvain-la-Neuve. It simplifies the patient setting, but its mechanical complexity makes it sensitive to troubles. It must be pointed out that all neutron collimators are giving a larger halo around the neutron beam, than what is observed with photon or electron beams.

In the first neutron facilities then was only one fixed beam. To obtain the equivalent to a cyclotherapy one needs to rotate the patient in front of the beam. With a vertical beam, to assure the patient confort one is then limited to treatment of the body lower part. If an horizontal beam is available then the patient can be seated on a rotating chair. This is an inexpensive solution, compare to the use of an isocentric rotating gantry available in a few treatment rooms. A superconducting proton cyclotron has been built by H. Bloser and his group. It is mounted on an isocentric gantry for neutron beams.

In this short paper, we tried to summarize for proton and neutron-therapy the problems that must be solved to obtain beam with a good therapeutic officiency. Due to the lack of space, we dont give any detail about accelerators. We refer the interested readers to the proceeding of accelerator conferences, in particular the cyclotron's conference, of whom the last one met in Vancouver last july.

REFERENCES

(1) E. PEDRONI, to be published in Proc. of XIIIth Int. Conf. on cyclotrons and their applications, Vancouver 1992.

(2) P.H. FOWLER and D.H. PERKINS, Nature, 189 (1961), 524.

(3) E. PEDRONI, in Treatment planning for external beam therapy, G. Burger et al. Ed., (1981), 60.

(4) P. MANDRILLON et al., to be published in Proc. of XIIIth Int. Conf. of Cyclotrons and their Applications, Vancouver 1992.

(5) W. BEECKMAN et al., Nucl. Inst. and Meth. in Phys. Res., B56/57 (1991), 1201.

(6) R. PRECHTER, Science Appl. Int. Corp., Int. Report (May 12, 1987).

(7) H. BLOSER et al., Report MSUCL 760a, Michigan State University (1991).

(8) P. PIHET et al., 8th Cong. Rad. Research, Vol. 1 (1987), 61.

PARTICLE BEAMS FOR CONFORMAL THERAPY

J.C. ROSENWALD, A. MAZAL, R. BELSHI, D. PONVERT
Institut Curie Paris et
Centre de Protonthérapie d'Orsay

Conformal radiotherapy consists in giving a high homogeneous dose to a well defined target volume, following closely the shape of this volume while protecting all the surrounding tissues. It can be thought as the ultime refinement of conventional radiotherapy where basically the goal is the same, but the requirements in terms of geometrical accuracy and the technical efforts developped are not so high. Not all patients could be treated with conformal therapy for both economical and pratical reasons, but there is without doubt a number of them for which such an approach would be beneficial both to increase the probability of local tumor control and to reduce the risk of complications.

The achievement of conformal therapy implies a number of steps listed below :

- acquire anatomical and pathological data
- delineate volumes of interest
- define "optimal" dose distribution (prescription)
- define beam parameters used for optimization
- search the "best" technique (3D treatment planning)
- express this technique in patient coordinates
- check patient set-up relatively to the beams
- perform treatment with proper control of irradiation

ANATOMICAL DATA

Anatomical data are required to define the aim of irradiation in terms of target volume and organs at risk. The target volume normally encompasses the tumor volume and comprises a safety margin accounting for microscopic spread of the disease. In addition, the external shape of the body and the detailed description of the tissue inhomogeneities (shape, position, composition) are necessary to calculate the dose distribution within the patient. This anatomical description must be related to a system of coordinates consistent from the very begining of the procedure, to the treatment itself. It is therefore necessary to immobilize the patient using various devices such as casts or mechanical accessories.

For brain tumors an accurate solution consists in screwing in the skull a stereotactic frame used as reference as well for imaging as for beam set-up. Alternatively, anatomical or added metallic markers can be used.

The anatonomical data base most often consists of a series of parallel slices acquired on an X-ray computed tomography scanner (CT). In each of them, the structures of interest (target volume, organs at risk, markers...) must be carefully delineated allowing future reconstruction and dose calculation. It is very useful to combine several imaging modalities (such as CT and magnetic resonance imaging) to provide better identification of the tumor volume.

METHODS TO CONFORM DOSE TO TARGET VOLUME

. *longitudinal adjustment*

In the beam direction the problem is very different for conventional photon beams and for charged particle beams. In photon beams the interposition of any material in the beam path will result essentially in a modification of the dose rate. Conversely, in particle beams, the resulting effect is a change of energy giving full and flexible control of the maximum depth of penetration (particule range). Except for electrons, the sharp increase of dose in the so called Bragg peak region can be used to focus the dose on the desired region.

By "stacking" Bragg peaks of different energies one can produce a dose modulation over a given depth. Two possibilities exist (fig. 1).

a) Generate the same modulation over the whole target volume. In that case the modulation is chosen to cover the maximum thickness and there is an unwanted irradiation of some of the normal tissues located in the proximal vicinity of the target volume.

b) Generate a variable modulation according to the exact thickness of the target volume measured on each beam path through the target volume.

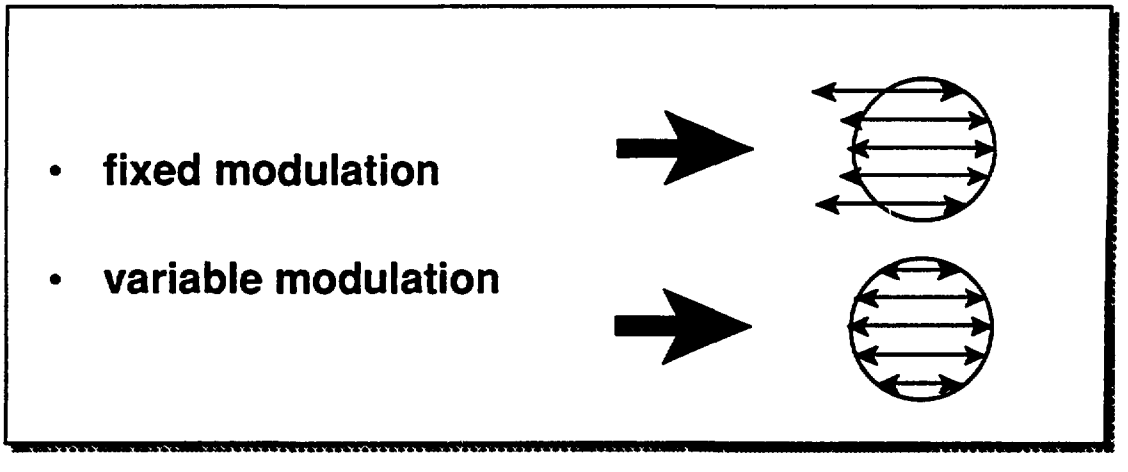

fig. 1
In fixed modulation the same spread out of the Bragg peak (SOBP) is applied over the whole target volume, while in variable modulation the SOBP differs according to the target thickness along the beam path.

In clinical practice, up to now, only fixed modulation is used by interposition in the beam of a "wheel" consisting of sectors of different thicknesses and weighted as to produce a uniform "biological" dose distribution along the required distance. 3D boluses shaped accordingly to the distal edge of the target volume and taking into account the external shape of the body and the internal inhomogeneities, are eventually added. It can also be thought of changing the particle energy by direct tuning of the accelerator on a pulse by pulse basis. This is theoretically possible when a synchrotron is used but is has still to be proven to be clinically feasible.

Variable modulation is only possible in conjunction with variable collimator and/or scanning technique, as will be discussed later.

. *Lateral adjustement*

Starting from a narrow pencil beam coming out of the accelerator, the charged particles must be spead over the cross section of the target volume. The simplest solution consists in using a high Z scatterer eventually shaped to produce a uniform dose density over a wide area.

Another solution consists in scanning the pencil beam whether continuously or pixel by pixel (Chu 1991, Pedroni 1991). In this case, one can produce on purpose an inhomogenous dose distribution by varying the sweeping speed or the dwelling time according to the location.

For "passive" conformation systems where there is no beam steering, an additional collimator is mandatory to limit the exposed area to the cross section of the target volume.

Multileaves collimators, such as used in photon beams, provide more flexibility to cover any shape with remote computerized control. If a scanning system is used, provided that the beam position is accurately monitored and that the spot size is small enough, a collimator is theoretically no longer necessary. In addition, a variable modulation in depth can be obtained by changing the lateral spread of the beam (shape of the cross section) for each Bragg peak depth (energy) sequentially selected.

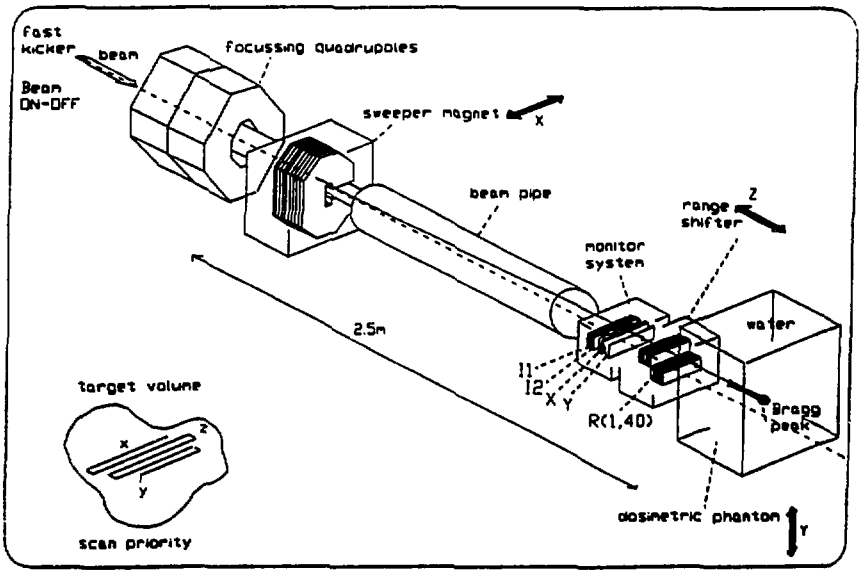

Fig. 2 Example of pixel by pixel scanning technique : project developped at PSI (Pedroni 1991)

An example of such a 3D conformal system presently under investigation is shown on fig. 2. A summary of the main characteristics of the different methods for dose conformation appears in table I.

	scattering	continuous spot scan	discrete spot scan
variable SOBP modulation	no	with variable collimator	yes
control of dose density	no	variable speed	variable dwelling time
additional collimation	mandatory	recommended	optional ?
flexibility	± (many accessories)	yes	yes
treatment time	no dead time	small dead time ?	larger dead time
required beam monitoring	total particle fluence	local particle fluence	position + dose
sensitivity to instability			
of beam energy	yes	yes	yes
of dose rate	no	high	no if good control
of beam position	±	±	?
of patient position	small	average	yes
simplicity	yes	±	no
reliability	good	±	?
cost	low	average	high

Table I

. *Combination of multiple beams*

It must be realized that the dose to skin and to healthy tissue located on the beam path is far from being negligible, which presents a serious limitation to the use of single beams.

Therefore a combination of several beams, penetrating through different ports is often necessary. Isocentric techniques with continuous irradiation while rotating the beam around the patient as practiced in photon therapy could be of some interest. But the technical difficulties and the cost of such an installation, even for protontherapy, makes it difficult to implement in the near future.

TREATMENT PLANNING

The choice fo the "best" technique for a given patient results from an interactive process conducted on a computer console and referred to as treatment planning.

A 3D dose calculation model is used in this process which must be fast and realistic. Most of the algorithms clinically used are based on an analytical description of the dose distribution with more or less refined corrections for inhomogneities. In general multiple scatter is ignored and further efforts should be made to improve the accuracy of these models.

After application of the calculation to the anatomical data, the treatment planning systems display the dose distributions in different cross sections of the patient. In addition, informations such as dose volume histogram within specific organs can be useful to assess the quality of the proposed treatment and to correct the beam parameters (direction, weight, shape...) until the result is considered satisfactory.

The systems presently in use in conjunction with charged particle therapy are generally able to automatically design the beam modifiers (range shifter, bolus, collimator) to be chosen for a given target volume and a given beam incidence.

However, algorithms allowing automatic optimization of voxel by voxel scanning techniques are being developped, starting from a desired dose distribution and proposing the optimal weight at each voxel for a given beam configuration (Brahme 1989).

TREATMENT

The treatment itself requires careful beam set-up with proper machine adjustment, positionning of beam modifiers and systematic quality control before each session. The patient is then immobilized and placed in proper position relatively to the beam using the coordinates defined during treatment planning.

A radiological check is performed and the patient position is iteratively adjusted until it is consistent with digitally reconstructed radiographs generated from treatment planning.

Only then, the irradiation can start with proper beam steering, independent and redundant beam monitoring and permanent control of patients movements.

CONCLUSION

It is recognized that for local cancer treatment, significant improvement is expected from conformal therapy. Charged particle beams are particularly well suited for this purpose provided that major effort and time are dedicated to any single patient.
Technology is progressing rapidly and sophisticated ways of beam shaping are being devised. However, before applying them to clinical practice all sources of uncertainties must be precisely identified and quantified. Overall, it should be remembered that safety is more important than accurate conformation.

References :

- *Brahme A., Källman P. and Lind B.K.*
  Optimization of proton and heavy ion therapy using an adaptative inversion algorithm. Radioth. and Oncol. 15, 189 - 197 (1989).

- *Pedroni E., Blattman H., Böhringer T., Coray A., Lin S., Scheib S., Schneider U.*
  Voxel Scanning for protontherapy in Proceedings of the NIRS International Workshop on Heavy charged Particle Therapy p. 94 - 109 Chiba, Japan, July 1991.

- *Chu W.T., Ludewight B.A., Marks K.M., Nymon M.A., Renner T.M., Singh R.P. and Strodner R.*
  Three dimensional conformal therapy using light ion beams in proceedings of the NIRS International Workshop on Heavy Charged Particle Therapy p. 110 - 123 Chiba, Japon, July 1991

POSITRON EMISSION TOMOGRAPHY FOR DOSE LOCALIZATION AND BEAM MONITORING IN LIGHT ION TUMOUR THERAPY

W. Enghardt, W.D. Fromm, P. Manfraß, J. Pawelke, M. Sobiella
FZ Rossendorf, PF 19, DO-8051 Dresden, Federal Republic of Germany
H. Geissel, H. Keller, G. Kraft, A. Magel, G. Münzenberg,
F. Nickel, D. Schardt, C. Scheidenberger
GSI Darmstadt, PF 110552, D-6100 Darmstadt, Federal Republic of Germany

In-vivo measurements of the ranges of β^+-radioactive beams by means of positron emission tomography (PET) is regarded as an essential component for treatment plan verification in a future light ion therapy [1,2]. For this purpose suitable positron camera systems that considerably differ from those applied in nuclear medicine have to be developed and tested at accelerator beams. A positron camera of two high-density avalanche chambers [3] with a sensitive area of $50 \times 28\,\mathrm{cm}^2$ was installed at the beam line behind the fragment separator FRS [4] of the Gesellschaft für Schwerionenforschung (GSI) in Darmstadt.
Beams of β^+-radioactive ions were obtained from projectile fragmentation of ^{20}Ne primary particles ($E = 500\,\mathrm{MeV/u}$) in a $4\,\mathrm{g\,cm^{-2}}$ Be target and subsequent in-flight separation in the FRS. The radioactive beams of $1 \ldots 5 \times 10^5$ particles/spill containing ^{19}Ne as the main component (fig. 1) were implanted into phantoms of plastic or water placed in the camera field of view. The beam pulse repetition time was 3.5 s, the spill length amounted to 0.5 s. In order to detect the short lived positron emitters as e.g. ^{19}Ne with $T_{1/2} = 17.2\,\mathrm{s}$ with high efficiency, the annihilation events were recorded in list mode between the beam pulses. Longitudinal tomograms [5] were constructed from these data by backprojection and iterative reconstruction [6] in a three-dimensional image space of 33 × 33 × 33 voxels.

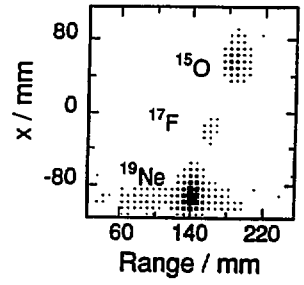

Fig. 1: Components of the β^+-active beam behind the fragment separator. The tomogram displayed represents a 2 cm thick slice through the plastic phantom containing the beam axis. The lateral beam position is denoted by x.

By this technique several tomograms of the range distributions of implanted radioactive beams have been taken. As an example we show in fig. 2 the range distribution of a monoenergetic ^{19}Ne beam in a plastic phantom, where minor density variations can be clearly resolved.

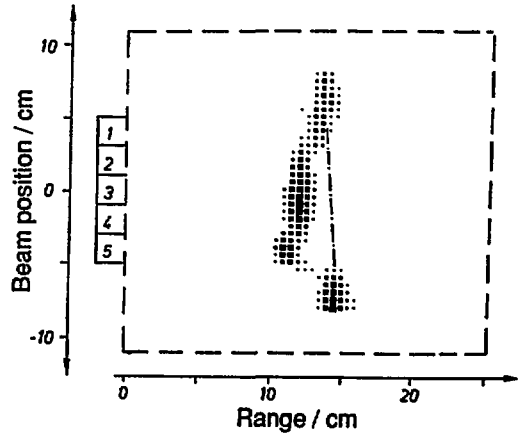

Fig. 2: Positron emitter distribution in a plastic phantom (dashed line) generated by irradiation with a monoenergetic ^{19}Ne beam (E = 406 MeV/u). Small density deviations have been simulated by mounting five pieces (2 cm thick) of different materials in front of the phantom:
1 - balsa wood, $\rho = 0.22\,\mathrm{g\,cm^{-3}}$;
2 - PE, $\rho = 0.92\,\mathrm{g\,cm^{-3}}$;
3 - PMMA, $\rho = 1.18\,\mathrm{g\,cm^{-3}}$;
4 - PVC, $\rho = 1.40\,\mathrm{g\,cm^{-3}}$;
5 - PTFE, $\rho = 2.20\,\mathrm{g\,cm^{-3}}$.
The dashed-dotted reference line has been measured without the extra material.

In real therapy such range measurements using a β^+-active beam for treatment plan verification and adjusting the therapy beam parameters should be done with low doses of radiation. Therefore, it is desirable to measure the ranges from a low number of annihilation events. Fig. 3 shows that for a beam of ^{19}Ne the centroid of the range distribution can be rather precisely calculated from several hundreds of registered annihilation events.

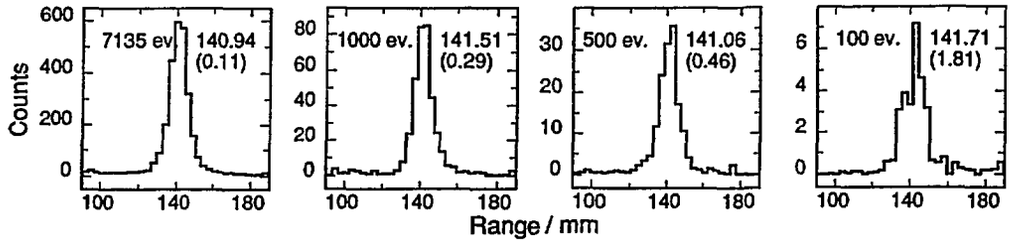

Fig. 3: Comparison of the ranges of a ^{19}Ne beam (E = 406 MeV/u, width: 26.9 mm FWHM) deduced from tomographic slices of 2 cm thickness which have been reconstructed from different numbers of annihilation events. The graphs have been obtained by projecting the tomograms onto the range axes. The mean ranges calculated by a Gaussian fit are given in mm with the errors in parantheses.

In a further experiment we took tomograms of the spatial β^+-activity distribution generated by stopping ions of 406 MeV/u (10^8 particles/spill) of the stable nucleus ^{20}Ne in a plastic block. This distribution (fig. 4) shows a pronounced maximum close to the range of the primary beam particles that has been calculated using the stopping power code of [7]. The radioactivity distribution is composed from several β^+-emitters with atomic masses $A < 20$ produced by projectile and target fragmentation. The shape of the distribution can be qualitatively understood from a simple Monte Carlo approach of the stopping, fragmentation and decay processes [8]. These results offer the possibility of beam monitoring and control by means of PET techniques during the tumour therapy.

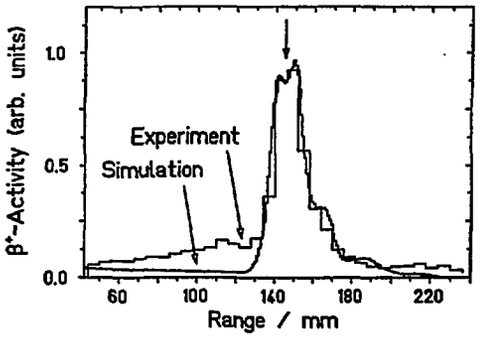

Fig. 4: Measured and calculated distributions of positron emitters in a plastic block induced by a ^{20}Ne beam of 406 MeV/u. The activation time was 5 min. The flat part of the spectrum at low ranges results from target fragmentation. Projectile fragmentation causes the peak involving β^+-activity from Ne, F and O and a long range tail of N and C isotopes. The calculated range of the primary ^{20}Ne ions is indicated by an arrow.

This work is supported by the "Bundesministerium für Forschung und Technologie" of the Federal Republic of Germany (grant 06DR102 3).

References

[1] J. Llacer, Nucl. Sci. Appl. **3** (1988) 111
[2] W. Enghardt et al., Phys. Med. Biol. **37** (1992) 791
[3] P. Manfraß et al., Nucl. Instr. Meth. **A273** (1988) 904
[4] H. Geissel et al., Preprint **GSI-91-46**, GSI Darmstadt, 1991
[5] L.T. Chang et al., IEEE Trans. Nucl. Sci. **NS-23** (1976) 568
[6] W. Enghardt, Physica Medica **VII** (1991) 119
[7] Th. Schwab, Report **GSI-91-10**, GSI Darmstadt, 1991
[8] W. Enghardt et al., Preprint **FZR-92-01**, FZ Rossendorf, 1992

CALCULATIONS OF CROSS SECTIONS AND DEPTH-DOSE DISTRIBUTIONS WHEN USING HEAVY ION BEAMS

L. Sihver and T. Kanai

NIRS, Division of Accelerator Research
Chiba-shi, Inage-ku, Anagawa 4-9-1
Chiba 263 Japan

The use of heavy ions, as compared to conventional radiation techniques, is expected to result in significant advantages in therapeutic and diagnostic medicine (ex. Heavy Ion CT). The heavy ions are, among other things, expected to be very effective in treating deep tumors located near vital structures.

The properties of charged-particle beams are affected by their interaction with matter to a grater degree than those of other types of radiation. When using heavy ions for medical treatments it is therefore essential to understand the behavior of these ions in human tissues. To calculate the total depth-dose distributions in a medium, the energy loss (dE/dx) and the range of a specific fragment in the medium must be known. We have therefore developed a computer code for calculating the stopping power (dE/dx) and range distributions for protons and heavy ions in any media[1]*. Our calculations is in good agreement with the best previous calculations for incident energies ≥ 1 MeV/nucleon.*

It is also very important to know how the nuclear interactions contribute to the depth-dose distributions. Sometimes when a heavy ion beam impinges upon a target, the collision results in nuclear fragmentation. Depending on impact parameters, these events are characterized as projectile and/or target fragmentation. On the one hand, the target fragments are large, high Z fragments, which carry little momentum. These fragments might have biological effects, but as they have a small effect on the dose distributions, we assume we can neglect the effect from these fragments. On the other hand, the projectile fragments loose very little momentum and travel nearly in the beam direction with relatively minor deflection. These latter fragments generally have lower charge than the incident beam, i.e. their stopping power is less than that of the primary beam. Therefore, they lower the average ionization relative to that of the incident beam, and they will make up a "tail" which extends beyond the stopping region of the primary beam (i.e. beyond the Bragg Peak).

To calculate how much these "secondary" fragments contribute to the dose distributions, one must know their partial cross sections. To do that, we have constructed a procedure for calculating the partial nucleus-nucleus cross sections[1,2]*, by scaling the semiempirical proton-nucleus partial cross section systematics. The scaling is done by a scaling parameter, which is based on a Bradt-Peters-type*[3] *law and takes advantage of the weak-factorization property*[4] *of projectile fragments. All products from the Z of the projectile down to Z=2 can be calculated with our procedure. The agreement between the calculated partial cross sections and the experimental data is better than all earlier published results. Figure 1 show the calculated partial nucleus-*

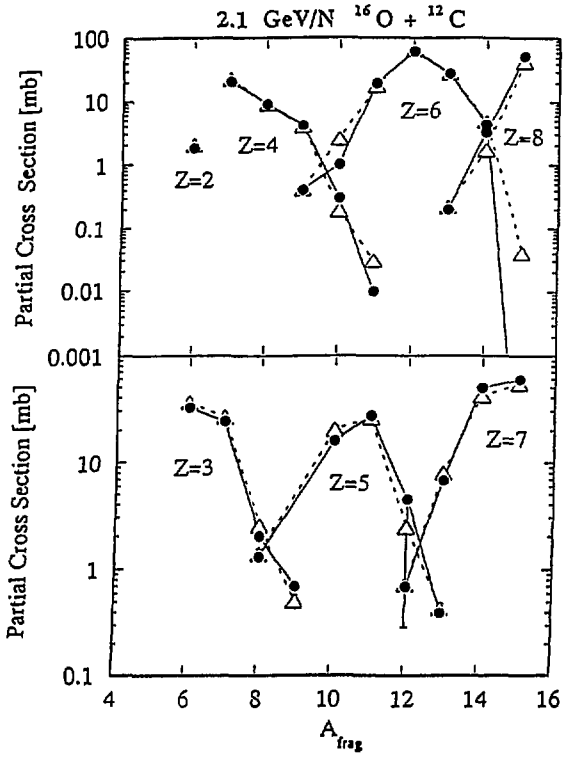

Figure 1.

nucleus cross sections (filled circles) for the reaction of 2.1 GeV/nucleon ^{16}O with ^{12}C, together with the experimental data [4] (open triangles) as an typical example.

To calculate the beam attenuation, we have also developed semiempirical total reaction cross section formulas for proton-nucleus (nucleus-hydrogen) and nucleus-nucleus reactions [1,2]. The formulas are applicable for incident energies from 10 MeV, and 100 MeV/nucleon respectively. The proton-nucleus formula is applicable for targets with $Z_t \leq 26$, and the nucleus-nucleus formula for projectiles and targets with $Z_{p,t} \leq 26$. The agreement between our calculated cross sections and the experimental data is much better than all earlier published semiempirical calculations. The calculated σ_R, together with experimental data [5], for the reactions of protons with Be, B, C and Al.

In our model to calculate the depth-dose distributions for heavy ions, we include range straggling for the primary particles, but not for the secondary and the tertiary particles, as a first approximation.

The first 400 MeV/N ^{20}Ne beams was delivered by SIS at GSI (Germany) recently and the first measurements of the fragmentation of this beam in water was done [6]. The measured mean free path was 163 ± 8 mm. We have calculated this mean free path, using our reaction cross section formulas. Our calculated value is 163 mm, i.e in total agreement with the experimental value.

REFERENCES

1. *L. Sihver and T. Kanai, NIRS-M-87, HIMAC-002, July 1992.*
2. *L. Sihver et al., Phys. Rev C (submitted).*
3. *H.L. Bradt and Peters, Phys. Rev. 77, 54 (1950).*
4. *D.L. Olson et al., Phys. Rev. C28, 1602 (1983).*
5. *W. Bauhoff, Atomic. ta and Nucl. Data Tables 35, 447 (1986).*
6. *I. Schall et al., GSI Scientific report 1991, p. 306.*

PRESENT STATUS OF HIMAC

T. Kohno, H. Ogawa, S. Yamada, Y. Sato, T. Yamada, T. Murakami, A. Kitagawa, J. Yoshizawa, K. Sato, A. Itano, M. Kumada, E. Takada, M. Kanazawa, K. Noda, K. Kawachi, F. Soga, M. Endo, T. Kanai, S. Minohara, M. Sudou, H. Koyama-Ito and Y. Hirao

Division of Accelerator Research,
National Institute of Radiological Sciences,
4-9-1 Anagawa, Inage-ku, Chiba-shi, Chiba 263, Japan

Introduction

HIMAC is a heavy ion accelerator complex dedicated to medical use, especially clinical treatments of tumors. It comprises two ion sources, an RFQ linac, an Alvarez linac, two synchrotron rings, a high-energy beam transport(HEBT) system and an irradiation system. The ion species required for the clinical treatments range from ^{4}He to ^{40}Ar and the maximum energy of 800 MeV/u is determined so that silicon ions have a range of about 30 cm in the soft-tissue of a human body. The beam intensity from the synchrotron is determined to satisfy the requirements for a dose rate of 5 Gy/min in order to permit completion of one fractional treatment within one minute. This paper describes an outline of HIMAC and its present status. The general descriptions have already been given in other articles[1]-[5].

Outline of HIMAC

The injector system comprises a PIG source for light ions, an ECR source for heavier ions, an RFQ linac of 100 MHz and an Alvarez linac with the same frequency. The ion sources are put on the high voltage platforms for the injection to the RFQ linac and heavy ions are accelerated up to 6 MeV/u through both linacs. A debuncher cavity will be installed in an output beam transport line in order to reduce a momentum spread. Both linacs accept heavy ions with a charge-to-mass ratio as small as 1/7, and only one charge stripper is installed at the end of the Alvarez linac to raise the charge-to-mass ratio to a value higher than 1/4. An experimental room is prepared to use the beams from the injector system directly.

The synchrotron system has a pair of separated function type synchrotron rings with a strong FODO focusing structure. They are installed on upper and lower floors and operated independently except that the magnets of these rings are excited 180 degrees out of phase each other. The output energy of each ring is designed to be variable in a range from 100 to 800 MeV/u for ions with q/A=1/2. The circumference of the ring is 129.6 m and the maximum magnetic rigidity is 9.75 Tm. The repetition rate is in a range of 0.3-1.5 Hz depending on extraction energies of the rings. Each ring has a slow extraction system connected to the HEBT system, and a fast extraction system can also be installed in the upper ring in the future. The fast beam will be used for experiments or for injection to the lower ring which is possible to operate under a two stage acceleration mode or a storage ring mode.

The HEBT system consists of a horizontal and a vertical beam line. The horizontal line transports the beam up to 800 MeV/u from the lower ring to two treatment rooms(B, C) and two experimental rooms(Physics, Secondary Beam). The vertical line is designed to guide the beam up to 600 MeV/u from the upper ring and that from the lower ring through a junction beam line to two treatment rooms(A, B) and one experimental room(Biology). Therefore we can irradiate

a patient by the horizontal and the vertical beam simultaneously in the treatment room B. The beam should be switched within about 5 minutes from one treatment course to the other by only adjusting the current of a switching magnet in order to use the beam efficiently. The beam position must be reproduced within +/- 2.5 mm after the beam switching.

The irradiation system of each treatment room has a pair of scanning magnets(wobbler magnets), a beam scatterer, a range shifter, a ridge filter, a multileaf collimator and several beam monitoring devices. The uniform intensity distribution is generated by the combination of the scatterer and the scanning magnets. The maximum field size of 22 cm in diameter and the uniformity within +/- 2 % inside the field are required at the position of irradiation. The fine tune of the range is done by inserting the range shifter in the beam axis. The ridge filter spreads the narrow Bragg peak according to the thickness of a tumor.

Present Status

The beam tests of the PIG and the ECR source were finished with satisfactory results. The requirements for the beam intensities were fully met for all ion species. The tuning of the RFQ linac and the high power tests of the Alvarez linac at Niihama Works of Sumitomo Heavy Industries, Ltd. showed good performance of these devices. All components were carried in the HIMAC building in March, and the setting and the alignment of them have been completed. The wiring work is now under way and the beam test of the injector system is expected to start in the spring of 1993.

In the synchrotron system, the magnetic field distributions of dipole magnets were measured and the values of the integrated field strength were adjusted among the magnets by using detachable pole end pieces. The tests of power supplies for the dipole and the quadrupole magnets of the rings are now in progress at Hitachi Works of Hitachi, Ltd. In the high power test of an rf acceleration system, an rf frequency was swept successfully in 0.7 sec from 1 to 8 MHz with an acceleration voltage of 9 kV. The installation of the major part of the synchrotron system will be started in the middle of October.

Most of the magnets of the HEBT system have been fabricated and some of them have already been carried in the HIMAC building and roughly set. Power supplies are being carried in just now. The alignment of the horizontal line will be finished by the end of November.

In the irradiation system, the design work of the components has almost been completed. The scanning magnets and the scatterer have already been fabricated. The other devices are now under fabrication favorably.

The beam tests of the synchrotron, the HEBT and the irradiation system are scheduled during 1993.

References

[1] Y. Hirao *et al.*, Proc. 2nd European Accelerator Conference, Nice, France, 1990, p.280.
[2] S. Yamada *et al.*, Proc. 8th Symp. Accel. Sci. Technol., RIKEN, Saitama, Japan, 1991, p.28.
[3] K. Sato *et al.*, Proc. 8th Symp. Accel. Sci. Technol., RIKEN, Saitama, Japan, 1991, p.31.
[4] K. Noda *et al.*, Proc. 13th Int. Conf. on Cyclotron and their Applications, Vancouver, Canada, 1992(to be published).
[5] T. Kohno *et al.*, Proc. Int. Conf. on Accelerator and Large Experimental Physics Control Systems, Tsukuba, Japan, 1991(to be published).

WHAT IS THE BEST PARTICLE FOR THE HEAVY ION RADIATION THERAPY?

T.Kanai, L.Sihver and K.Kawachi

Division of Accelerator Research,
National Institute of Radiological Sciences,
4-9-1, Anagawa, Inage-ku, Chiba-shi, CHIBA 263 JAPAN

Heavy ion therapy is expected to be superior to the conventional radiation therapy using high energy photon because of their excellent dose localization and high LET effects of the biological responses. At NIRS in JAPAN, the heavy ion therapy using from He to Ar beams will start in 1994. In order to perform the heavy ion radiation therapy, it is necessary to have a guide line to choose appropriate heavy ion beams for the various situations of the radiation therapy. We understand that it is very difficult to deduce a clear conclusion on this issue. However, we think that scientific approach to establish this guide line is required and is very important even it has some assumptions. This paper presents only preliminary results in the way of establishing the guide line.

To compare the therapeutic gain of the heavy ions, it is firstly required to derive physical characteristics of heavy ion beams. Semi-empirical formula for total nuclear reaction cross sections and fragmentation production cross sections were developed, which is presented in different papers[1),2),3)]. Based on these formula, we calculated depth dose distribution of high energy heavy ions in water including fragmentation effects[3)]. In this calculation, dose contributed from primary heavy ions, secondary fragmented nuclei produced by the primary ions, and tertiary fragmented nuclei which is produced by the secondary fragments are all included. Fluence distribution and dose average LET distribution of the primary beam and the fragmented nuclei can be obtained by this calculation. Preliminary results of the dose distribution and the dose average LET distribution were obtained. There are very limited experimental data concerning this kind of fluence and LET distribution except relative ionization distribution. The comparison of the calculated results and the experimental results are not completed yet.

In order to deduce the therapeutic gain of the various heavy ions, we started the investigation from obtaining a cell response curve for various LET heavy ion beams. We choose V79 cell line for estimating the universal biological response for the heavy ions. Experimental data of the survival curves of V79 cells for different LET values were fitted to the linear quadratic model. LET dependence of the coefficients, α and β, are then obtained from the experimental data by an eye fitting. LET dependence of OER is also necessary for the calculation of the therapeutic gain of the heavy ions. OER of V79 cells as a function of LET was obtained from the experimental data by an eye fitting.

From the above physical and biological data for heavy ion beams, we can estimate survival fractions of V79 cells for any mono-energetic heavy ion beams whether they are in a aerobic or hypoxic condition. In order to simulate biological responses at therapy conditions, we made various kind of spread Bragg peaks for various heavy ion beams. In order to estimate survival curve or RBE for the ridge filter beams, we assumed the RBE for the mixed beam is dose average RBE of the original beams as follows[4)];

$$(RBE)_{mix} = f_1(RBE)_1 + f_2(RBE)_2$$

where $f_i = d_i / D$; dose fraction of i-th radiation

OER for the mixed beam was also calculated according to Lam theory.

Assuming these relation, we designed spread Bragg peaks for helium, carbon and neon beams. In this spread Bragg peak designing, we tried so that dose multiplied by RBE(biological dose) in the spread peak is uniform. We also calculated OER distributions of the spread Bragg peaks. Biological dose and OER distributions were calculated for 27 cases of spread Bragg peaks, which are combinations of 3 types of heavy ions(He, C, Ne), 3 different energies (ranges are 10, 15 and 20 cm in water) and 3 different width of spread Bragg peaks(3, 6, and 9 cm). Fig. 1 shows the results of the biological dose and OER distributions in case of 15 cm range beams.

To compare the figure of merit of the various heavy ion beams, we defined a therapeutic gain factor as $\{\text{dose x (RBE)}\}_{\text{spread peak}} / \{\text{dose x (RBE)}\}_{\text{entrance}} / (\text{OER})_{\text{spread peak}}$. As shown in Fig. 1, the value of (OER) is not uniform in the spread Bragg peak. we took the $(\text{OER})_{\text{spread peak}}$ as the highest value of (OER) in the spread Bragg peak. This factor represents therapeutic gain when the irradiation is performed by a single port and all target cells are in hypoxic condition. In this limited comparison of therapeutic gain between helium, carbon and neon beams, carbon had a best score.

As discussed in this paper, we had preliminary conclusion that carbon is the best particle for the heavy ion radiation therapy although the difference between the three ions is very small. In this derivation of the conclusion, following considerations are lack;

1) Multiple scattering of the charged particles in human body was neglected, which becomes important when protons are included in the comparison.
2) When multi-port irradiation technique is applied, a different conclusion may be derived.
3) RBE of higher survival level should be analyzed.
4) Fractions of hypoxic cells in the target volume should be varied.

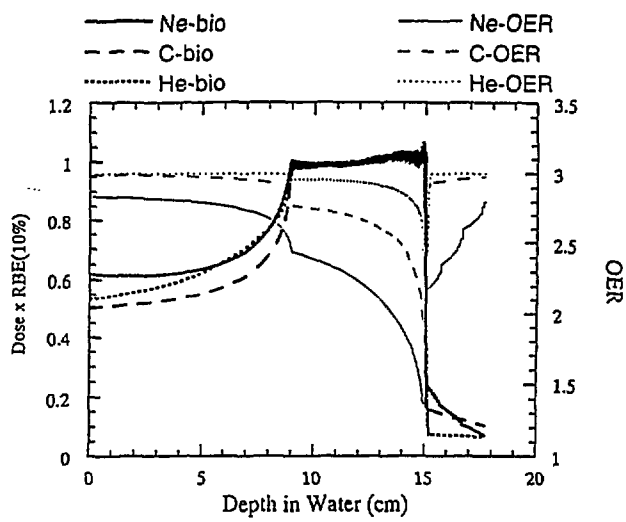

Then, in order to derive more certain conclusions, we have to simulate many cases which are more realistic of heavy ion radiation therapies. At present, we barely have had tools to investigate these simulation to obtain the therapeutic gain factor.

References

1) L.Sihver and T.Kanai, NIRS report, HIMAC-002.
2) L.Sihver et al., submitted to Phys. Rev. C.
3) L.Sihver and T.Kanai, BARN92
4) G.K.Y.Lam, Radiat. Res. 110, 232 (1987).

SPATIAL ASPECTS OF LIGHT IONS TRACKS

V. Michalik

Institute of Radiation Dosimetry, Prague, Czechoslovakia

In radiation biology as well as in radiation dosimetry the knowledge of radiation track structure is very important. It seems that from the biophysical and biological point of view the decisive is energy deposition in the nanometer regions of particle tracks together with the formation of energy deposition clusters in these regions[1]. The radiation track structure was simulated by the Monte Carlo code TRION[2] and further analyzed by the method described in detail elsewhere[3]. This method allows partitioning of ionizations formed along particle track into clusters of a given size, where cluster size determines the maximum allowed distance between any of two ionizations belonging to the same cluster. The mean absolute frequency of clusters of a given size, containing a given number of ionizations, produced by a radiation per unit of deposited energy can be computed from a sufficient number of particle tracks and can be considered as a characteristic of radiation reflecting its ability to form energy deposition clusters. A detailed discussion of their properties can be found elsewhere[4].

Double strand break (dsb) is considered to be one of the most important lesions in radiation biology. Based both on the experimental and theoretical data it is reasonable to suppose that dsb can be correlated with the formation of energy deposition clusters[5]. Provided threshold model for dsb induction constraints on cluster sizes and thresholds were derived[4]. It can be concluded that clusters containing at least 3 to 6 ionizations localized in sites with 1 to 4 nm diameter, respectively, can be correlated with the dsb induction.

It has been shown in recent years that different particles with comparable LET yields similar RBE's for dsb induction but different ones for cellular endpoints such as survival and mutation[6]. This indicates that dsb's produced by different track structures are not equivalent and/or their spatial distributions are different. If dsb's can be correlated with the energy deposition clusters then the spatial distribution of dsb's should in some way reflect the spatial distribution of these clusters. Therefore the distance distributions for energy deposition clusters of sizes and thresholds corresponding to the dsb induction were investigated[6].

The most interesting is the case of two particles with the same LET. Protons (0.7 MeV/amu) and alpha particles (5 MeV/amu) with comparable LET about 30 keV/μm have been compared. In the case considered there are not great differences between alphas and protons in respect to the formation of clusters with the size and orders corresponding to the dsb induction. Their absolute yields show that protons are a little more efficient then alphas, the ratio of yields is about 1.2-1.4. The distance distributions have been compared for all four "permitted" combinations of cluster

sizes and thresholds. It can be concluded that protons are more efficient then alphas in the production of clusters correlated at small distances < 100 nm by a factor ranging from 1.4 to 1.8.

If two dsb's produced sufficiently close together in chromatin are required for particular final effect then cluster analysis of track structure indicates that low energy ions with higher ionization density should be very effective in producing such final effect. In case of two particles with the same LET the particle with a smaller charge should be more effective than the particle with a greater charge, in spite of the fact that initial dsb's are produced with similar yields. The results obtained correspond very well to the data of Belli et al.[7] showing that for V79 cell inactivation and mutation induction protons of 20 keV/μm are more effective than alpha particles of the same LET by a factor ranging from 1.4 to 2.0.

REFERENCES

1. Goodhead, D.T. *The initial physical damage produced by ionizing radiations.* Int.J.Radiat.Biol. 56 623-634 (1989)
2. Lappa, A.V., Bigildeev, E.A., Vasilev, O.N., and Burmistrov, D.S. *TRION code for radiation action calculations and its application in microdosimetry and radiobiology.* Radiat.Environm.Biophys. in press, (1992)
3. Michalik, V. *Particle track structure and its correlation with radiobiological endpoint.* Phys.Med. Biol. 36 1001-1012 (1991)
4. Michalik, V. *Energy deposition clusters in nanometer regions of charged particle tracks.* Radiat.Res., submitted, (1992)
5. Ward, J.F. *DNA damage produced by ionizing radiation in mammalian cells: Identities, mechanisms of formation and reparability.* Prog.Nucl.Acid Res.Mol.Biol. 35 95-125 (1988)
6. Michalik, V. *Distance distributions for energy deposition clusters in different particle tracks.* Radiat.Prot.Dosim. (1992) in press
7. Belli M., Cera F., Cherubini F., Goodhead D.T., Ianzini F., Jenner T.I., Moschini G., Nikjoo H., Sapora O., Simone G., Stevens D.L., Stretch A., Taboccini M.A. a Tiveron P. *Relevance of experiments with different charged particles having the same LET for biophysical modelling of radiation effects.* in Biophysical Modelling of Radiation Effects, (ed. K.H.Chadwick, G.Moschini and M.N.Varma), pp.285-292 (1992)

DEVELOPMENT OF A MONTE CARLO CODE FOR THE SIMULATION OF THERAPEUTIC PROTON BEAMS

Joakim MEDIN and Pedro ANDREO
Department of Radiation Physics, Karolinska Institute and University of Stockholm, P O Box 60211, 104 01 Stockholm, Sweden

In radiation therapy the knowledge of the precise absorbed dose is of great importance since both, dose-response curve for tumours and dose-complication curve for normal tissues may be steep. In this context accurate dosimetry plays an essential role. Monte Carlo calculations have been extensively used in the development of electron and photon dosimetry. Physical constants, parameters and correction factors have been calculated with the method and are in clinical use today for therapeutic beams. For the dosimetry of heavy charged particles the development has however not followed a parallel trend, and it is recognized that there are insufficient basic data available on physical constants to ensure the desired accuracy in the dosimetry of therapeutic beams [1].
In order to improve the present status of the dosimetry for therapeutic proton beams a Monte Carlo code is under development. The code differs from existing Monte Carlo codes for proton transport at therapeutic energies in a number of aspects, the most important being the production of secondary electrons along the proton-track and the low cut-off energy for the transport of protons. Secondary electrons may play an important role in describing boundary effects between different materials and in simulating response of ionization-chambers in proton dosimetry. Despite of their low energy they can cross the air volume of an ionization chamber and therefore change the amount of energy assumed to be deposited in the chamber cavity [2].
The Monte Carlo code under development, PETRA, is a Class-II type MC code [3], where single proton-electron collisions yielding energy losses greater than a given cut-off are considered individually. This is achieved with the sampling from the Bahba cross section between the cut-off energy and the maximum possible energy transfer in a single proton-electron collision, which implicitly considers energy straggling with great accuracy in that energy region. Below the cut-off energy for inelastic processes, restricted collision stopping-powers, based on unrestricted collision stopping-powers from a forthcoming ICRU report [4], are used to calculate the *csda* energy loss. The method avoids the use of approximate energy straggling-distributions, although at the cost of very long computation times due to the relatively small fraction of energy lost in single collisions. Work is under development to implement additional energy-straggling sampling below the cut-off energy to enable larger step-lengths (energy losses) in calculations where accuracy requirements can be relaxed.
Proton scattering angles after a randomly selected pathlength are sampled from the full Molière's distribution, including Fano's correction factor for the scattering by atomic electrons. It has been found that for very short path-lengths, as those occurring in MC sampling, the braking-down of Molière's multiple scattering theory occurs. This makes the sampling of the polar angle questionable in numerous steps of existing electron and photon Monte Carlo simulations, where the validity of the theory is pushed down to one or to $\underline{e}$ collisions [5]. The limits of the theory that yield a "mathematically homogeneous" distribution have been investigated, taking into account the influence of using a large number of terms in the Molière's series (up to 7). A limit between B=3.4-3.7 (about 10 collisions) has been found, depending on the number of terms, which mathematically allows using the theory for smaller step-lengths than what the strict use of Moliere's

B_{min}=4.5 dictates, but is considerably larger than the limit currently used in some MC codes [5]. Below this limit, and to avoid "Molière's wiggles", only the Gaussian term is used, which coincides with the method used in the ETRAN MC code [6] for short electron paths in front of a boundary. Although the physics dictates the more accurate sampling from single scattering angular distributions, or the use of a few scattering formalism, this possibility might be considered in a later stage.

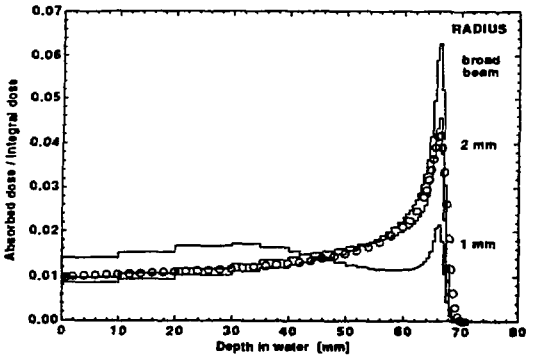

Fig. 1. Monte Carlo calculated depth-dose distributions for proton beams of 92 MeV having different radii (histograms). Circles are experimental data for a nominal 100 MeV beam incident on a Pb/brass double scattering foil [Grusell and Montelius priv. comm.].

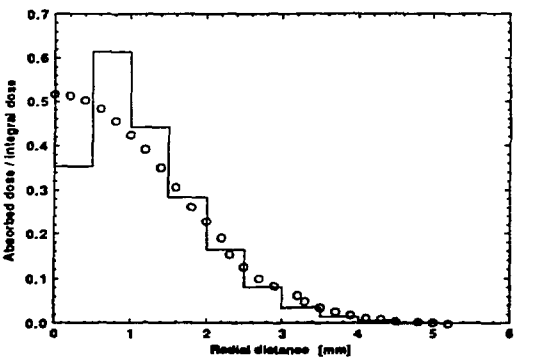

Fig. 2. Monte Carlo calculated radial dose profiles at 65 mm depth in water for a 92 MeV proton pencil beam (histogram). Circles are experimental data for the same beam as in fig. 1 .

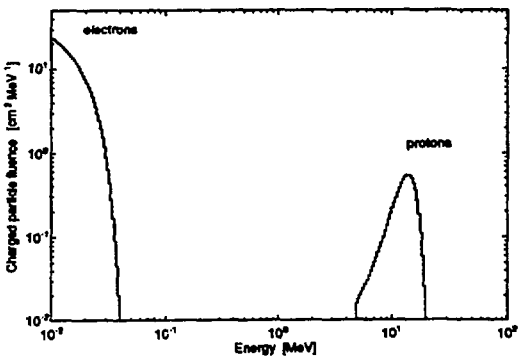

Fig. 3. Monte Carlo calculated proton and electron fluence, differential in energy, at 65 mm depth in water for a 92 MeV proton pencil beam.

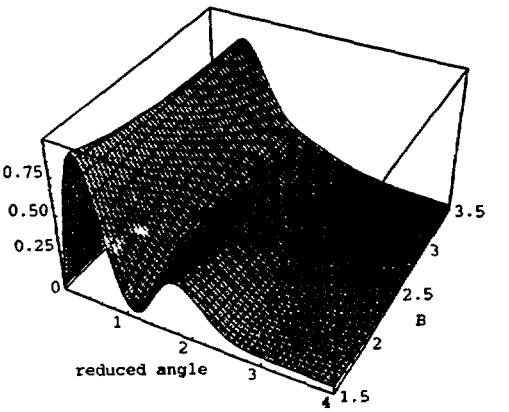

Fig. 4. The braking-down of the universal Molière's multiple scattering distribution as a function of parameters B and reduced angle ϑ using three terms in the expansion series.

References:

[1] J Medin, P Andreo. *Nucl Instr Meth* **B69** 64 (1992).
[2] N Laulainen and H Bichsel, *Nucl. Instr. Meth.* **104** 531 (1972).
[3] M J Berger, in: *Methods in Computational Physics,* Vol. 1, p 135. Alder, Fernbach and Rotenberg eds (Academic Press, New York, 1963).
[4] International Commission on Radiation Units and Measurements (ICRU), *Stopping Powers for Protons and Alpha Particles,* to be published.
[5] W R Nelson , H Hirayama and D W O Rogers, *The EGS4 Code System,* Report SLAC-265 (Stanford, CA: SLAC) (1985)
[6] S M Seltzer, *Appl. Radiat. Isot.* **42** 917 (1991)

HEAVY ION TRACK STRUCTURE CALCULATIONS

M. Krämer, G. Kraft, GSI, Postfach 11 05 52, D-6100 Darmstadt, Germany

Introduction

For the understanding of ion induced radiation effects a detailed knowledge of track structure is mandatory. The radiation damage is initiated by the ionization caused by the projectile and the emitted δ-electrons. A Monte Carlo (MC) simulation has been developed to model the primary ionization and the transport of the created δ-electrons in matter, particular in water. Each collision of a heavy ion or an electron with a molecule is treated individually. This strategy allows to study the ionization distribution on an event-by-event basis on a nanometer scale.

Electron Transport

The outline of the electron transport calculation follows to some extent the recipes given by various authors ([1, 2]). The basic interactions elastic scattering, excitation and ionization are considered. Experimental total and differential cross sections were used where available [3, 4]. The correctness of the transport model was verified by comparing calculated electron backscattering coefficients, W-values and electron depth dose profiles with experimental data.

δ-Electrons from Heavy Ions

In order to describe the electron emission from the collisions of heavy ions with water or other light target molecules the Binary Encounter Approximation (BEA) was chosen, mainly due to its simplicity [5]. It assumes basically a binary collision between the projectile (P) and

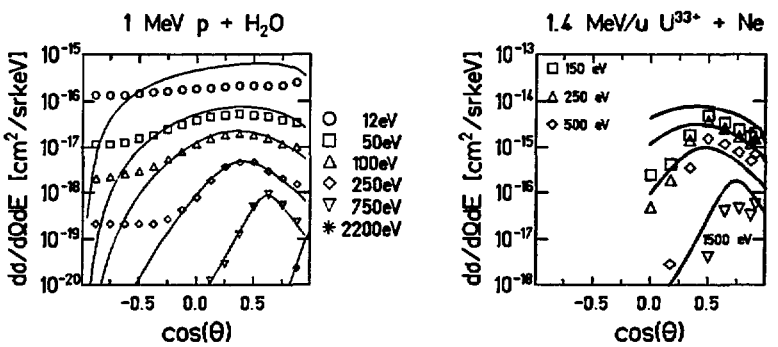

Figure 1: δ-electron angular distributions. Symbols: measured, curves: BEA calculations.

an electron (e) from the target molecule. The absolute height of the BEA cross section scales with the effective projectile charge as Z^2_{eff}, which is calculated according to the Barkas formula [6], and is approximately proportional to the number of weakly bound target electrons. Figure 1 compares experimental [7, 8] and BEA cross sections. The overall agreement of BEA and experiment is quite good. A major deficiency of the BEA theory is the underestimation of backward emission. For very heavy projectiles like uranium the theory overestimates the yield around 90^0. The overall agreement is still surprisingly good, keeping in mind the complexity of the reaction of the partially stripped very heavy projectile with a multi-electron target.

Dose Calculations

The dose as a function of distance from the ion path was calculated and compared with experimental results. Experiments usually determine the dose by measuring the ionization current caused by the passage of heavy ions in a chamber filled with gas at low pressure. The dose distribution is obtained by multiplying the measured currents with the W-value. This procedure

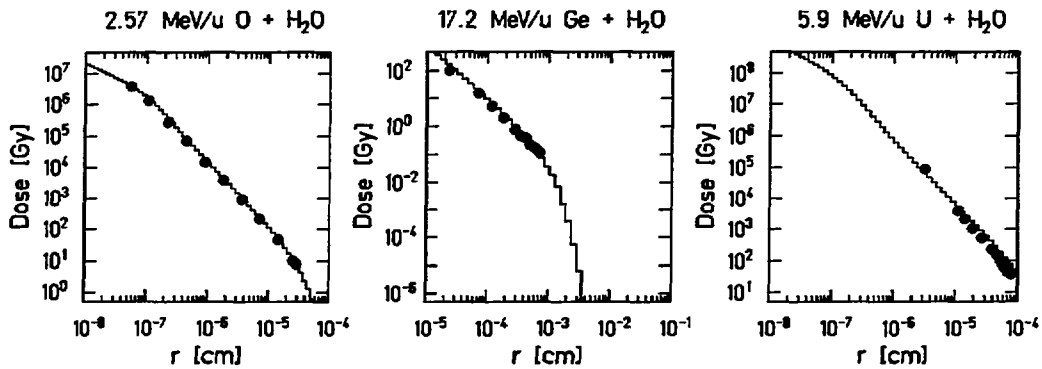

Figure 2: Measured (symbols) and simulated (histograms) dose distributions.

is simulated in the MC code. Figure 2 shows experimental dose distributions for oxygen [9], germanium and uranium [10]. They are well reproduced by our calculations assuming water vapour of unit density. However, the BEA is originally not well suited to obtain the correct primary electron distribution for very heavy projectiles. In order to estimate how changes in the primary spectrum affect the radial dose, the measured and the calculated distributions for uranium (Figure 1) were used as input to transport calculations. The resulting dose curves differ by a factor of 2 at small distances ($< 1 \times 10^{-5}$), mainly due to the overestimation of the cross sections around 90^0. At large distances, corresponding to electron energies > 1 keV, the curves coincide due to the better agreement of experimental and theoretical input spectra.

References

[1] Grosswendt B. and Waibel E. (1978), *Nucl. Instr. and Meth.* **155**, 145

[2] Paretzke H. G. (1978), *Proc. 6th Symp. on Microdosimetry* Eds. Booz, Ebert H. G. (Brussels: Harwood)

[3] Trajmar S., Register D. F. and Chutjian A. (1983), *Phys. Rep.* **97/5**, 219

[4] Schutten J. at al., (1966), *Journal of Chemical Physics* **44/10**, 3924

[5] Bonsen T. F. and Vriens L. (1970), *Physica* **47**, 307

[6] Barkas W. H. (1963), *Nuclear Research Emulsions,* (New York: Academic Press)

[7] Toburen L. H. and Wilson W. E. (1977), *J. Chem. Physics* **66/11**, 5202

[8] Ch. Kelbch at al., *J. Phys. B* **22** 2171-2178 (1989).

[9] Varma M. N., Baum J. W. and Kuehner A. V. (1977), *Rad. Res.* **70**, 511

[10] L.H. Toburen et al., *Rad. Prot. Dosimetry* **31**, No 1/4 199-203(1990).

International Workshop on Biological Applications of Relativistic Heavy Nuclei (BARN 92)

Problems of Radiation in Space

Walter Schimmerling

Universities Space Research Association
Washington, D.C.

Human space exploration in the 21st century holds exciting prospects for the advancement of science and the expansion of our experience. Projected missions include an outpost on the Moon and a piloted mission to Mars. However, for space exploration to proceed, adequate protection of crew members must be ensured against the hazards presented by the harsh environment of space; in particular, against the hazards of ionizing radiation. While much still remains to be learned in all aspects of radiobiology, major unresolved issues for human activities in space are:

- radiation protection against large fluxes of high energy protons from solar energetic particle (SEP) events,
- the possible existence of new or qualitatively different biological effects, either not seen, or not seen at comparable radiation levels, for conventional (low-LET) radiation such as x-rays or γ-rays, and
- the uncertainties associated with predicting biological effects, even when these are known, based on extrapolations from low-LET data and sparse high-LET data.

The space radiation environment consist of protons and electrons trapped in the Earth magnetic field, protons (and some heavier particles) emitted in the course of solar disturbances (SEP), and protons and the energetic nuclei of other elements (HZE particles) that constitute galactic cosmic rays (GCR). The HZE particles, although contributing less than 1 percent of the GCR flux, make a much larger contribution to the dose due to their higher rate of energy deposition, and may be biologically the most significant component of GCR radiation.

Energies of the GCR particles range from less than a few MeV per nucleon to over 10,000 MeV per nucleon. According to calculations by G. Badhwar at the NASA Johnson Space Center, approximately half the dose equivalent in free space is due to GCR particles with energies above 1 GeV/nucleon (although this proportion depends on shielding thickness). L. Townsend, at the NASA Langley Research Center, has calculated that seven components, nuclei of H, He, C, O, Mg, Si, and Fe, contribute more than 70% of the dose equivalent due to GCR, again depending on shielding thickness. However; with increasing shielding thickness their contribution increases. Of these components, the most important are protons and iron nuclei. Calculations by J. W. Wilson, also at NASA/Langley, indicate that GCR constitute a significant component of cell transformation, even in low Earth orbit (LEO) radiation fields. The LET spectrum can extend to ~1000 keV/μm, leading to large quality factors assigned for the purposes of radiation protection.

The scientific knowledge required to predict radiation risk in space from first principles is not currently available. Therefore, predictions of radiation risk in space need to be derived from models based on empirical data. The data need to be sufficiently detailed to minimize interpolation errors, and they need to cover a wide range in order to minimize the errors introduced by extrapolation of measured quantities to the space environment.

A schematic description of the rationale for the overall approach to the program goals is given in Fig. 1. Since the purpose of research is to assure the protection of humans in space, significant results of their exposure to radiation cannot be expected. Furthermore, it is generally more cost effective to perform scientific research on the ground.

Direct ground-based data on radiation effects in humans are only available as a byproduct of medical treatment (e.g., cancer therapy), of accidental exposures, and as the result of analyses of atomic bomb survivors. Therefore, the estimation of radiation effects on humans will, of necessity, be based on chains of inference, using the best judgment of the scientific community as to what links to accept or require in forging such chains.

Mammals are the organisms most similar to humans, and it is logical to assume that investigations of biological effects of radiation on mammals are an important component in the necessary research. Small mammals afford the best statistical basis for such studies and have the added interest that a substantial data base exists for studies with conventional types of radiation. However, we currently lack the knowledge to make reliable extrapolations from animal studies in

one species to another and, therefore, to human beings. For this reason, studies are required to elucidate the mechanisms of radiation action and their modification in intact tissues, organs and organisms.

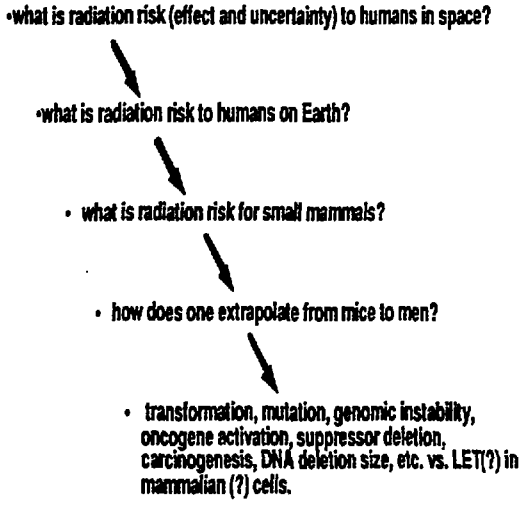

Figure 1. Rationale for space radiation research

The most important biological hazards associated with ionizing radiation particles are so-called "late effects," occurring during the remaining life span of the individual after exposure. Life threatening and life shortening effects, in particular, cancer, are of greatest concern. Mutagenesis and tissue damage, including cataract formation, are also significant adverse health effects. Neurological and behavioral effects and their consequences for crew performance likewise need to be understood.

The biological effects of exposure to radiation and, in particular, the resulting risk of cancer, depend on a multitude of factors. Among the most important are: the dose, the dose rate, the rate of energy deposition along a particle trajectory ("linear energy transfer" or LET), the age at exposure, the organ or organs irradiated, etc. The same dose, delivered by different types of radiation, does not always result in the same biological effect.

A fanciful, but intuitive way to illustrate the different behavior of different types of radiation may be obtained from Fig. 2.[1] In previous ages of exploration, the radiation hazard may more likely have consisted of infrared radiation, originating in the fire under the pot to the left. As with x-rays, radiation in this situation could be reflected, absorbed, and transmitted by shielding. A thermometer is a highly effective dosimeter in this situation, because there is an equilibrium state and the temperature is approximately the same anywhere in the water bath.

On the contrary, a thermometer would have no utility at all in the "high LET" cartoon on the right. On the one hand, if it were placed in the hip pocket of the executed man, out of the way of the bullets, its indication of a zero dose would be irrelevant to the actual circumstances. On the other hand, if the thermometer were placed in the shirt pocket, in the way of the bullet, it might register a lethal "dose" but in reality save the life of the prisoner: equilibrium no longer holds.

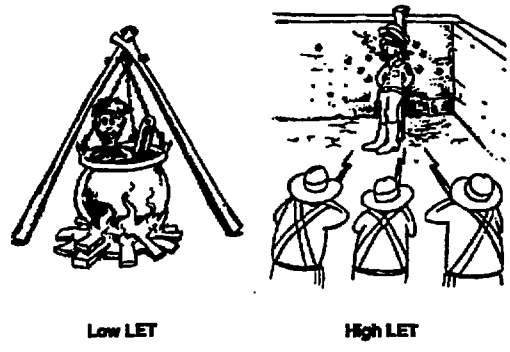

Figure 2. The difference between low LET and high LET.

A calculation of the energy required to raise the temperature of one kg of water from ambient to boiling requires a "dose" of approximately 250000 Gy (J/kg). If this is regarded as an approximation to a "lethal" dose of heat radiation, the comparable energy dissipated by a bullet of 0.1 kg mass, exiting from a rifle with a muzzle velocity of 2200 m/sec, in an 80 kg body, is approximately 3000 Gy. If one assumes that 10 bullets are required to ensure hitting the target, then the lethal dose would be 30000 Gy, resulting in an RBE value of 8, not bad for such a comparison!

There are large uncertainties associated with every step in the complex chain of reasoning leading from evaluation of the radiation fields to prediction of any biological effects resulting from exposure to radiation in the course of lunar habitation or a trip to Mars. The spacecraft designed by engineers must take these uncertainties into account in order to keep the radiation exposure within safe margins, which may be one or more standard deviations. As a consequence, additional shielding mass will be required, leading to increased costs associated with launching the extra mass into space. A diagram of this process is shown in Fig. 3.

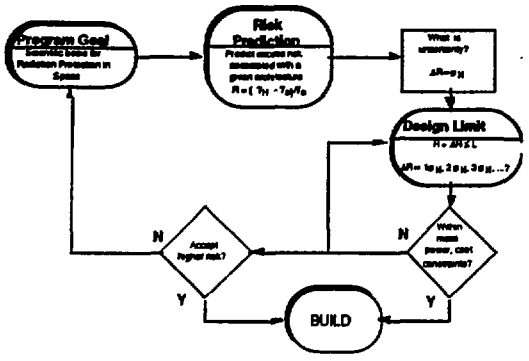

Figure 3. Uncertainties: the engineering perspective

Wilson *et al.* [2] have made a model calculation of the costs resulting from a one-standard deviation safety margin in the shielding required to limit radiation exposure to current LEO radiation limits, as a function of uncertainty in HZE dose-equivalent only. The results are shown in Fig. 4

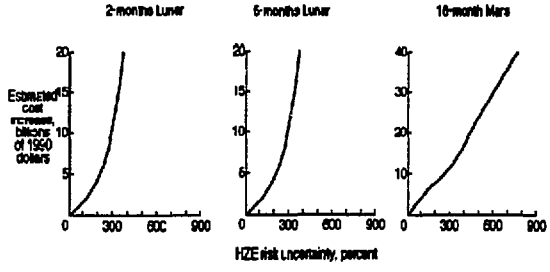

Figure 4. Estimated cost increase (in billions of 1990 dollars)

From such studies one can conclude that

1. Worst case calculations (based on order of magnitude estimates instead of detailed calculations) lead to unacceptable engineering designs.

2. The most efficient way to reduce the costs of space exploration missions is by research leading to reductions in the uncertainty of risk predictions.

Neither of these conclusions should be surprising in itself. Given that the costs of launching materials into space are extraordinarily high, especially when these materials have to include human life support, the benefit of appropriate research by far outweighs the costs incurred by attempts to compensate for large uncertainties in risk prediction. It is clear that these uncertainties need to be reduced below the 200 percent level in order to limit costs of shielding to a reasonable level. However, most subsequent reductions in uncertainty are likely to more than pay for themselves as well.

---

[1] I thank Mr. A. Joyce of the Lockheed Engineering and Science Corp. for translating my crude sketch into an artistic cartoon.

[2] J. W. Wilson, J. E. Nealy, W. Schimmerling, F.A. Cucinotta, and J. S. Woods, "Effects of Biological Uncertainty on Deep Space Mission Shield Design." In Preparation.

NUCLEAR FRAGMENTATION AND THE SPACE RADIATION PROBLEM

J. Miller, K. Frankel, W. Gong, L. Heilbronn and C. Zeitlin, Lawrence Berkeley Laboratory
W. Schimmerling, Universities Space Research Association
M. R. Shavers, Texas A&M University
L. W. Townsend and J. W. Wilson, NASA Langley Research Center

The following is a very brief description of some heavy ion fragmentation results from the LBL Bevalac. The program was originally begun in support of the Bevalac heavy ion radiotherapy program, and in recent years the applications to space radiation risk assessment have also become apparent.

$^{20}Ne + H_2O$. Fragment linear energy transfer (LET) spectra have been measured and compared with the results of two heavy ion transport codes [1,2]. Most recently [3], we have used the LBLBEAM transport code written at NASA-Langley Research Center [4] to investigate the relative biological effectiveness (RBE) of light fragments. When RBE's from model and physics experiment are compared for particles with $4 \leq Z \leq 10$, they are found to agree within 5% (Fig. 1), reflecting the good agreement between the model and experimental LET spectra from which the RBE is calculated. We have also used the model to look beyond the range of the experiment by including all charged fragments (Fig. 2) and comparing the RBE from the biological data [5] with the RBE calculated from the model fragment fluences. The difference between the solid and short dashed curves is a measure of the contribution of nuclear fragmentation to the biological effects of heavy ions.

^{56}Fe + polyethylene. We have recently begun a program to measure fragment fluences produced by iron nuclei, the most significant heavy component of the dose-weighted galactic cosmic radiation (GCR). Preliminary, relatively normalized LET spectra for 510A MeV iron nuclei incident on several thicknesses of polyethylene are shown in Fig. 3. The number of fragments relative to the iron peak increases with increasing target thickness, as expected. Further physics measurements and comparisons with biological data are in progress [6-8].

^{93}Nb + Nb, Al. Transport calculations indicate that neutrons from nuclear interactions of the GCR will make a significant contribution to the radiation dose behind shielding [9], and it is important to verify these calculations experimentally. In a recent experiment, niobium nuclei with energies of 250A MeV and 400A MeV were stopped in niobium and aluminum targets and the emerging neutrons detected. Figure 4 shows the preliminary laboratory angular distribution of neutrons produced by 250A MeV niobium nuclei stopping in 1.27 cm of aluminum. The spectra exhibit the sharp forward-angle peak and Fermi-boosted high momentum tail, characteristic of projectile fragmentation at these beam energies.

REFERENCES

1. W. Schimmerling et al., *Radiat. Res.* **120**, 36 (1989).
2. M. R. Shavers et al., *Radiat. Res.* **124**, 117 (1990).
3. M. R. Shavers et al., Submitted to *Radiat. Res.*
4. J. W. Wilson et al., *Radiat. Res.* **122**, 223 (1990).
5. W. Schimmerling et al., *Radiat. Res.* **112**, 436 (1987).
6. J. Miller, in the proceedings of the XXIX COSPAR Plenary Meeting, Washington, D.C., Aug. 28–Sept. 5, 1992, to be published in *Adv. Space Res.*
7. E. J. Ainsworth et al., *ibid.*
8. B. Worgul et al., *ibid.*
9. L. C. Simonsen et al., SAE Tech. Paper Ser. 911351.

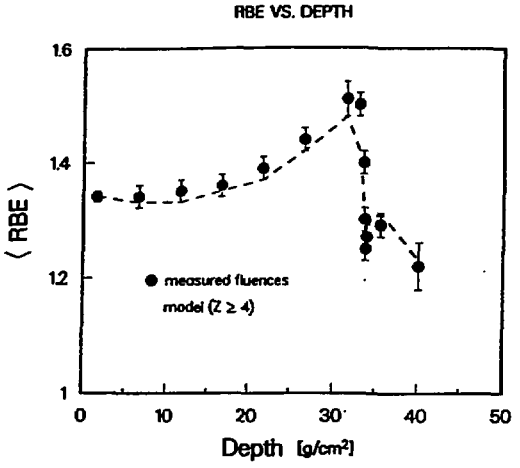

Figure 1. Relative biological effectiveness (RBE) calculated from measured fluence spectra (filled circles) and from fluence spectra predicted by LBLBEAM for fragments with $Z \geq 4$ (dashed curve), as discussed in [3].

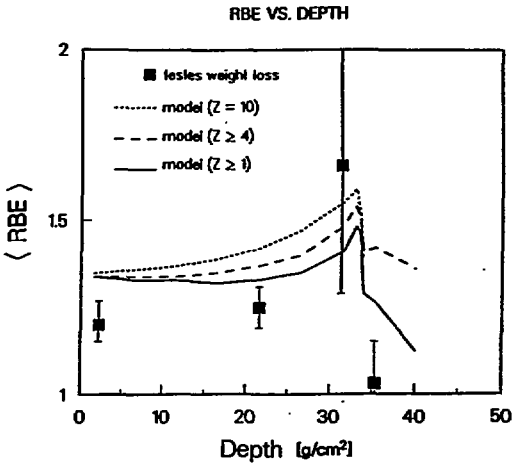

Figure 2. Filled squares: RBE from testes irradiation. Solid curve: RBE from model fluence spectra for particles with $1 \leq Z \leq 10$. Long dashes: RBE from uncorrected model spectra for primary neon and fragments with $Z \geq 4$. Short dashes: RBE from uncorrected model spectra for primary neon only.

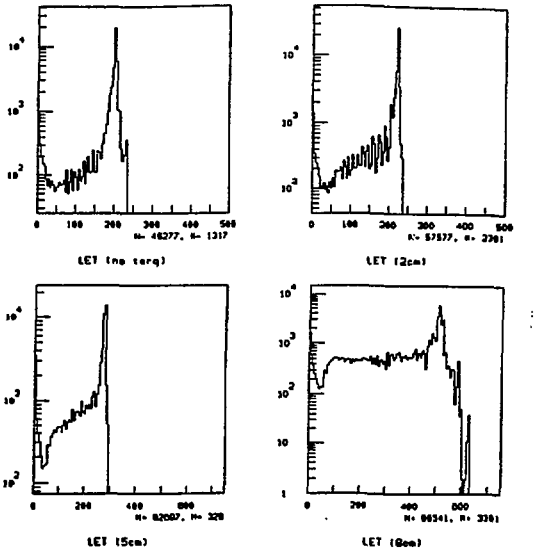

Figure 3. Preliminary, relatively normalized LET (in keV/μm) spectra for iron nuclei and fragments after passage through 0, 2, 5 and 8 cm of polyethylene.

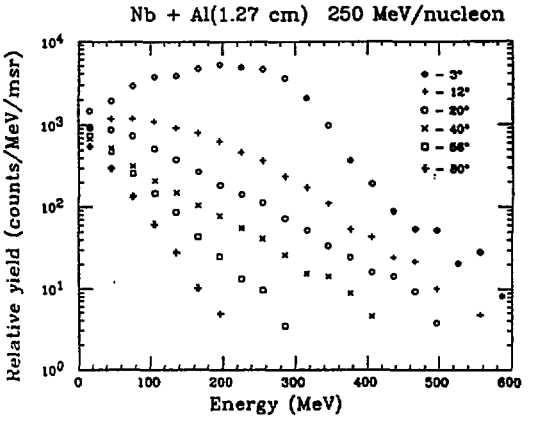

Figure 4. Spectra of neutrons produced at laboratory angles between 3° and 80° by 250A MeV ^{93}Nb incident on 1.27 cm of aluminum. The data are relatively normalized.

RISK FROM RELATIVISTIC HEAVY IONS ON MANNED SPACE MISSIONS

Stanley B. Curtis

Life Sciences Division
Lawence Berkeley Laboratory
University of California
Berkeley, CA 94720 U.S.A.

The risk from exposure to radiation posed to space travelers outside the magnetic shielding provided by the geomagnetosphere will come from two sources: the slowly varying but low intensity high-energy galactic cosmic rays and the more intense predominantly low-energy protons from large solar particle events associated with magnetic disturbances originating sporadically on or within the solar surface during the active period of the eleven-year solar cycle. The energy spectra of the protons in solar particle events are quite soft, with large numbers of low-energy protons and a rather steep decrease of the energy spectra with increasing energy. This allows for the possibility to provide, within the space vehicle or habitat, a well-shielded area sometimes called a 'storm shelter' or 'safe haven' where the travelers could gather during the largest particle events. Intensity rise-times on the order of a half hour or more and overall event durations of one to two days would make actively seeking a well-shielded shelter for the duration a distinct possibility. The high-energy and penetrating nature and relative constancy of the galactic cosmic rays, on the other hand, do not allow the use of highly shielded areas as a means of protection against them. The first question to answer becomes: what is the risk to human health from the galactic cosmic rays? We need to have a good idea of the answer to this question before we can address the problem of how to best protect human health or, indeed, whether any specific measures need to be taken.

Considerable information is available on the intensities, energy spectra, composition and time-variation of the galactic cosmic rays. They comprise all the ions in the periodic table, 87% are protons, 12% are heluim ions, with the rest being heavier particles. There is a preponderance of even over odd charge number and there is a peak at iron (Z=26), presumably reflecting large abundances of iron in the galactic source (or sources). They permeate near-earth space isotropically and their intensities vary on the order of a factor of two over the eleven-year period of increasing and decreasing solar activity. The intensities are at a maximum during the time solar activity is at its minimum, and are at a minimum when solar activity is at its maximum. The variation is due to the modulating effects of the solar magnetosphere which screens out the galactic particles more effectively during highly active solar periods. In addition, it is now known that, for every second solar cycle, the solar magnetic field changes its direction by 180 degrees. This causes a 22-year periodicity that is also reflected in the galactic cosmic ray intensities. Every second solar minimum is associated with higher cosmic ray intensities. Thus, the intensities in the solar minimum periods of 1954 and 1976-77 were larger than in 1965. It has been estimated that the galactic cosmic ray intensities can now be estimated to within 10-13% accuracy throughout the solar cycle.

The next problem is the modulation of the primary radiation by the space craft or habitat shielding and body self-shielding of the space travelers themselves. An extensive effort has been going on at NASA Langley Research Center, among other places, to develop a computer code to calculate the radiation transport through space craft shielding and human tissue of the galactic cosmic rays. Nuclear interactions of all the primary and secondary particles, including neutrons, are propagated through the total shielding to body organs of interest. The approximations used are that the secondary projectile fragments from the nuclear interactions emerge straight ahead, i.e., at zero degrees to the incident primary direction and with the same velocity as the primary. These calculations produce curves that have been estimated to have uncertainties of less than 35% due to our lack of knowledge of the nuclear cross sections.

The final aspect in the evaluation of the risk is the determination of the effects of the radiation on the tissues being exposed. Unfortunately, we know very little indeed about the hazards of human exposure to galactic cosmic ray particles. There is no counterpart to this kind of radiation on earth, except, of course, for the individual components at very well-defined energies in beams accelerated in a small and dwindling number of high-energy accelerators. There is, of course, no experience of

exposure of humans to these beams. It is believed that the light flashes seen on Apollo missions, the joint American-Soviet orbital mission (ASTP), as well as on other low earth-orbital missions, were caused by direct optical stimulation from the passage of galactic cosmic rays (for the Apollo mission) and trapped protons (for the earth-orbital missions). It is not expected that these flashes caused permanent damage to the eye, but they provide dramatic testament that single-particle effects are detectable by the human body.

The only risk that is presently thought to be well-established from the galactic cosmic radiation is the risk of cancer. It is believed that cancer arises from single transformed cells, and radiation-induced cancer is a well-established end point in many different species of animals, and excess cancers have been found over background levels in radiation-exposed human populations such as the atomic-bomb survivors of Hiroshima and Nagasaki. Most of the human data, which include the Japanese data, however, have been gathered from populations exposed to gamma radiation, a sparsely ionizing (low-LET) radiation. Although there is much cellular and animal experimental evidence to show that highly ionizing (high-LET) radiation such as found in the galactic cosmic rays are more efficient per unit of absorbed dose in producing biological effects, very little data are available from the high-energy heavy-ion beams directly relevant to galactic cosmic ray risk assessment. The conventional method of detemining risk from a mixed environment of low-LET and high-LET radiation is to multiply the absorbed dose distribution by a Quality Factor, which is a weighting factor that is a function of LET and was designed to account for the higher efficiency of the high-LET components, and then integrating to obtain what is called the dose equivalent. The dose equivalent can be thought of as the amount of gamma radiation necessary to produce the same amount of damage (or risk) as the radiation in question. At present, we lack values of the relative efficiency of the heavy-ion component to cause molecular damage relevant to the carcinogenic process.

Finally, other risks that need to be evaluated are cataractogenesis and the effects of neural damage that might accumulate in the central nervous system over long exposure times. The question that should be answered regarding cataractogenesis is whether the total fluences of particles accumulated over a two or three year mission outside the geomagnetosphere is high enough to be above the threshold for human cataractogenesis. The question of irreparable damage accumulating in neural networks by the passage of high-energy heavy ions is at present just a conjecture. Such damage could cause degradation of brain function and/or neuroreceptor function elsewhere in the body. Well-designed animal experiments should be performed to measure end points related to the slow degradation of central nervous system functioning over long exposure times.

In sum, it is not established that all the human risks from galactic cosmic radiation have been identified. In view of this, and because the Relative Biological Effectiveness of high-energy heavy ions beams (particularly iron) have been obtained on only a few biological systems to date, some of them of questionable relevance to cells and tissues in the human, it is clear that our uncertainty in risk assessment on extended missions back to the moon or on to Mars is predominantly due to our lack of understanding about the biological effects of the heavy components of the galactic cosmic rays. A somewhat subjective but, I hope, not unrealistic guess is that our uncertainty in the biological effects result in an uncertainty in risk estimation of a factor of between 2 and 5. Regardless of what the true numerical uncertainty in our risk estimates is, it is clearly dominated by our uncertainty in the biological effects. Much work needs to be done on high-energy heavy-ion accelerators using representative beams of iron and other particles with energies in the 0.5 to 2.0 GeV/ nucleon range in order to evaluate adequately the risks from this unique type of radiation.

Acknowledgements

This work is supported by the National Aeronautics and Space Administration under Order No. T-9310R, and by The NASA Specialized Center of Research and Training (NSCORT) awarded to the Lawrence Berkeley Laboratory/Colorado State University Consortium.

PLANT DEVELOPMENT IN SPACE

Perbal Gérald
Laboratoire CEMV, Bât. N2
Université Pierre et Marie Curie
75252 Paris Cedex 05 France

Gravitropism, growth of organs either toward (roots) or away from gravity (shoots) plays an important role in the development of plants.

When root is placed horizontally its tip curves in order to orient itself with respect to gravity. Curvature is due to differential growth in the upper and lower sides of the root. The perception of gravity occurs in special cells (statocytes) which are located at the very tip of the root. These cells possess voluminous organelles (amyloplasts) the density of which is greater than that of the surrounding cytoplasm. Amyloplasts are therefore able to move in the direction of gravity. The pressure of these organelles on the cytoskeleton should be responsible for an assymmetrical signal (lateral transport of a hormon) which leads to the differential growth and the bending. There are two different target cells which respond to the gravity stimulus : those of the upper part of the meristem (zone of cell proliferation) and those of the lower part of the cell elongation (zone where cell differentiation occurs).

The early pioneering space experiments do not give very clear cut results since the culture conditions are not well defined and it is therefore impossible to discriminate between the actions of gravity an those due to cosmic rays or cabin atmosphere. Progressively, the idea of a "space control" is becoming evident. As it is well known that plant organs react to centrifuged acceleration as they do to gravity, seedlings are now grown on a 1 g centrifuge in parallel with others grown in microgravity. In principle, both samples are subjected to the same "space factors" except microgravity.

In microgravity, roots do not grow straight, and their elongation is less than on the 1 g centrifuge. However, they are able to sense gravity since they curve as soon as they are subjected to a centrifuge force. Cell proliferation in the meristem and cell differentiation in the elongation zone are perturbed in absence of gravity. In effect, the mitotic index is

greater in microgravity than on the 1 g centrifuge and cell differentiate closer to the root tip in absence of gravity.

The growth of roots is thus regulated by gravity on the ground even if this organ is in the vertical position.

The polarity of the organelles in gravisensing cells is slightly different in microgravity than on the 1 g centrifuge. This could be due to the relaxation of the cytoskeleton which is responsible for the location of the organelles in the cell.

Gravity is thus necessary for a normal growth of plant organs. In space, it should be necessary to subject plants to a low level of artificial gravity (centrifugal acceleration) in order to obtain their full development.

INTERACTIONS OF 1.3 GeV/nucl ^{84}Kr NUCLEI IN EMULSIONS

L. Just, M. Karabová, K.Kudela
Institute of Experimental Physics, Košice, Czechoslovakia

Abstract. Basic experimental data are presented on the mean free path, parameter of fragmentation and on angular distribution in the interactions of ^{84}Kr nuclei of 1.3 GeV/nucl.

Experiment. The stacks of NIKFI BR-2 emulsion pellicles 9.5x9.5 cm^2, 0.4 mm thick were exposed at BEVALAC by the 1.366 GeV/nucl ^{84}Kr beam parallel to the pellicles and scanned by the along-the track minimum bias scanning yielding in 602 interactions. For all of them the numbers of fast and slow particles (β <0.7, N_h; β>0.7, n_s), number of grey and black tracks (N_g,N_b), multicharged fragments (Z=2, N_α; Z>2,N_f) and relativistic particles with emission angle θ<7° deduced from single charged fragments (n_p) were found. Deflection angles of fragments were determined for part of the material. The errors in charge and in the angles are 10% and 0.05° respectively.

The following average values were obtained: $\langle n_s \rangle$=12.53±1.67, N_g=4.44±0.81, N_h=6.04±0.78, N_h=10.48±1.33, n_p=4.31±0.45, n_α=2.58±0.34 . Fig.1 shows the dependence of the inverse of mean free path ($1/\lambda$) on $A_p^{2/3}$ for BR-2 emulsion. Experimental data are ^{12}C, ^{22}Ne at 4.2 GeV/n [6], ^{56}Fe at 1.9 GeV/n [7], ^{40}Ar at 1.2 GeV/n [8], and from this experiment corrected for hydrogen. The lines correspond to $1/\lambda$ values deduced from modified Bradt-Peters formulae (BP [1]) using approaches [2-5]. Fig.1 shows that the result obtained in this paper is consistent with those of other papers. The best fits for BP are r_0=1.32 fm and b=0.85.($A_p^{-1/3}$+$A_T^{-1/3}$).

Fragmentation parameter (P_{ij}) is the average number of fragments of type j created in splitting of primary nucleus of type i. The histogram of frequency distribution of fragments with charge Z is in Fig.2 which manifests decrease of numbers of fragments with lower Z. This fact is observed also in [9] reporting exposure of CR-39 stack by ^{84}Kr at 0.45 GeV/n. Table 1 gives the P_{ij} results obtained in this experiment (lowest row) compared with other experimental data. The groups of fragments are named according to the way used in cosmic ray studies (L-group: 3<=Z<=5; M: 6<=Z<=9; H: 10<=Z<=19; VH: Z>=20).Average emission angles (in degrees) are given in Tab.2.

Tab.1. Fragmentation parameters P_{ij} (errors are in the brackets)

react\fragm	p	α	L	M	H	VH
^{12}C+Em [6]	1.18(.04)	0.81(.03)	0.14(.02)	0.04(.01)		
^{22}Ne+Em[6]	1.41(.05)	0.84(.04)	0.14(.01)	0.28(.01)	0.05(.01)	
^{40}Ar+Em[8]	2.04(.09)	1.13(.08)	0.12(.01)	0.15(.02)	0.55(.04)	
^{56}Fe+Em[7]	3.74(.26)	1.51(.13)	0.12(.05)	0.10(.03)	0.20(.03)	0.29(.03)
^{84}Kr+Em	4.31(.45)	2.58(.34)	0.13(.06)	0.09(.04)	0.23(.05)	0.49(.03)

Tab.2. Average emission angles (°)

react\fragm	p	α	L	M	H	VH
^{40}Ar+Em[8]	3.80(.15)	2.99(.24)	2.01(.21)	1.24(.12)	0.78(.04)	
^{56}Fe+Em[7]	2.63(.03)	2.44(.07)	2.00(.10)	1.63(.08)	1.08(.08)	
^{84}Kr+Em	2.67(.05)	2.21(.06)	2.06(.15)	1.94(.12)	1.12(.07)	0.64(.04)

Discusslon . The results show that P_{ij} (j 1,2) , for the interactions with the "average" nucleus of emulsion, is decreasing with increasing Z or mass of primary nucleus (i). Dependence P_{ij} on i (j=1,2) is stronger than linear. The ratio P_{i2}/P_{i1} for stripping fragments is decreasing with i from

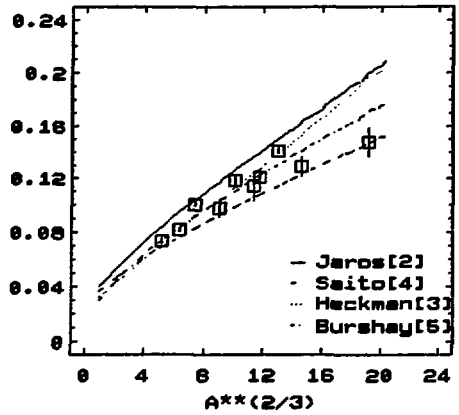

Fig.1.Values $1/\lambda$ vs $A^{2/3}$.Points correspond to experiments.

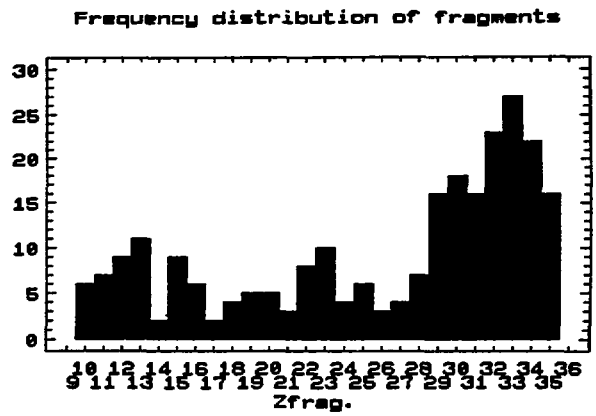

Fig.2.Distribution of fragments Z

0.69 (C) to 0.5 (Kr). P_{iL} is insignificantly dependent on i. P_{iM} is nonmonotonic with maximum for ^{22}Ne interactions. This result can be explained using the simple "geometric" approach to the collision process. For peripheral interactions, being of high probability, the primary nucleus loses several nucleons and only slightly changes its charge (ΔZ=1 - 2). For the "more central-like" collisions the ΔZ is larger and that is why the P_{iM} can have the nonzero value for sufficiently massive nucleus. This simple approach explains also the small value of P_{CM} (by loosing one proton the ^{12}C nucleus is shifted to group L). Also large value of P_{NeM} and small value of P_{NeH} can be explained in such "geometrical" approach, since only for those interactions with ΔZ=0 the fragment remains in group H.Such interactions (ΔZ=0) are only 5% of the whole statistics. For heavier nuclei (^{40}Ar, ^{56}Fe and ^{84}Kr) the contribution of fragments with Z>10 is approaching to 50%. This is related to high charge of impacting nuclei. The fragmentation parameters of these nuclei into M-group are much lower than those obtained for neon.

Summary. The mean free path for the inelastic collisions ^{84}Kr + Em obtained in this study is in good agreement with earlier published data on exposure of emulsions by ions. For the Bradt-Peters modified formula the best fits deduced from the presented data are r_0=1.32 fm and $b=0.85.(A_p^{-1/3}+A_T^{-1/3})$.The increase of number of fragments with increasing mass of primary nucleus is observed. Ratio of the yields of double to single-charged fragments is clearly decreasing with increasing the degree of overlapping of the impacting nuclei.

Acknowledgement. The paper was prepared under grant 37 of the Slovak Academy of Science.

References.

1. Bradt,H.L., and Peters,B., Physical Review 77, 54, 1950
2. Jaros, J. et al, Physical Review C, 18, 2273, 1978
3. Heckman, M.H., et al, Phys. Rev. C, 17, 1735, 1978
4. Saito, S., Jour. Phys. Soc. Japan, 38, 282, 1975
5. Burshay, S., Dover, C.B., and Vary, J.P., Phys. Rev. C11, 860, 1974
6. Collaboration Alma-Ata, ...,Ulan-Bator, Report JINR Dubna, P1-85-692, 1985
7. Dudkin, V.A., et al, Nuclear Physics A509, 783, 1990
8. Antonchik, V.A., et al,Proc. 20 ICRC, vol.5, 109, Moscow 1987
9. D.P.Bhattacharyya, et al, Nucl. Instr. Methods, 1992 (in press)

The biological action of heavy charged particles

G. Kraft
GSI-Biophysik
Planckstr.1
6100 Darmstadt/Germany

Although we are not encountered in our daily life with the biological action of heavy ions, beams of heavy charged particles are of special interest in radiobiological research: firstly, with heavy ion beams of various energies and atomic numbers the physical parameters of the energy deposition can be varied to a large extend and the corresponding variation in the biological response can be used to test the correctness of models and theories of radiation action. Secondly, the knowledge of heavy ion action is important for radioprotection as well of neutrons as of cosmic radiation. Finally heavy ions are used in radiotherapy because they represent the optimal solution of tumorconform dose profiles, combined with a maximal protection of the healthy tissue around the target volume.

The biological action of heavy ion differs from sparsely ionizing radiation and is determined by its inhomogenous dose distribution. While sparsely ionizing radiation like x- or gamma rays interact stochastically with electrons of the target material, heavy particles produce a dense track of primary ionization and electron emission along their path. This yields an extremely inhomogenous dose distribution - on a more macroscopic scale - of areas affected by particle hits and target areas not affected by any energy deposition. But also in a microscopic scale, the dose is distributed extremely inhomogenous inside the particle track. In good agreement with many experiments and calculations is a $\frac{1}{r^2}$ decay of the dose with increasing radial distances up to a maximum value corresponding to the range of the most energetic electrons emitted in heavy ion impact (ref. 1). These inhomogenous dose distribution produces a characteristic pattern of radiation response wich is determined by the physical distribution and by the nature of the biological object. In figure 1 the inactivation cross sections of different biological objects bacteria, yeast and mammalian cells are shown as a function of the linear energy transfer LET (ref. 2). In spite of the diversity of the biological objects, the measured σ-LET dependencies are very similar. This is based on the structure of the biological organisation: The biological cell represents the basic subunit and the DNA inside the cell carries all the information on the biological structure. Therefore the DNA represents in the most cases the target of radiation action and the response of the biological object is determined by two parameters: first by the probability to have a particle

track going through the critical, DNA containing cellular target and second by the physical and biological characterization of the induced DNA lesion.

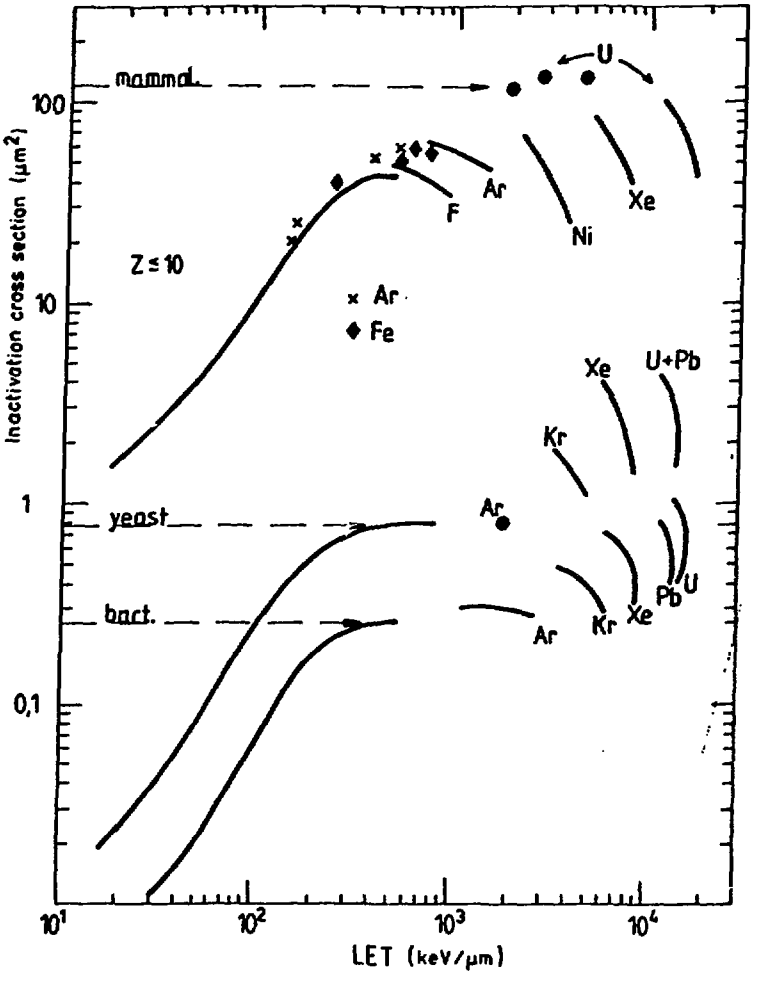

Figure 1: Action cross for cell inactivation i.e. the loss of colony forming ability as funciton of linear energy transfer LET. The experiments are performed with V 79 Chinese hamster cells, Yeast cells and Bacteria spores.

DNA damage can occur in various sites of the DNA molecule and can be classified into base damage, single and double strand breaks of the DNA and DNA-protein cross linking. The most important of these lesions are the double strand breaks especially when they are

produced in clusters destroying a larger part of the genetic information which can not be repaired correctly.

Sparsely ionizing radiation like x- or gamma rays can be characterized by the production of isolated ionization events and in consequence by a predominant induction of single lesions. Double lesions occur only according to the statistical probabilities of an inhomogenous event distributions.

In contrast, particle produce a high amount of correlated damage in the areas of elevated ionisation density in the track. Therefore, the ratio between the induction of double strand breaks and single strand breaks changes with the radiation quality (ref. 3). But also the nature of the double strand breaks seem to be affected by the radiation quality as indicated by a drastically deminished repair ability after heavy ion exposure. This might be due to the destruction of larger fractions of the DNA molecules or due to the simultaneous induction of crosslinks with the proteins at the damaged DNA site inhibiting repair.

At present, many of the necessary data for the understanding and calculation of these processes are not or only incompletely known. On the physical side the production rate, angular and energy distribution of the emitted electrons in a condensed target are not measured and gase phase measurements indicate large discreapancies compared to theoretical approaches. On the biological side, the size of the critical target inside the cells is frequently not known with good precission. But, probably more improtant, the molecular nature of the lethal DNA damage is not known at all. In conclusion, there is a large open field of research using the methods of modern molecular biology but also using the improved resolution of molecular microscopy.

References

1. G. Kraft, M. Krämer, M. Scholz, LET track structure and models, *Radiat Environ Biophys* **31** 161-180 (1992)

2. G. Kraft,Radiobiological effects of very heavy ions, *Nucl Sci Appl* **3** 1-28 (1987)

3. J. Heilmann, H. Rink, G. Kraft, DNA strand break induction rejoining and cellular recovery in mammalian cells after heavy ion exposure, *submitted to Radiat Res* (1992)

ASSESSMENT OF COMPONENTS OF RADIATION ACTION BY RELATIVISTIC NUCLEI

D.E.Watt and J.Storey, Department of Physics and Astronomy, University of St Andrews, St Andrews, Fife, KY16 9TS, Scotland, UK.

INTRODUCTION

In previous work a model for the biological action of ionising radiations, for various end-points in mammalian cells, has been derived. Each stage of development of the model was guided by reference to empirical data and the criterion in the selection of model parameters was the need to optimise unification of data, for all charged particle types. Heavy particles were found to act predominantly by single track direct action on targets presumed to be the DNA - a double-strand break being the lethal lesion[1]. Photons and electrons have a significant component of indirect action due to radical diffusion over short distances from the tracks. Indirect action in mammalian cells is deduced from empirical data for targets known to obey single hit, single target kinetics e.g. enzymes. Poisson statistics are then applied to deduce the probability of induction of double-strand breaks in the DNA[2]. A repair factor is incorporated. It is found that the common target dimensions for cell inactivation, mutations, transformation, chromosme aberrations, and DNA double-strand breaks is about 2 nanometres[3]. Here, a simplified version of the model is applied to determine the proportion of inactivation damage attributable to fragmentation products produced by irradiation of mammalian cells by relativistic protons.

MODEL

The survival fraction of targets is given by:

$$F=\exp[-N_T.K(t_i)] \quad \text{------ (1)}$$

where N_T is the total initial number of double-strand breaks produced in the intranuclear DNA by the radiation. $K(t_i)$ is a factor giving the fraction of double-strand breaks remaining unrepaired after a time that damage can be considered 'fixed' i.e. at mitosis.

Three process are considered for induction of double strand breaks: direct action, indirect action and a mixture of direct and indirect action - all for single charged particle tracks. Two track action, as for example in dual action, is thought to occur only at very high doses of photons or electrons.

The problem reduces to evaluating the number of double-strand breaks, N_T.

N_T is given by $N_T = N_D + N_I + N_M$

where N_D, direct action, $= \sigma_g.n_o.(1-e^{-\lambda_o/\lambda}).\Phi_S$ ------ (2)

N_I, indirect action, $= n_t.(\sigma_{ssb})^2.\Phi_S/\sigma_g$ ------ (3)

N_M, mixed action, $= 2.n_o.(1-e^{-\lambda_o/\lambda}).\sigma_{ssb}.\Phi_S/\sigma_g$ ------- (4)

Here, σ_g is the geometrical cross-sectional area of a DNA segment; n_o is the mean number of segments traversed by the track along a mean chord; λ_o = 2nm; λ is the mean free path for ionisation of the relevant charged particle in the equilibrium spectrum; Φ_S is the equilibrium fluence of charged particles; n_t is the total number of DNA segments at risk in the cell nucleus. All of these parameters are well-defined quantities obtainable from independent sources with the exception of the cross-section for production of single strand breaks, σ_{ssb}.

σ_{ssb} can be written as: $a_1.L_T.\exp(-a_2).(1-\exp(-a_3.L_T/C_{DNA})$, where the constants a_1, a_2 and a_3 can also be expressed fully in terms of physical and biological quantities that can be determined independently but some of which are not yet known. Note that, on the basis of this model, damage is due predominantly to the correlated spacing and number of events along single heavy particle tracks and not to energy deposition. *Any heavy particle with the same λ (>2nm) will have the same quality.*[7] There is therefore no advantage to be gained in choosing particles of mass > He for radiotherapy. Absorbed dose ($\Phi_S.L_T$) has a minor role in the indirect action (through σ_{ssb}) and is not therefore a satisfactory parameter for specifying effects[4].

DAMAGE BY FRAGMENTATION NUCLEI.

Assessment of damage by fragmentation nuclei is made by applying the direct action component of the model to each product nucleus released in spallation collisions, assuming that there is no overlap of tracks. Cross-sections $\sigma_{i,j}$, for production of nucleus type j by incident primary particle type i, and the fragment average energies for 1 GeV protons incident on carbon and oxygen nuclei were taken from the work of Cucinotta et al[5]. Mean free paths for ionisation and track average LET's of the fragments were taken for liquid water[6]. Fluences of each type of fragment products were calculated for a soft tissue medium. Consequently the predicted mean number of DNA double-stranded breaks is given by;

$$X_j = \sigma_{eff}.\Phi_j$$

where Φ_j ($=A_t.\sigma_{i,j}.\Phi_p.R_j$) is the fluence of a fragment type j having csda range R_j. A_t is the concentration of target nuclei and σ_{eff} is given by equation 2. As such, the magnitude of X_j gives the contribution of the individual ion type j towards cell killing. The total contribution of the fragments is given by the summation $\Sigma_j X_j$. In addition to the action of the fragment tracks there will be the contribution of primary protons which lose energy by ionisation but which do not undergo collisions causing fragmentation. The effect of these residual protons is given by X_{rp}. Thus the survival fraction is given by:

$$F = \exp[-\Sigma X_j + X_{rp}],$$

where $X_{rp} = (1-f).\Phi_p.\sigma_{eff}$ and f is the fraction of the total collisions which produce fragmentation. Assessment of contributions towards dose were made via:

$$D(\text{gray}) = 1.6\text{x}10^{-9}.L_{T,av}(\text{keV}/\mu\text{m}).\Phi_j(\text{cm}^2)$$

for each fragment, type j, and for the residual protons.

Although the total fluence of fragments is approximately only 0.04 times that of the initial primary protons, the dose attributed to them is about 24 times greater than that for the residual primary protons. The low energy high LET fragments are the major contributors towards the localised dose and, i.e. those fragments formed as a result of the 'stripping' of one to three nucleons from the target nuclei (typically boron, carbon and nitrogen nuclei) by an incident proton are the most damaging. These nuclei produce saturation damage as their mean free paths for ionisation are less than 2 nm and they have sufficient range to penetrate neighbouring cell nuclei. The direct ionisation effect due to the incident 1 GeV protons is small. No attempt has been made to include either the effects of neutron fragments produced or of proton-proton interactions which contributions will be small but not negligible.

This work was partially supported by the Commission of the European Community under contract CEC BI7-040-C(A) in their Radiation Protection Programme.

REFERENCES.

1. Cannell, R.J. and Watt, D.E. Biophysical mechanisms of damage by fast ions to mammalian cells in vitro. Phys.Med.Biol. vol.30, 255-258, 1985.

2. Watt, D.E.and Hill, S.J.A. An empirical model for the induction of double-strand breaks in DNA by the indirect action of ionising radiations. Eleventh symposium on microdosimetry. Gatlinburg, Tennessee. 13-18th Sept. 1992.

3. Watt, D.E., Al-Affan, I.A.M., Chen, C.Z. and Thomas, G.E. Identification of biophysical mechanisms of damage by ionising radiation. Radiat.Protect.Dosim. vol.13, 285-294, 1985.

4. Simmons, J.A. Absorbed dose - an irrelevant concept for irradiation with heavy charged particles? J.Radiol.Protect. vol.12, no.3, 173-179, 1992.

5. Cucinotta, F.A. Hajnal, F. and Wilson, J.W. Energy deposition at the bone-tissue interface from nuclear fragments produced by high-energy nucleons. Health Physics vol.59, no.6, 819-825, 1990.

6. Watt, D.E. Track structure calculations for charged particles in liquid water. Part 2: heavy charged particles. University of St.Andrews Report, BIOPHYS/20/92. St Andrews, Fife KY16 9TS, Scotland, UK.

7. Watt, D.E. On absolute biological effectiveness and unified dosimetry. J.Radiol.Protect. 9, 33-49, 1989.

COMPARISON BETWEEN CROSS SECTION OF DEUTERONS AND PROTONS FOR CELL INACTIVATION AND MUTATION INDUCTION

M. Bellia[a,b], F. Cera[c], R. Cherubini[c], A.M.I. Haque[c], F. Ianzinia[a,b], G. Moschini[c,d], O. Sapora[b,e], G. Simone[b,f], M.A. Tabocchinia[a,b] and P. Tiveron[c]

[a] *Laboratorio di Fisica, Istituto Superiore di Sanità, I-00161 Rome, Italy*

[b] *INFN-Sezione Sanità, I-00161 Rome, Italy*

[c] *Laboratori Nazionali di Legnaro-INFN, I-35020 Legnaro (Padova), Italy*

[d] *Dipartimento di Fisica, Università di Padova, I-35131 Padova, Italy*

[e] *Laboratorio di Tossicologia Comparata ed Ecotossicologia, Istituto Superiore di Sanità, I-00161 Rome, Italy*

[f] *Istituto di Fotochimica e Radiazioni di Alta Energia (FRAE)-CNR, I-40126 Bologna, Italy*

There is an increasing interest to investigate the biological effects of radiations of different quality to test biophysical models useful for radioprotection and several medical applications, and to get an insight of the basic mechanisms involved in the interaction of the radiations with the living matter.

In recent years, we carried out extensive studies on inactivation and mutation induced by protons in V79 cells[1-3] showing that protons are more effective than alpha-particles at the same LET for both end-points. These results gave experimental evidence of a Z-dependence of the Relative Biological Effectiveness (RBE) of the light ions as already pointed out in literature for heavy ions (see for instance ref. 4).

More recently, to extend the investigated range of LET for charged particle with Z=1 overcoming the inherent limitation of the proton range in biological matter, we have undertaken a systematic investigation with deuteron beams[5,6]. They possess twice the range of protons with the same LET, thereby the same velocity, and are expected to have the same track structure as protons, therefore the same biological effectiveness.

Log-phase Chinese hamster V79-753B cells were irradiated with monoenergetic deuteron beams at the radiobiological facility of the 7 MV Van de Graaff CN accelerator of the INFN-Laboratori Nazionali di Legnaro (LNL), Italy Irradiation conditions, dosimetric measurements, colture methods and biological tests for cell inactivation and mutation induction have been described in details elsewhere [1,2,6].

Deuteron primary energies in the range 3.82-6.50 MeV were chosen to obtain unrestricted LET in cells at 3 μm depth ranging from 57.0 to 13.4 keV/μm (see Table I). As far as the mutation induction is concerned, irradiation experiments have been performed so far using only primary deuteron beam of 4.2 MeV. The dose-response relationships were evaluated in the range 0.5-4.0 Gy at the dose rate of about 1 Gy/min. Each curve was evaluated by 4-10 independent experiments.

Inactivation data were fitted by linear-quadratic equations ($S=\exp(-\alpha D-\beta D^2)$) for LET lower or equal to 20 keV/μm, while those for higher LET values were fitted by linear equations ($S=\exp(-\alpha D)$). The mutation data were fitted by linear equation ($M=\alpha D$). Best fits of the data were performed with the weighted least-square methods.

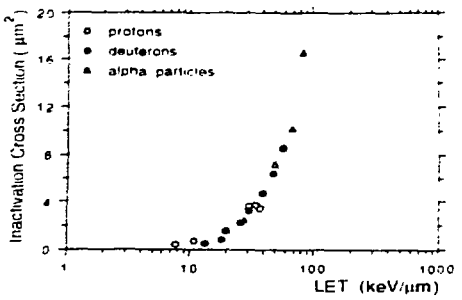

Fig. 1- Inactivation cross-section curves as a function of LET for V79 cells (see text).

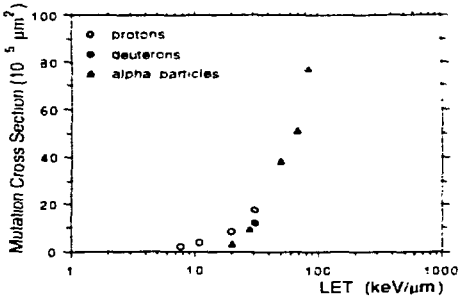

Fig. 2- Mutation cross-section curves as a function of LET for V79 cells (see text)

From the dose-response curves we have evaluated the cross-sections for both effects in terms of the linear coefficients (i.e. of the initial slope of curves), (see Table I).
In figures 1 and 2 the inactivation and mutation cross section curves as a function of LET for V79 cells irradiated with deuterons are reported together with those obtained from our previously proton data. Data for alpha-particles obtained by Thacker et al[7] on V79-4 cells are also shown.

TABLE I - Beam and curve parameters (see text)

DEUTERON BEAMS			SURVIVAL	MUTATION
E_{beam} (MeV)	E at 3 μm depth (MeV)	LET at 3 μm depth (keV/μm)	σ± s.e. (μm^2)	σ± s.e. (μm^2) x10^{-5}
6.500	4.87	13.4	0.52±0.08	
5.200	3.16	18.4	0.85±0.14	
4.400	1.89	26.3	2.22±0.03	
4.200	1.51	30.8	3.23±0.03	11.78±0.02
4.000	1.06	39.5	4.73±0.17	
3.900	0.80	48.0	6.40±0.33	
3.820	0.62	57.0	8.58±0.18	
PROTON BEAMS				
6.000	5.01	7.7	0.38±0.03	1.93±0.00
4.500	3.20	11.0	0.65±0.06	3.66±0.00
3.300	1.41	20.0	1.51±0.11	8.22±0.01
3.000	0.76	30.5	3.63±0.07	17.32±0.02
2.955	0.62	34.6	3.61±0.14	
2.930	0.57	37.8	3.41±0.07	

The differences, of several order of magnitude, found between the cross sections of the two end points are related to the differences in the size of relevant targets. Comparison between protons and deuterons shows some discrepancies, in the effectiveness per particle track, implying that these particles should have different energy deposition patterns within the relevant biological targets.Further deuteron irradiation experiments are in progress to complete the mutation indution data and to collect information of effectiveness on other biological end-points.

REFERENCES

1. Belli et al.(1989), Int. J. of Radiat. Biol. **55** 93-104 .
2. Belli et al.(1991), Int. J. of Radiat. Biol. **59**, 459-465 .
3. Belli et al.(1992), Int. J. of Radiat. Biol. **61** 145-146 .
4. Kraft (1987), Nuclear Science Applications **3** 1-28 .
5. Cera et al.(1991), in: GSI-91-29 Report. Extended Abstracts_ Fourth Workshop on Heavy Charged Particles in Biology and Medicine, GSI, Darmstadt, Germany, Sept. 23-25, 1991.
6. Belli et al (1992) Eleven Symposium on MICRODOSIMETRY, Gatlinburg, TN, USA, Sept. 13-18,1992. To be published in Radiat. Prot. Dosim.
7. Thacker et al.(1979), Int. J. of Radiat. Biol. **36**, 137-148 .

BIOLOGICAL EFFECTS OF ^{20}Ne ION IRRADIATION ON TUMORAL AND HEALTHY RODENT CELLS.

JL Poncy[1], M Dhilly[1], Y Archimbaud[1], R Bimbot[2], R Anne[3], F Clapier[2], B Kubica[2], O Sorlin[2], G Tousset[3], C Tribouillard[3], J Herault[4], R. Freemann[5], and R Masse[1].

1- CEA, DSV/DPTE/LRT, 91680 - Bruyères le Châtel.
2- Institut de Physique Nucléaire, 91406 - Orsay.
3- GANIL, 14021 Caen. 4- Centre Antoine Lacassagne, 06054 - Nice.
5- Centre de Recherches Nucléaires, 67023- Starsbourg

The development of high-linear energy transfer (LET) radiotherapy induces a great interest in the biological effects of heavy ions on mammalian cells. The purpose of this study was to determine the relative biological effects of ^{20}Ne ions (95 MeV/u) on tumoral and normal rodent cells in comparison with different kinds of gamma radiations (cobalt 60 and iridium 192) with variable energies. To minimize the disturbance of cell-cell interactions, cells will be irradiated in vivo. Tumoral cells (P77 cell line established from a radio-induced rat lung fibrohistyocitoma) have been inoculated in the hind leg or the upper part of the back in rats. Ten days after injection of 10^6 cells in suspension, tumor grafts (about 8 to 10mm in diameter) were irradiated. The doses used were 0, 5, 15 and 30Gy and the dose rates were 3.3, 1.1 and 0.9 Gy/min for ^{20}Ne, ^{60}Co and ^{192}Ir respectively. For cobalt and iridium the dose correspond to the skin dose value. It will be considered that the 1cm depth dose (internal part of the grafted tumor) for iridium irradiation was about 40% of the skin dose

About 15 to 20 hours after exposure, tumors were excised from three non exposed or irradiated rats, minced in culture medium to obtain cell suspensions. Then, using cell culture methods, the biological effects observed were both the survival of tumoral cells after exposure, considering their abilities to cloning, and the growth kinetics of the irradiated and non irradiated cells after successive passages (measurement of the population doubling level for each passage). On the second group of animals, the survival of tumor bearing rats after irradiation were compared to the non exposed controls and the secondary pathological effect on healthy tissue will be observed.

The figure shown the dose response curves established in vitro for survival of P77 cells irradiated in vivo with ^{20}Ne ions and γ-rays of ^{60}Co or ^{192}iridium. Survival decreased exponentially when the dose of Ne ions increased. After γ-rays exposure, the survival curves had smaller shoulder from 0 to 5 Gy and decreased exponentially above 5Gy. Then the slope of the curve was greater for Co γ-rays than Ir γ-rays. This fact might be due to the dose distribution of 350keV γ-rays of Ir in the mass of the tumor.

The relative biological effectiveness (RBE) for survival of cells isolated several hours after irradiation was measured for survival fractions of 10%. ^{20}Ne ions had an RBE of about 3.2 relative to ^{192}Ir γ-rays and about 3.8 relative to ^{60}Co. With a dose of 15Gy, curves shown that the surviving fraction was more than 10% and little different after gamma-rays exposure than after Ne ions. These observations shown the low radiosensitivity of the P77 tumor cells to the γ-rays. Number of DNA damage might be repaired during

the recovering time before in vitro cloning test for cell survival after irradiation.
The table compared the growth kinetics of cells irradiated by γ-rays (Ir) and Ne ions, by comparing the accumulation of population doubling levels (PDL) at various passage. At passage 1, PDL decreased with doses in the irradiated cell population. The growth rate remained constant in control cells and recovered completely before passage 2 in γ-rays irradiated cells.

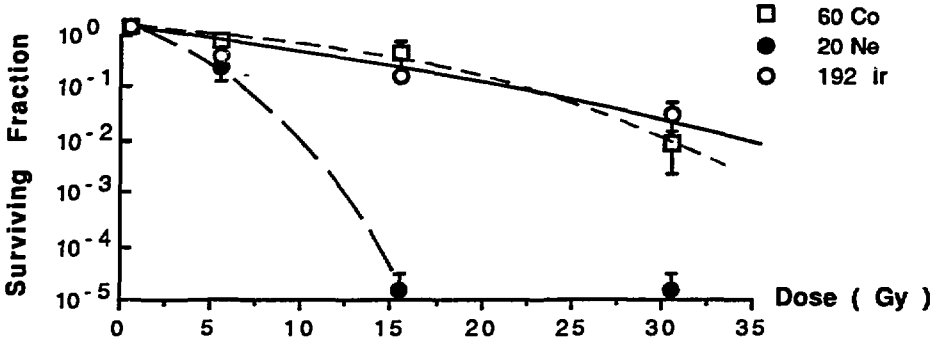

Figure : Dose survival curve of P77 cells irradiated in vivo by ^{20}Ne ions and γ-rays of ^{60}Co and ^{192}Ir. Each point corespond to the mean value from cultures of cells isolated from three control or irradiated rats

After Ne ion irradiation, cells did not proliferated after passages 1 and 2, the growth rate increased thereafter but did not reach the control value until passage 6. Comparatively with the survival curve of cells exposed to heavy ions, this observation was ambiguous. A small fraction of tumoral irradiated cells would be not killed and could reproliferated after a long period of quiescence

		Population doubling level					
		Passage numbers :					
	dose (Gy)	1	2	3	4	5	6
Ne	0	9.6	9.6	9.3	9.7	9.8	9.8
	5	4.5	9.0	9.2	9.6	9.6	9.6
	15	0.0	0.0	7.0	8.6	8.2	8.7
Ir	0	8.0	9.6	9.4	9.5	8.8	-
	5	5.7	9.4	9.3	9.3	9.9	-
	15	2.6	9.1	9.8	9.2	9.1	-

Table: Population doubling level (PDL) in cells at different passages numbers following exposure to Ne ions or gamma rays from iridium 192. PDL is expressed as ln(n7-n0)/ln2 where n7 is the number of cells after 7 days in culture and n0, the initial number of seeded cells

All the non irradiated bearing tumors rats, used for life survival analysis, died about 21 days after tumoral cell injections. A delay in the tumor growth had been observed after irradiation, however 7 months after exposure to ^{20}Ne ions at doses of 15 and 30 Gy, 2 rats were still alive. 5 rats in each dose group were initially presents. Rats had died with growing tumors because a small part of tumor was probably out of the heavy ion beam. The surviving rats will be examined at death to determine the long term effect of heavy ion irradiation on the healthy tissue near the initial tumor area.

RADIATION RESPONSE OF HUMAN TUMOUR CELL LINES TO HEAVY CHARGED PARTICLES

A. Courdi, C. Caldani, M. Scholz
Centre A. Lacassagne, 36 Voie Romaine, 06054 Nice, France,
and GSI, Planckstr. 1, Darmstadt 11, Germany

Whereas the radiation response of human tumour cell lines to low LET radiation is well documented, little is known about the effect of heavy charged particles on these cells. Charged particles offer physical and biological advantages over conventional irradiation (1). In vitro studies on human tumour cell lines would contribute to the selection of tumour types most likely to benefit of this novel therapy, and would help selecting the optimum particle and energy. Further, measuring cell inactivation using human cell lines is necessary for space and nuclear radiation safety.

CAL 1, a melanoma cell line (2), CAL 51, a breast carcinoma cell line (3), and CHP 100, a neuroblastoma cell line (4) were exposed to the following ions: 400 MeV O , 400 MeV Ni , 11 MeV Ne, 14 MeV Ar, 7 MeV Ar, 13 MeV Kr and 11 MeV Au, having respective LET values of 19, 220, 400, 900, 1500, 4000 and 9000 KeV/μm. The high energy beams O and Ni were produced by SIS, other beams of low energy were produced by Unilac, Darmstadt. The response was compared to that of Co gamma rays. The in vitro colony method was used to assess survival.

Table I

	DNA index	nucl. area (μm^2)	α (Gy^{-1})	β (Gy^{-2})	MID (Gy)	SF_2
CAL 1	1.16	117	0.344	0.0277	2.23	0.45
CAL 51	1.00	148	0.338	0.0498	2.00	0.42
CHP 100	1.73	199	0.031	0.1630	2.10	0.49

The DNA index, the nuclear area, and the radiosensitivity parameters to low LET radiation are shown in Table I (α and β are the linear and the quadratic terms, MID is the mean inactivation dose or the area under the curve in linear coordinates (5) and SF_2 is the survival after 2 Gy). After particle irradiation, survival curves became more linear, and the β term was no more apparent at 900 KeV/μm and higher values. Linearity with particle irradiation, in contrast to low LET radiation, led to the observation of an increase in RBE with the decrease in dose. Figure 1 illustrates the response of CAL 51 to the different particles.

RBE values were highest for the 400 MeV Ni beam (LET = 220 KeV/μm). They were lowest for the densely ionising Au beam (LET = 9000 KeV/μm) (Fig. 2).

In general, response to high LET radiation was related to response to low LET radiation, this was observed up to LET values of 1000 KeV/μm. The RBE was highest for the cell line with the lowest α and the highest β after gamma irradiation. This relationship with the intrinsic radiosensitivity parameters was also not observed for very high LET beams.

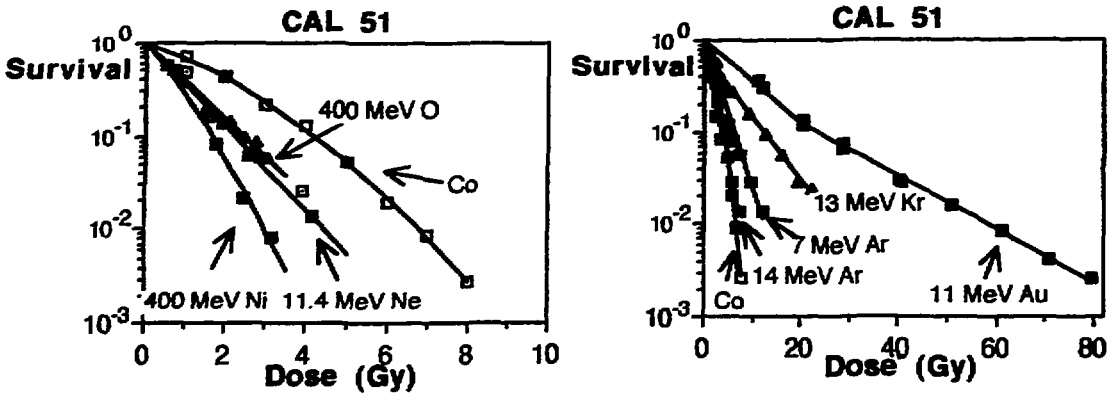

Fig. 1

Inactivation cross sections were highest at LET values of about 1000 KeV/µm. Finally, there was a link between the inactivation cross section and the nuclear area: the bigger the nucleus, the higher the sensitivity (Fig. 3).

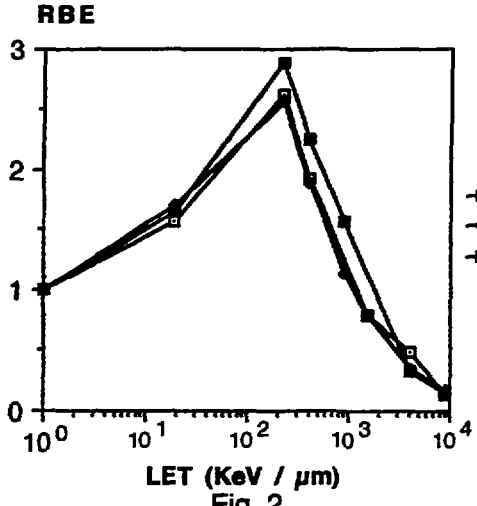

Fig. 2

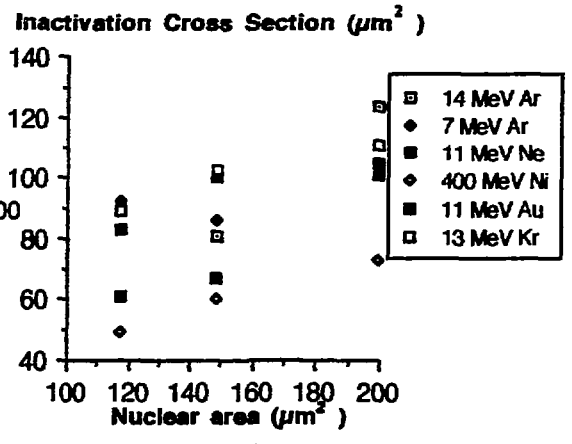

Fig. 3

The highest cross section equals approximately 70 % of the nuclear area, suggesting that not all particle traversals through the nucleus are lethal to the cell.

Supported in part by grants from the EULIMA project and the ARC, Villejuif.

References

1) P. Chauvel - J. Chim. Phys. 88: 1125-1136, 1991
2) A. Courdi, J. Gioanni, C.M. Lalanne, J.L. Fischel, M. Schneider, F. Ettore, J.C. Lambert - In Vitro 19: 453-461, 1983
3) J. Gioanni, D. Le François, E. Zanghellini, C. Mazeau, F. Ettore, J.C. Lambert, M. Schneider, B. Dutrillaux - Br. J. Cancer 62: 8-13, 1990
4) H.R. Schlesinger, J.M. Gerson, P.S. Moorhead, H. Maguire, K. Hummeler - Cancer Res. 36: 3094-3100, 1976
5) B. Fertil, H. Dertinger, A. Courdi, E-P. Malaise - Radiat. Res. 99: 73-84, 1984

B.A.R.N. 92

CHROMOSOMAL INSTABILITY INDUCED BY HEAVY IONS IN HUMAN FIBROBLASTS

Laure SABATIER, Berta MARTINS, M. Ricoul and Bernard DUTRILLAUX

Commissariat à l'Energie Atomique, DSV/DPTE/LCG, BP6 92265 Fontenay-aux Roses

Abstract

The cytogenetic study of normal human dermis fibroblasts irradiated with heavy ions showed the appearence of de novo chromosomal instability (around the 15th passage after irradiation). Our results exhibited that this instability 1) can be induced in normal human cells, for a wide range of high LET radiation; 2) is transmissible through many cell divisions and is mainly reflected by the emergence of dicentric chromosomes; 3) does not occur at random but affects certain specific telomeric regions and 4) leads to clonal chromosomal imbalance and rearrangement, as frequently observed in human solid tumour.

Introduction

The biological effects of irradiation by heavy ions remain poorly understood (Tobias, 1985; Lett et al, 1986, 1992). The unusual characteristics of chromosome lesions induced by hight LET particles was recently demonstrated. These lesions are more complex than those induced by X or γ-rays, involve several chromosomes, and their complexity increases with LET's (Sabatier et al., 1987; 1990). The frequency of cells carrying such lesions is reduced by 30% at each generation (Al Achkar et al, 1988). Thus, in a few cell generations, all or almost all cells carrying heavy ions induced chromosome rearrangements diseappear, which is in agreement with the strong efficiency of these particles to induce cell death (Kraft et al, 1987, Kiefer, 1989). However, it could be possible that a few cells carrying radiation induced rearrangement survive and develop as proliferative clones, which would fit with the efficiency of heavy ions to induce cell transformation (Yang et al, 1985, Suzuki et al, 1990).

Recently Kadhim et al (1992) demonstrate that irradiation by α-particles of Pu-238 (LET=120keV/μm) induce a transmissible instability in mouse hematopoietic cells. Working with human dermis fibroblasts irradiated by heavy ions in a large range of LET (386-13600 keV/μm) we also showed that an instability could also be acquired by human cells and that particular chromosomes were recurrently involved (Sabatier et al 1992).

Results and discussion

The study of the 7 cultures irradiated at GSI (Darmstadt) by Neon ions (E=10.74 MeV/u, LET=386 keV/μm), (fluences of 10^6, 2.10^6 and 4.10^6 particles/cm^2), Argon ions (E=10.52 MeV/u, LET=1207 keV/μm), (fluences of 10^6, 2.10^6 and 4.10^6 particles/cm^2) and Lead ions (E=9.5MeV/u, LET=1360 keV/μm), (fluence of 2.10^6 particles/cm^2) shows identical results and permits us to propose the following scheme :

- irradiation by heavy ions induce multiple chromosomal alterations proportionally to the fluence of the particles,

- many cells directly affected by the track of one (or more) particle either die or do not give rise to viable descendants. This results in the observation of a majority of normal karyotypes in metaphases around the 5 - 10th passage,

- a few passages later, however, a transmissible chromosome instability is observed in descendant cells,

- specific chromosomes are involved(25% of the chromosome break points are located on chromosome 13,

- this instability affects some chromosome structures preferentially, and in particular telomeric regions of chromosome 13 and of 1p, 16p and 16q arms,

- some clones, characterized by chromosome rearrangements and imbalances, progressively develop and invade all the cultures around passage 25th after irradiation,

- Both chromosome instability and selection of imbalances, particularly deletions, suggest that the surviving cells have acquired anomalies shared by transformed or malignant cells.

The occurence of de novo radiation-induced chromosomal instability has never been observed after low LET-irradiations of human cells. However, chromosomal instability is generally observed in senescent cells, in premalignant or low grade malignancies (Benn, 1976, Kovacs et al., 1988; Mandhal et al., 1985; Pathak et al., 1988; Aledo et al., 1988). Chromosomal instability would be one of the mechanisms which lead a normal diploid cell to become a transformed aneuploid cell.Thus, after heavy ion irradiation, the surviving fibroblasts have performed one step towards cellular transformation.

References

Al Achkar, W., L. Sabatier and B. Dutrillaux (1988) Mutation Res., 198, 191-198.
Aledo R., M. F. Avril, B. Dutrillaux and A. Aurias (1988) Cancer Genet Cytogenet., 33, 29-33.
Benn P.B. (1976) Am.J.Hum.Genet., 28, 465-473.
Fry R.J.M., P. Powewers-Risius, E.L. Alpen and E.J. Ainsworth (1985) Radiation Res., Suppl. 8, 104, S-188-S-195.
Kadhim M.A., D.A. Macdonald, D.T. Goodhead, S.A. Lorimore, S.J. Mardsen and E.G. Wright (1992) Nature., 355, 738-740.
Kiefer J. (1989) In Biological Radiation Action Ed Springer-Verlag.
Kovacs G., R. Muller-Brechlin and Szucs S (1987) Cancer Genet Cytogenet., 32, 93-101.
Lett J.T., A.B. Cox and D.S. Bergtold (1986) Radiat. Environ. Biophys., 25, 1-12.
Lett J.T. (1992) Radiat. Environ. Biophys., (in press).
Mandahl N., S.Heim, V. Kristofferson , F. Mitelman , B.Rooser , A.Rydholm and H.Willen (1985) Hum Genet., 71,321-324.
Patak S., Z.Wang, M.K. Dhaliwal and Saks P.C (1988) Cytogenet Cell Genet., 47, 227-229.
Sabatier L. W. Al Achkar and B. Dutrillaux (1990) In frontiers in radiation Biology Ed. E. Riklis, VCH., 287-294.
Sabatier L., W. Al Achkar, F. Hoffschir, C. Luccioni and B. Dutrillaux (1987) Mutation Res., 178,91-97.
Sabatier L., B. Dutrillaux and B. Martins (1992) Nature (London)., 357, 548.
Suzuki M., M. Watanabe, K. Suzuki, K. Nakano and I. Kaneko (1989) Radiation Res., 120, 468-476.
Tobias C. A. (1985) Radiation Research., 103, 1-33.
Yang T. C., L.M. Craise, M.T. Mei and C.A. Tobias (1985) Radiation Res., 104, S-177-S-187.

RELATIVE BIOLOGICAL EFFECTIVENESS OF 65 MeV PROTONS AT BEAM ENTRANCE AND AT THE SPREAD-OUT BRAGG PEAK

A. Courdi, N. Brassart, J. Hérault, P. Chauvel
Centre A. Lacassagne, 36 Voie Romaine and 227 Avenue de le Lanterne, Nice, France

High energy proton beams offer a substantial physical advantage over the conventionally used photons or electrons in radiotherapy. The maximum dose deposition is delivered at the Bragg peak, a smaller dose is delivered at the beam entrance where normal tissues are situated, and the dose abruptly falls off beyond the peak. This peak is spread-out (SOBP) in order to deliver an homogeneous dose to the tumour. There is a consensus to adopt an RBE value of 1.1 when proton doses are compared to Cobalt doses (1), and previous findings using a human melanoma cell line in our laboratory agree with this value (2). In this study, we have exposed the melanoma cells CAL 4 (3) to 65 MeV protons produced by the cyclotron Medicyc in Nice at 2 depths, using 2 mm or 20 mm perspex, and a half range modulator, corresponding respectively to the beam entrance and the SOBP. The aim is to find out if there is a difference in effect between the beam entrance and the SOBP. Survival was assessed by the in vitro colony method and the linear-quadratic model was used to fit the experimental points.

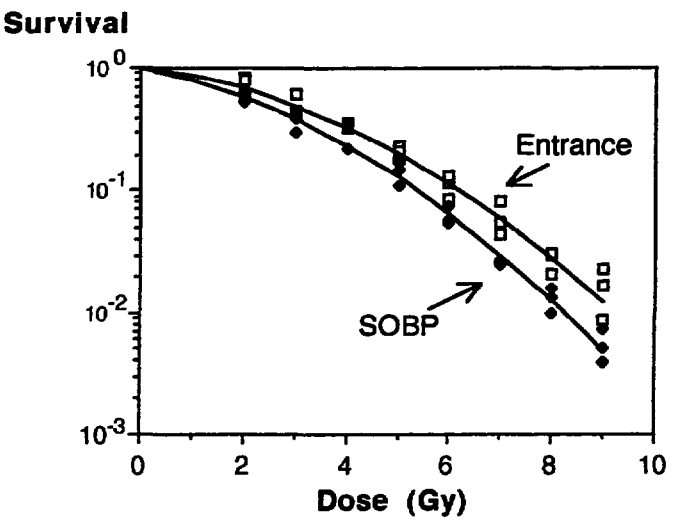

Fig. 1

Figure 1 illustrates survival of 3 independent experiments. At beam entrance, the linear term α was 0.0982 ± 0.021 Gy^{-1}. It was 0.1750 ± 0.026 Gy^{-1} at the SOBP ($p = 0.048$). There was no difference in the β term. The average sensitivity, as measured by the mean inactivation dose (4), which is the area under the curve in linear coordinates, was respectively 3.33 ± 0.103 Gy and 2.75 ± 0.087 Gy ($p = 0.001$). The RBE of the SOBP relative to the entrance beam is shown in Fig. 2, the shaded area represents the 95 % confidence interval.

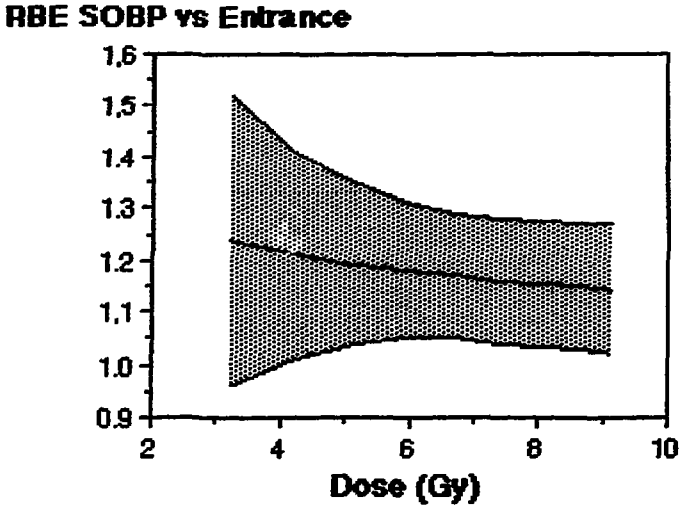

Fig. 2

Relative RBE values can be represented as the followings: Proton entrance vs Co: RBE = 1. Proton SOBP vs Co: RBE = 1.1. SOBP vs entrance: RBE = 1.1. For a Co equivalent dose of 60 Gy, and a physical entrance/SOBP dose ratio of 67 %:

	Proton dose	RBE	Co equivalent dose
SOBP	54.5 Gy	≈1.1	60 Gy
Entrance	36.5 Gy	≈1.0	36.5 Gy
Ratio	67 %		61 %

Using the LQ model, survival ratios at the end of a treatment can be derived knowing the ratios of the doses per fraction (5). The relative efficiency (E_1) of a treatment giving p% of the dose d is given by the formula:
$E_1 / E_2 = p[(\alpha/\beta) + d.p] / [(\alpha/\beta) + d] = K$
Assuming same α and β values at entrance and at SOBP, and for a final survival of 10^{-9} and d = 13.6 Gy (15/1.1), the surviving fraction at entrance would equal 10^{-9K}.
For an entrance dose = 0.67 SOBP dose, the ratio of cells to be spared = $4. 10^4$. If the small RBE difference is taken into account, the ratio of cells to be spared = $1.8. 10^5$, which means a further 4.5 fold sparing of cells.

Supported in part by grants from the Ligue Nationale Française Contre le Cancer, Comité Départemental du Var, and the Fédération des Centres de Lutte Contre le Cancer de France.

References

1) M. Urano et al. Int. J. Radiat. Oncol. Biol. Phys. 10: 509-514, 1984
2) A. Courdi. Eurocancer 92, Paris, 21-23 Avril 1992
3) A. Courdi et al. - In Vitro 19: 453-461, 1983
4) B. Fertil, H. Dertinger, A. Courdi, E-P. Malaise - Radiat. Res. 99: 73-84, 1984
5) A. Courdi et al. Int. J. Radiat. Oncol. Biol. Phys. 19: 1225-1228, 1990

PROTONS AND NEUTRONS VERSUS X OR GAMMA RAYS EXTERNAL RADIOTHERAPY : ALTERNATIVE OPTIONS ?

A - UVEAL MELANOMA, PROSTATE ADENOCARCINOMA

R. ROZAN, F. BACIN, E. ALBUISSON, B. GIRAUD, J.J. BARD, D. DONNARIEIX

(CLERMONT-FERRAND, FRANCE)

My colleague, Pr Kantor and myself, will show four examples which can be treated both by protons or neutrons but also by photons. Both have an equal chance of success but certainly slightly different therapeutic indications.

I - UVEAL MELANOMA

Uveal melanoma is a tumor developed from choroid and ciliary body.

In the USA, one thousand and two hundred new cases are detected every year. In France, it is not possible to establish precisely the exact figure of new cases due to the absence of epidemiologic record. A diagnosis of malignant melanoma of the uvea is established from the results of clinical examinations, indirect ophtalmoscopy, biomicroscopy, angiofluorography and A and B ultrasonography.

For many years enucleation has been the usual treatment for choroidal malignant melanoma because it was considered that this radical operation gave the patient the best chance of survival. In 1978, Zimmerman et al. proposed the hypothesis that enucleation caused metastatic dissemination and they therefore recommended alternative therapeutic approaches.

The method we describe is similar to that developed by Stallard for monopthalmic patients. It is a conservative brachytherapy treatment of intraocular tumours using a specially designed applicator. This applicator is a cobalt-60 plaque. Cobalt-60 has a half-life of 5.3 years. The opthalmic plaques are formed of concentric rings of cobalt-60 inserted into a platinum matrix which eliminates the beta rays and ensures that only gamma rays are used for the treatment. A set of isodose curves is available for each type of applicator and specifies the dose rate distribution as a function of depth for a standard activity of the plaque.

In Clermont-Ferrand, since 1983, patients have been treated using a cobalt-60 plaque but from 1986 we have used ruthenium-106 plaques, either on its own or in combination with cobalt-60 plaques.

The ruthenium-106 source has a half-life of 1 year and through beta decay produces rhodium-106 which has a half-life of 30 seconds and emits high energy beta rays together with photons whose energy is less than 700 keV. At a depth of 3 mm, the dose is only 50 % of the value found at the plaque surface.

The surgical procedure is carried out under general or local anaesthesia. It consists in approaching and exploring the operating zone subsequent to conjunctival disinsertion and tensioning of the oculomotor muscles.

The phases of the procedure are delineation of the tumour base using transillumination, measurement of the tumour base and choice of plaque, temporary suturing of the dummy plaque, insertion and suturing of the radioactive plaque.

RESULTS : SURVIVAL

84 patients have been treated in Clermont-Ferrand with plaque : 43 patients have been treated using a cobalt-60 plaque, 25 using a ruthenium-106 plaque and 16 in combination.

We have compared survival rate of our 84 patients treated with plaque brachytherapy with 59 patients treated by enucleation by the same surgeons.

The characteristics of the two groups of patients are comparable in terms of tumour dimensions. Survival rates of the two groups are non statistically different.

In the literature, regarding to the use of plaques as well as of charged particle radiation in the treatment of uveal malignant melanoma, the best survival results are those of Bornfeld, but the results from the various series are very similar, regardless of treatment technique. Gragoudas et al. (1990) suggest that the absence of significant differences can be explained by the presence of micro-metastases existing prior to treatment.

FUNCTIONNAL RESULTS

The functionnal results can be assessed by the frequence of enucleations and the retention of the treated eye's visual acuity.

The visual acuity will decrease as complications appear and therefore the follow-up period is of great importance for proper assessment.

The best results are those from treatment using protons.

However, the results from the different series are difficult to compare because of the different follow-up periods.

Some variables are associated with modifications to visual acuity : the larger the volume of tumour, the closer the tumour is to the fovea and papilla, the older the patient, the more the detachment of the retina is exudative and the poorer the visual acuity is at the start of treatment, the quicker is the loss of sight.

A large amount of published data as well as our own observations indicate that conservative treatment of malignant melanoma of the uvea by means of irradiation does not subject the patient to any more important risks than the radical treatment of enucleation.

The indications and contra-indications of brachytherapy versus charge particles are uncertain. A prospective trial comparing iodine versus helium therapy is in progress (D.H. Char, T.R. Castro et al.).

II - LOCALIZED CARCINOMA OF THE PROSTATE

Carcinoma of the prostate is, when skin cancer is excluded, the second most common malignancy in males in most of industrialized countries. The increasing age of the population causes a relative increase in the incidence of prostate cancer.

Radiation therapy has been demonstrated to be an accepted therapeutic modality in the management of patients with localized carcinoma of the prostate. Twenty-five MV photons from a linear accelerator are used to administer 45 or 50 Gy to the pelvis and additional 20 or 25 Gy to the prostate. The development of CT-planned limited field external beam radiation led to a fall off in treatment-related morbidity.

About a series undertaken by the French Federation of Anticancer Institutes in 1991, we analyzed 1100 cases from 16 Institutes.

We choose to analyze them using multivariate analysis. We used a cox model, Kaplan-Meier curves and a tree-structured regression method : the cox model and the

Kaplan-Meier curves confirmed two main explicative factors : stage ($p < 0.0001$) and tumor grade ($p < 0.001$). Poorer evolution occurs in extracapsular forms (ECE) and grade I has better survival than others.

According to a review of the literature, for disease limited to prostate (DLP) the radiotherapeutic results and surgical results are the same.

Another method of treatment consists of putting radioactive sources inside the prostate.

Use of radioactive implants is theorically appealing because it allows the highly-localized radiation dose with a minimum effect on surrounding structures. ^{125}Iodine implantation was popularized by Whitmore and Hilaris at Memorial. Most of published data regarding results of implantation have come from the use of retropubic technique. Local control rates are generally equivalent with implantation, external beam irradiation or prostatectomy.

Radiation therapy is the most effective technique available for stage ECE. However, the results are poor and the optimal treatment for this stage is always a controversial issue. Radical surgery has not been widely practiced. The results of endocrine manipulation or some combination of these techniques are not clear. Next speakers will describe the role of fast neutrons in the treatment of patients with stages ECE disease. It is hoped that the development of this new treatment machines will result in a further improvement in the results of treatment in this disease.

PROTONS AND NEUTRONS VERSUS X OR GAMMA RAYS EXTERNAL RADIOTHERAPY : ALTERNATIVE OPTIONS ?

G. KANTOR and P. LAGARDE - M.D. - A. CHEMIN - Ph
Regional Comprehensive Center, Fondation Bergonié, 33076 Bordeaux - France

Protons and Neutrons have ballistic or biological properties different of X or gamma rays commonly used in external radiation therapy. Actually, the place of treatment with protons and neutrons compared to other external radiation therapy technique can remain controversary.
Two clinical indications are discussed to individualise the respective places of the different available techniques :
- first : artérioveinous malformations (AVM) and the possibility to treat with external stereotactic radiotherapy or with protons.
- second : soft tissue sarcoma (STS) and the choice between external radiotherapy and neutrons.

I - ARTERIO-VEINOUS MALFORMATION AND RADIOSURGERY

Radiosurgery is a technique that delivers with a single fraction a high dose of radiation (10 to 50 Gy) in an acurrate defined intra cranial wolume.
First medical treatments have been performed with a special cobalt unit with multiple sources or with protons units. To assume a high definition of the Target volume stereotactic means are mandatory.
Recent developpments with linacs commonly used in radiotherapy allow a wide extension of radiosurgery (at least 8 centers in France use radiosurgery with linacs).
At present time, arterio-veinous malformation (AVM) are the main clinical indications.
The obliteration of abnormal communications between arterious and veinous is achieved after a delay of two years.
For AVM less than 30 mm diameter, the rate of obliteration varries from 60 to 80 %.
Results for proton therapy are comparable for the ranges of size and dose used.
For AVM larger than 30 mm diameter, few informations are avalaible for treatment with cobalt and photons X. First results with protons for larger AVM seems interesting.

II - SOFT TISSUE SARCOMAS

Soft tissue sarcomas are rare diseases (less than one per cent of all cancers). Due to the high ratio of benign tumors, there is a high rate of unexpected malignant tumors and the first surgical procedure can be inadequate.
For the local control, the mains prognostic factor is the quality of the surgical procedure. A wide resection, with safety margins, plus radiation therapy (with X or gamma rays) provides the same local control rate than a radical excision.
For soft tissue sarcomas of the extremities a 70 % range of local control can be achieved after wide resection and radiation therapy. The risk of metastasis depends mainly about depth of the tumor and histopronostic grading.
Thus, for operable tumors, quality of diagnostic, grading, surgical procedures, volume and dose of irradiation are more relevant than the choice of the type of radiation.
For non operable tumors, the role of radiation therapy and the place of heavy particules are not yet well defined.

NEUTRONTHERAPY : FROM RADIOBIOLOGICAL EXPECTATION TO CLINICAL REALITY.

N. Breteau (1) , **A. Wambersie** (2)

(1) Sce de Radiothérapie, C.H.R. B.P. 6709 - 45067 ORLEANS Cedex 2
(2) U.C.L. Cliniques Universitaires St-Luc, 1200 BRUXELLES

The radiobiological data available today indicate that high LET radiations could bring a benefit in the treatment of some types of tumours (typically slowly growing, well differenciated). Radiobiology also suggests some mechanims through which this benefit could be achieved : hypoxic gain factor, kinetic gain factor and less repair.

Among the high LET radiations, fast neutrons are the less expensive and the most widely used in therapy. Seventeen centres are today involved in neutrontherapy and more than 15 000 patients have been treated so far.

The difficulties when reviewing the clinical results are mainly due to the apparent high value of expected therapeutic gain in the seventies : in fact, at that time, all the radioresistant tumours were so considered because of hypoxia and such a high potential benefit allowed therapists to consider that it overcame the insufficiant physical selectivity of neutron facilities.

As a matter of fact, a lack of proper patient selection according to characteristics of tumour and normal tissue at risk and use of neutrontherapy in suboptimal (or even poor) technical conditions can obscure or worsen the clinical results. Then it is difficult to separate what is really due to the high LET radiations from that due to inclusion of patient with suboptimal (or even contra-) indication and/or to the technical treatment conditions.

Nevertheless, radiobiological and clinical data at present available are in complete agreement, and among the clinical indication for fast neutrons, the following are most recognized :

- inoperable or recurrent salivary gland tumours,
- locally extended tumours of the paranasal sinuses,
- tumours of the head and neck area with fixed nodes,
- soft tissue sarcomas, osteosarcomas and chondrosarcomas grades I and II,
- locally extended prostatic adenocarcinomas,
- palliative treatment of melanomas.

From technical point of view, the situation has been significantly improved with the introduction of high energy hospital-based cyclotrons isocentric mounting and variable collimators.

Today, the indications of neutrontherapy represent about 10 to 15 % of the patients currently referred to the Radiation therapy Departments.

Finally, two important conclusions can be derived from clinical and radiobiological data :

- need for adequate patient selection which can be partly solved by randomized clinical data and the development of predictive tests such as specific cell radiosensitivity or T-pot.
- need for a high physical selectivity : it is possible nowaday, to reach the same physical selectivity with neutrons than with high energy photons with an acceptable cost for the community.

Only under these conditions can the real role of fast neutrontherapy be correctly evaluated.

CLINICAL INDICATIONS FOR PROTONTHERAPY

P.Chauvel [1], J-L.Habrand [2]
1 - Centre Antoine-Lacassagne-Cyclotron Biomédical 227 avenue de la Lanterne. 06200 Nice France
2 - Centre de Protonthérapie d'Orsay Campus Universitaire d'Orsay Bat 101. 91400 Orsay France

The last seventy past years experience in radiation oncology demonstrates that each improvement in the radiation depth dose distribution is correlated with an improvement in therapeutic results, both in term of increasing tumor control and decreasing side effects of treatments. This was clearly established by the works of Bush and Allt for the cancer of the cervix: going from 200kV to Cobalt 60 and further from Cobalt 60 to 22MV photons increases the survival of the patients by a factor of 2 for each step. This was also the case for Hodgkin's disease, as shown by Kaplan , for oropharynx, as shown by Fletcher , for prostate carcinomas, as shown by Bagshaw , etc... All these results were summarized and presented during the "NCI Proton Workshop" on April 1989 (1) in Bethesda.

Rationale for the use of proton beams in radiation oncology

In parallel to this progressive enhancement of radiotherapy accuracy, a new kind of possibilities appeared in the 50's, with the therapeutic use of the first charged particle beams; due to their charge and heavy mass (1835 times that of electrons), protons present favorable absorption characteristics known as the Bragg curve. The protons energy at the entrance and the tissue density along their track, determine the depth of penetration of the beam and the position of the Bragg peak. Spreading out the Bragg peak, using modulating devices, allows to conform the plateau obtained to the thickness of the treatment volume. The heavy mass of the particle results in minimal deviation and therefore minimal side scattering. These main characteristics permit the radiation oncologist to give a dose in depth superior to the entrance dose, with sharp fall-off and penumbra.

The first proton beams were used in Berkeley (University of California San Francisco, Lawrence Berkeley Laboratory)(UCSF/LBL) in 1954, followed in 1957 by Uppsala (Uppsala University, the Svedberg Laboratory)(UU/SL) and in 1959 by Boston (Massachussets General Hospital, Harvard Cyclotron Laboratory)(MGH/HCL). These pioneers paved the way of charged particle therapy and demonstrated their superiority for some tumor sites untreatable by classical radiation treatments. Following these pioneers, some more facilities were opened for partial medical use, in previous USSR (Dubna 1967, Moscow 1969, Gatchina 1973), in Japan (Chiba 1979, Tsukuba 1983) and in Switzerland (Paul-Scherrer Institute, Villigen 1985)(PSI). Despite the fact that these accelerators were not installed in a medical environment but in Universities or Nuclear Physics Research Laboratories, several thousands patients were treated, the usefulness of proton beams established and thanks to this experience and to the knowledge acquired hospital-based machines now begin to be available for clinical purposes.

A relative advantage of proton beams over heavier charged particles consists in a Relative Biologic Efficiency (RBE) almost comparable to photon beams. This allows direct comparisons using the same fractionation schedules; under this condition a possible advantage of protons over photons is only attributable to dose localization accuracy. This advantage of proton beams accuracy has been established with the narrow beams used in "radiosurgery" at Berkeley, Boston and Uppsala. Dose levels of 45 to 200Gy in one or a few fractions have been successfully used to treat arterioveinous malformations, pituitary tumors, etc...using a small number of fields and stereotactic positionning, without major side effects (2).

Considering that each year, there are approximately 200000 patients whose primary tumor is treated unsuccessfully (3) in the United States, which number could be extrapolated

to 280000 for the European Community, there is a considerable need for new developments in the field of radiation oncology. Protontherapy is one of the possibilities and the results obtained in the "difficult-to-treat" tumor sites support the idea of opening new hospital-based protontherapy facilities, in parallel to all other developments of photontherapy.

Clinical results of protontherapy (3)

Around 30% of proton-treated patients were bearing an uveal melanoma, a rather uncommon tumor (5 new cases/million inhabitants/year). The results obtained are impressive: out of 2822 patients treated at MGH/HCL, UCSF/LBL and PSI, the local control rate is 96% and the survival at 5 years around 80%. These results are the consequence of two factors: the small volume of the tumors (64%<15mm) and the high doses delivered: 70CGE (Cobalt Gray Equivalent, which is the physical dose x RBE) in five fractions over 8-10 days for nearly all the patients treated at MGH and LBL, 60 CGE in 4 fractions and 4 days at PSI. These doses are exceptionally high, compared to photon radiation therapy and explain the high tumor control rates. The results obtained with radioactive plaques in tumors <15mm diameter and <6mm thickness are almost comparable, but the dose received by the sclera is about 200 to 400Gy to achieve a 70 Gy dose at the apex of the melanoma. Furthermore, protons seem to be more advantageous for the treatment of posterior pole tumors, the sharp fall-off of the beam allowing a better protection of the optic disc and/or fovea. Nevertheless some complications may occur as glaucoma, eyelid sclerosis etc..., essentially for large tumors and a phase III clinical trial comparing 50 CGE to 70 CGE (both in 5 fractions) is in progress at MGH/HCL. The goal of the study is to decrease the complication rate while maintaining the tumor control rate around 93 to 95%.

The second main result obtained by proton therapy concerns the tumors of the skull base. These tumors are untreatable in a curative intent by surgery or photontherapy, due to their complex anatomical relationship with adjacent healthy tissues which moreover are sometimes partially involved by the tumoral process: brain, brain stem, cranial nerves, blood vessels, eyes, middle ear. The local control achieved by photons (median dose 55 Gy) for 41 chordomas and 4 chondrosarcomas is 36% at 3.5 years (4). With protons, a dose in the range of 65-75 CGE (1.8 CGE/fraction) is achievable and able to dramatically increase the control rate. At MGH, the actuarial local control rates at 5 years in a series of 215 patients (130 chordomas and 85 chondrosarcomas are 91% for skull base and 65 % for cervical spine. The results obtained with Helium ions at LBL by J.Castro (5) are comparable: 65% at 3 years.

Some other tumor sites have also beeen successfully treated by protons at MGH; 16/16 benign recurrent inoperable meningioma are controlled with only one major morbidity. Craniopharyngioma demonstrate the same results: 14/14 local control, 1 major morbidity. 6 early stages rectal carcinomas have been treated after local excision and are locally controlled. 7/8 local control for soft-tissue sarcoma in the paravertebral tissues treated after local excision, without spinal cord injury. Carcinoma of the prostate have also been treated for a long time and the results judged sufficiently consistent to activate a phase III clinical trial comparing a proton boost to 75.6 CGE to a photon boost to 64.8 Gy, all patients receiving 50.4 Gy with photons prior to the boost. The local control rate on 190 patients entered in both arms of the study seems to be unusually high (81 and 89%) and the decoded results will be published in a few months. Nevertheless, a special effort has been made in target volume definition and coverage which certainly explains the high control rates in both arms. This is a spin-off of protontherapy for which were developped the first 3-D treatment planning programs, the concept of beam's eye view of the tumor in the beam, dose volume histograms, accurate positionning devices, all technologies now available for photon treatments.

Clinical indications for Protontherapy

Considering the results obtained for the above mentionned highly "difficult-to-treat" tumors, which constitute the basic indications for protontherapy, the need for hospital-based protontherapy facilities appears as a clear evidence; table 1 gives the possible numbers of patients concerned by these very restrictive indications for proton treatments in Europe.

	Incidence (per year/ 100000)	Absolute number of patients (EC°=345x10⁶)	Proportion suitable for protons (%)	Estimation of absolute number of patients
Chordomas	0.06	210	50	105
Chondrosarcomas	0.03	100	50	50
Basal meningiomas	0.32	1100	70	770
Meningiosarcomas	0.14	480	50	240
Schwannomas	0.33	1140	50	570
Neurofibrosarcomas*	0.017	60	50	30
Gliomas grade I & II	1.1	3800	40	1520
Pituitary tumors	0.3	1030	20	206
Optic nerve gliomas	0.05	170	90	153
Craniopharyngiomas	0.14	480	90	432
Choroidal melanomas	0.55	1900	30	570
Retinoblastomas	0.14	480	40	192
Glomus tumors	0.37	1280	20	256
Arteriovenous malformations	0.25	860	15	129
Total				*5603*

° European Community

* not associated with Recklinghausen's disease

Table 1: CNS or adjacent to CNS tumors; basic indications for protons in Europe

It seems that these indications have to be extended to some other tumor sites for which either tumor control rates are poor or healthy tissues unsufficiently protected against possible radiation injury or both. These tumor include locally advanced carcinomas of the head and neck and paranasal sinuses, bladder, uterus, rectum, sarcomas of the bones and soft tissues at uneasily accessible sites, high grade gliomas, tumors of the lung apex, carcinomas of the kidney, undifferentiated or anaplastic thyroid carcinomas and pediatric tumors for which dose localization is an essential deal; these potential indications represent around 40000 new patients/year, giving a *total number of 45000 patients/year in the EC.* Moreover, for some people it seems that lymphomas and seminomas, regarding their very long survival probability, could also benefit from protons, a better dose localization avoiding radiation induced tumors.

From an economic point of view, even if the cost of a proton treatment is around three times the cost of a photon treatment, we have to consider the benefit obtained from curing patients considering that the mean cost of a treatment failure is twenty times a photon treatment.

References

1 - Urtasun RC Does improved dose characteristics and treatment planning correlate with a gain in therapeutic results? Evidence from past clinical experience using conventional radiation sources. Int J Radiat Oncol Biol Phys 22: 235-239; 1991

2 - Perez CA, Brady LW eds: Introduction. In Principles and practice of radiation oncology. Philadelphia: Lippincott, 1987, 22

3 - Suit H, Urie M Proton beams in radiation therapy JNCI 84: 155-164; 1992

4 - Austin-Seymour M, Munzenrider JE, Goitein M et al. Progress in low-LET heavy particle therapy: intracranial and paracranial tumors and uveal melanomas. Radiat Res (suppl)8: S219-S226; 1985

5 - Castro JR Review of medical treatment with heavy charged particle beams. In Proceedings 2nd European Particle Accelerator Conference, Nice June 12-16, 1990. Eds P Marin, P Mandrillon, Ed. Frontières, Gif-sur-Yvette France, 1990, 369-373

OPTIMIZATION OF THE PROTONTHERAPY BEAMLINE IN NICE

N.Brassart, J.Hérault, P.Chauvel.
Centre Antoine-Lacassagne CyclotronBiomedical,
227avenue de la Lanterne 06200 Nice.France

Introduction: the treatment of ocular melanomas with a proton beam was developed in Boston"USA".In France two facilities began these treatments in 1991 : Nice (june) and Orsay (september). The success of the therapy program is highly dependent on the availability of a stable, reproducible and well controlled beam. The characteristics of the Medicyc cyclotron and general organization of the building have previously been described: the 65 MeV proton beam is transported down the beam line until the two treatment rooms : a neutrontherapy unit with a fixed vertical beam and a multi-leaf collimator and a protontherapy room with a horizontal beam.

The proton beam line: the proton beam is completly defocused after the last 90° magnet (8m from the entrance of the treatment room) : this provides a simple means of improving the beam profile homogeneity and avoids the use of a double diffuser; a simple 0.05mm tantalium foil has just been added (5m from the treatment room) to spread a little more the beam and to smooth it. The beam profiles are ajusted before the treatments by acting both on the last magnet which moves the beam horizontally and on a steerer to have more accurate horizontal and vertical fittings. Just before the entrance of the treatment room a first 50mm collimator begins to define the usefull beam and avoids too much irradiation in the treatment room.

The protontherapy unit: the beam runs under vacuum until the range-shifter/modulator combination(RS/MC). The position of this unity in the optical bench is a compromise between good profiles and loss of energy: initially the RS/MC was at 50 cm from the last collimator and because of the diffusion on the modulator and range shifter the shape of the profile and the penumbra were strongly dependent on the thickness of these elements and not satisfactory; the range in tissue was of 32.2mm. Moving away this RS/MC from the last collimator gives a loss in energy because of the longer beam path in air but greatly improves the profiles: as an example the penumbra (90%-10%) varies from 4.2mm to 2mm for a completly modulated beam as the RS/MC is shifted from 50cm to 240cm from the last collimator; the homogeneity is also improved: the ratio of 98% to 95% dose varies from 0.76 to 0.96 while the range in tissue decreases from 32.2mm to 30mm. The compromise adopted was to set the RS/MC at 190cm from the last collimator: the range in tissue is then 30.8mm(figure 1) sufficient to treat all the eye tumor even when using bolus. The penumbra is 1.6mm for a non modulated beam and 2.3mm for a completly modulated beam (Figure 2). The position and size of the collimators are also of great importance in the shaping of the beam. This has been tested in different situations. The diameter of the last collimator is 34mm ; as an example the profile is worse when adding a 35mm diameter collimator at 60cm in front of the last one (penumbra=6.1mm) than without collimator(penumbra=3.6mm) and it is greatly improved by a 45 mm diameter collimator located at the same position(penumbra=2.2mm). The beam has to encounter first the larger collimator sizes and the last one must have the smallest size. The beam is very slightly divergent: the witdth of the 50% isodose increases by 0.4mm when moving away from the last collimator from 1cm to 16cm
Two independent parallel plate transmission ionization chambers monitor the beam continuously: the response of these chambers has been tested with the variation of high voltage and beam current: the answer is identical between 200V and 400V. Anyway the high voltage supply is routinely 300 V and a security turns off the beam for variation larger than +/- 10% of this value. The variation of dose per monitor unit is about 0.6% when the proton beam current is multipled by 6 .

The measurement of the dose: the current measured by each of the transmission chamber increases a counter. These monitor units are then calibrated against ionisation chambers. The daily given dose delivered to patient is the mean of 5 measurements made in the middle of the plateau of the patient modulated beam using ionisations chambers according to "the Code of Practice for Proton Dosimetry". An intercomparison including an A150 calorimeter was held in April 1991 in Orsay; others intercomparisons between the centers of Clatterbridge, Louvain la Neuve, Orsay and Nice were held in Clatterbridge and Orsay.
Presently the dose per monitor unit is measured for every patient before each of the four fractions; the figure 3 shows the maximum difference between the four dose values per monitor unit: this difference, expressed as a percentage of the mean of these four values is, for the major part of patients, <1.5%. Larger differences until 3.7% may be due to lack of temperature and pressure equilibrium of the transmission monitoring chambers and in fact we observed for these treatment days large variations of pressure. The beam monitoring system is daily checked by measuring the dose per monitor unit in standard conditions on the middle of the plateau of a half modulated beam. This daily measurement

called the "top", which takes into account variations for temperature, pression and beam characteristics, may allow us to correct daily the dose per monitor unit made the first treatment day for every patient and so to simplifly the procedure of the daily measurement of the dose : in fact a study on 62 patients shows, for the major part of the patient, a variation between +/- 1% of the ratio of each day measured dose to each day calculated dose using the daily value of the "top" and the first day measured dose.

Quality assurance of the beam: mini beam explorers with small silicon photo diode are used to verify all the profiles and test the Bragg peak and the personalized modulator , range shifter and collimator of every patient. Each day before treatement are controled: the profile of the beam without any modulator and range shifter, the maximum range in tissue and broadening of the Bragg peak, the half range modulated Bragg peak and profile, the monitoring system of the beam, the beam line interlocks of the optical bench (presence or not of range shifter, modulator, field and macula light, polaroid film holder in the beam and speed of the modulator). It is impossible to treat if one of these elements is not correctly positionned. The dose delivery is monitored by computer but a manual emergency cutt off of the beam is always possible.

Radioprotection aspects: the beam in the treatment room is slightly diverging and the only notable activation occurs in the range shifter /modulator and first collimator unit as well as in the last collimator: soon after treatment the dose rate is about 100µSv/h in contact. During a treatment time(20s) no air activation was detected and the ambience dose rate is around 200µSv/h.This activity decreases in few seconds to about 3µSv/h; so no precautions have to be taken before entring the room after treatment. Before treatment 3 to 5 XRay pictures performed to control the positioning contribute to the integral dose to the patient. The total dose(XRay +20s treatment) to the patient varies from 8 to 10 µSv; the dose rate at the same position is about 2mSv/h. .

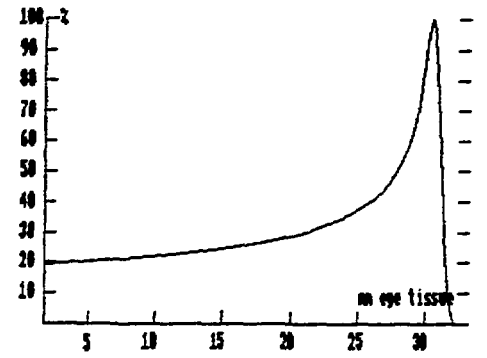

Bragg peak
Distal 90% at 30.8mm tissue
Full width half max=3.3mm tissue

Figure 1

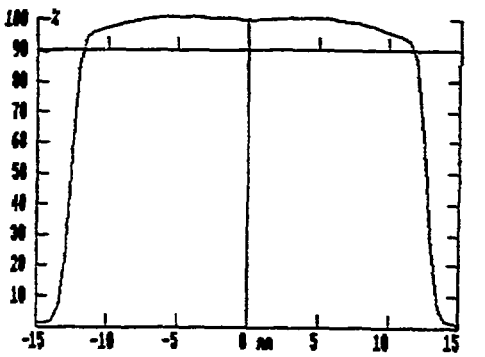

unmodulated beam profile
R(95%/90%)=0.91
Penumbra(90%-10%)=1.6mm

Figure 2

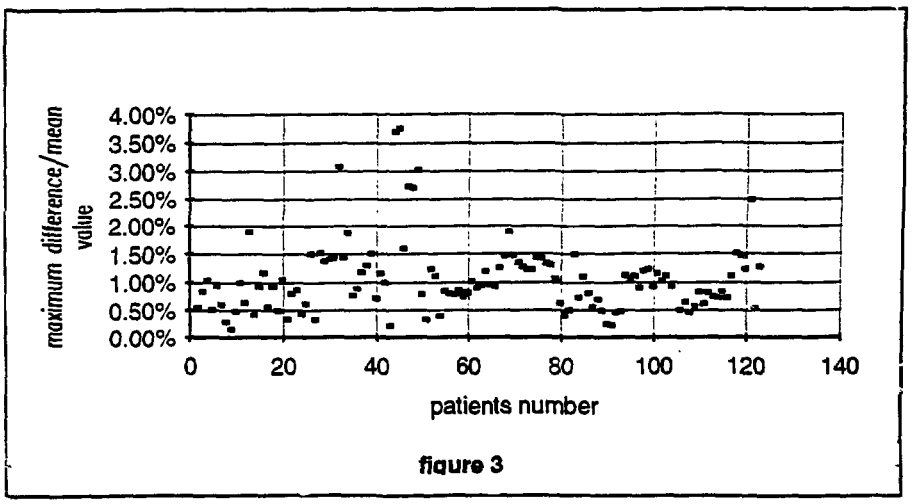

figure 3

A PROTONTHERAPY COOPERATIVE GROUP FOR UVEAL MELANOMAS : the SERAG (South Europe RAdiotherapy Group).

P.Chauvel[1,2], N.Brassart[1,2], J.Hérault[1,2], A.Courdi[1,2], JD.Grange[1], JP.Caujolle[1], L.Diallo-Rosier[1], F.Porta[1], N.Bornfeld[1], F.Bacin[1], J. Sahel[1], JP.Gérard[1], W.Sauerwein[1], V.Vitale[1], C.Carrie[1], G.Kantor[1], R.Rozan[1], JL. Lagrange[1,2], RJ. Bensadoun[1,2], E. Teissier[1,2], F. Demard[1,2].
SERAG(1) and Centre Antoine-Lacassagne (CAL)(2),
227 Avenue de la Lanterne 06200 NICE-France.

In December 1990, the first proton beams were extracted from the Medicyc Cyclotron installed in Centre Antoine-Lacassagne, one out of 20 French Comprehensive Cancer Centres. This hospital-based machine is mainly characterized by its axial injection providing negative hydrogen to be accelerated. The ions are produced in a multicusp source and accelerated by a RF system (2 opposed 75deg. dees, 24.8MHz, peak voltage 50kV). Protons are extracted at 65 MeV by stripping in a 60 µg/cm2 carbon foil. The proton beam is transported to the treatment room through focusing quadrupoles and bending dipole magnets. The maximum range is 32.2mm in eye tissue (measured on distal 90% isodose).The width of the unmodulated Bragg peak is 3.4mm on isodose 50%. The lateral penumbra is 1.7mm (10 to 90% isodoses). The Bragg peak is spread out by means of continuously variable thickness plexiglas propellers turning in the beam at 2000rpm; the homogeneity obtained in the spread out peak is +/- 1%. Range, modulation and collimation are individually adapted, range shifters, modulators and collimators being milled in the cyclotron workshops from files directly issued from the treatment planning system. Bragg peak and profiles of the beam are controled each day and dose measured before each fraction of each patient, despite the fact that variations are less than 2%.

5 years before the installation of Medicyc, a users group had been set-up around this future facility, including at this time South-East of France (Grenoble, Lyon, Marseille, Montpellier). This very convivial group progressively extended its members number and the SERAG (South Europe RAdiotherapy Group) includes now Comprehensive Cancer Centers and University Hospitals from South of France and adjacent regions in Germany, Italy and Spain (fig. 1). This cooperative group works around the Biomedical Cyclotron of Centre Antoine-Lacassagne in Nice for Protontherapy, Radiobiology, Medical Physics and very soon for Neutrontherapy. The group allows its members to directly participate in treatments protocols elaboration, treatment achievment, follow-up of patients, dosimetry and experimentations performed with heavy particles beams. For protontherapy, ophtalmologists and radiotherapists are invited to accompany their patients in Nice, in order to directly take part in the treatment planning and set-up.

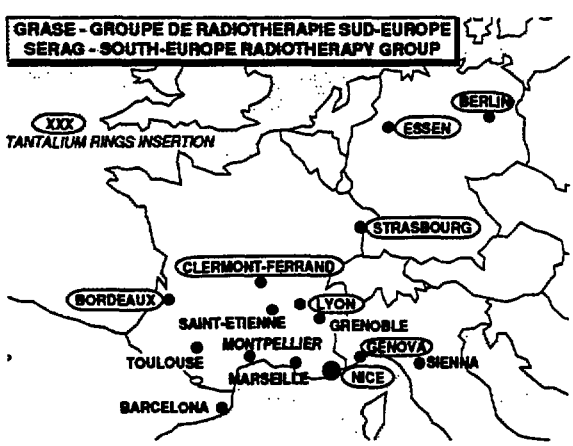

This organization maintains a close relationship between the different specialists referring patients, their patients and the cyclotron team. Moreover, the group gives to a large number of physicians and physicists the possibility to use a proton beam, enlarging the general knowledge on new radiotherapeutic modalities.

FIGURE 1 : the SERAG

Protontherapy started for France in Nice by June 17, 1991. Up to July 23, 1992, a total of 114 patients completed their treatment in Nice: 112 choroidal melanomas, 1 conjonctival melanoma, 1 retinoblastoma (5-years old boy, relapsing at the posterior pole, 4 years after left eye enucleation and right eye irradiation giving 40 Gy/photons. Dose delivered by protons: 48 GyCoEq/16 fractions/ 4weeks).

The series of uveal melanomas encompasses 53 men and 59 women, mean age 56 years (10<->84). Tantalium rings are inserted on the eye, delineating the tumor limits, by the surgeons participating in the group in Bordeaux, Clermont-Ferrand, Essen, Genova, Lyon, Nice and Strasbourg. Simulation and treatment planning are performed in Nice, optimally 10 to 15 days after the rings insertion, if possible in the week before treatment, in order to decrease the number of travels and consequently the total cost. The delay between surgery and simulation seems to be important: it contributes to avoid the small ocular mobility troubles following rings insertion, essentially for posterior tumors. The treatments are delivered in 4 consecutive fractions of 15 GyCoEq, each fraction lasting around 20 seconds. Table 1 shows the patients repartition by T classification and site. The majority consists in T3 and posterior pole tumors, indicating clearly that the group does not consider that protons have to substitute for plaques. A clinical trial aiming to define the real place of protontherapy in the treatment of ocular melanomas will certainly been proposed to the members of the GRASE during 1993. Presently we are trying to assess the real accuracy and the possibilities of proton beam targeting by reducing classical safety margins and using wedges and compensators in order to spare at its best healthy tissues and mainly optic disc and fovea (Fig.2 & 3)

Table 1 : 112 OCULAR MELANOMAS - CLASSIFICATION / SITE

	T1b	T2	T3	*Total*
CILIARY BODY	0	6(35%)	11(65%)	*17(15%)*
EQUATORIAL	4(3%)	4(13%)	22(74%)	*30(27%)*
POSTERIOR POLE	4(6%)	23(35%)	38(59%)	*65(58%)*
Total	*8(7%)*	*33(30%)*	*71(63%)*	*112*

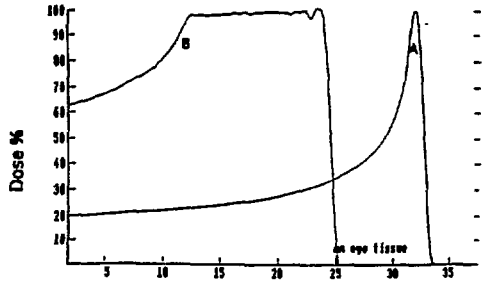

FIGURE 2
DEPTH DOSE CURVES FOR PROTONS IN EYE TISSUE : A- Bragg peak for 65MeV protons
B- Spread-out Bragg peak adapted to the characteristics of the tumor to be treated: range reduced to 24.1mm (calculated on distal 90%), modulation from 11.5 to 24.1mm. Entrance dose compared to plateau dose is 37% less giving a protection for healthy tissues ahead of the tumor.

C- Conformation of the beam: 2 dimensions are defined by the collimator (X,Y), 3rd dimension is given by the modulating propeller (Z) which superimposes Bragg peaks at different energies.

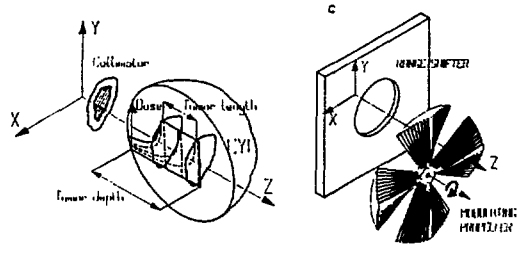

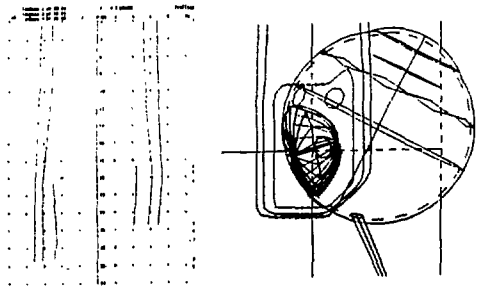

FIGURE 3
MODIFICATION OF DOSE DISTRIBUTION in the case of paramacular or parapapillar tumors, the use of plexiglass wedges helps to protect macula (as shown above) and/or papilla and optic nerve. Physical measurements in water demonstrate a good agreement with the result of treatment planning, considering the distal part of isodoses curves (left).

STATUS REPORT OF LABORATORI NAZIONALI DI LEGNARO RADIOTHERAPY PROJECT

F. Cera, R. Cherubini, A.M.I. Haque, G. Moschini, P. Tiveron
Laboratori Nazionali di Legnaro-INFN, I-35020 Legnaro (Padova) Italy

F. Calzavara, L. Tomio
Divisione di Radioterapia e Medicina nucleare, Complesso Clinico Convenzionato dell'Ospedale-Università, I-35100 Padova, Italy

G. Kraft
Gesellschaft für Schwerionenforschung (GSI) mbH, Darmstadt, Germany

The final goal of any radiotherapeutical treatment is to expose the tumour to a lethal dose of ionizing radiation, sparing thereby the surrounding healthy (normal) tissues to a maximum extent. The biological and physical advantages of high-energy charged particle beams, with respect to the electromagnetic radiations, have been established in cancer therapy over a number of years in a series of biomedical and clinical centres, mainly located where accelerators were designed for nuclear physics research, like the pioneer laboratories of Berkeley and Harvard in U.S.A.. In particular, the high precision in delivering the tumor dose and the increased biological efficiency in the high energy deposition region (at the end of particle tracks) are the more interesting features of heavy charged particles for use in therapy. Moreover, heavy charged particles, when penetrating through several centimeters of tissue, undergo nuclear reactions, some of which resulting in positron emitting isotopes. Taking into account that such isotopes have mainly the same direction and nearly the same range as the primary beam, it is possible through the monitoring of the annihilation gamma-rays *in vivo*, using appropriate γ-cameras, the penetration and the localization of the primary particle beam (in beam PET).

A heavy ion radiotherapy program has been proposed by the INFN-Laboratori Nazionali di Legnaro[1] in the framework of the development of the facilities already existing and under construction (XTU TANDEM + LINAC accelerator) for heavy ions constituting the ADRIA accelerator project (heavy ion beams; energy $\sim$1 GeV/amu) and constitutes a part of the final ADRIA proposal[2]. The ADRIA project has recently been inserted in the next "five years financial plan", starting from 1994, presented by the Istituto Nazionale di Fisica Nucleare to the Italian Government. The main features of ADRIA, of interest in medical applications, have already been reported[1]. Figure 1 shows the ADRIA accelerator complex (for details, see ref. 2).

From the clinical information it come out that in Italy 382.7 new cancer cases per year per 100,000 people are expected, of which 170 could be suitable for primary treatment with radiation therapy. In particular, as clinical targets for the radiotherapy program at ADRIA the following tumours have been identified: the Pancoast tumour, the carcinoma of the prostate, the tumour of the pancreas and soft tissue sarcomas of the retroperitoneum or pelvis. Table I reports the above clinical indications and the expected cases for the region of Veneto per year suitable for initial radiotherapy with heavy ions.

TABLE I

SITE	CLINICAL TARGETS	EXPECTED CASES/ YEAR
Thorax	Pancoast tumour	10
Abdomen	Pancreas	10
	Sarcomas of the retroperitoneum	5
Pelvis	Prostate	30
	Sarcomas	5

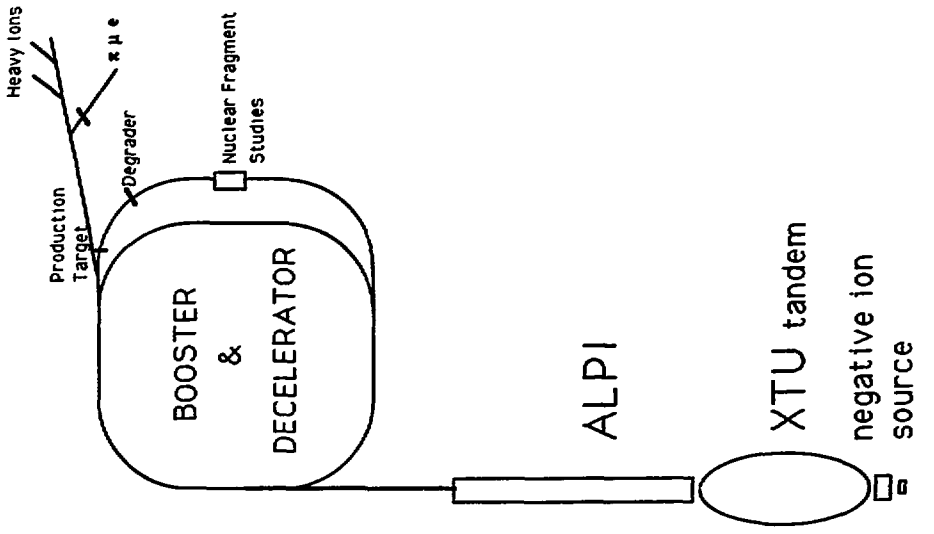

Fig.1 - Schematics of the ADRIA complex.

As far as the irradiation modalities are concerned, as initial choise, vertical and horizonthal beam lines will be prefered and the installation of a isocentric gantry is forseen. In order to profit a good beam quality and to perform optimized tumor conform treatment, a magnetic scanning techinique like that under development at the GSI[3], Germany, would be adopted. Profitting the opportunity offered by the PET Laboratory under installation at the LNL, the in beam PET monitoring is planned to be used to verify and optimize the tumour treatment.
Taking into account the number of initial expected cases to be treated (see Table I), a treatment room and few waiting rooms will be prepared in the medical area of ADRIA complex.

Moreover, besides the heavy charged therapy program, the prosed LNL proton therapy project[1] will profit of the proton beam available at the ALPI accelerator complex, based on a superconducting LINAC for heavy ions, presently under installation. At the final LINAC configuration, a proton energy of 56 MeV is expected and this turns out to be useful for the treatment of intraocular tumours (located in a range of 20.0 mm). The 56 MeV proton beams are planned for 1996 from ALPI.

REFERENCES

1. Cera et al.(1991), in: GSI-91-29 Report. Extended Abstracts– Fourth Workshop on Heavy Charged Particles in Biology and Medicine, GSI, Darmstadt, Germany, Sept. 23-25, 1991.
2. The ADRIA Proposal. LNL-INFN(REP)58/92, March 1992.
3. Kraft et al., Preprint GSI-91-15, März 1991.

HOW TO ORGANIZE A POSSIBLE FUTURE FOR PROTONTHERAPY, CONSIDERING THE PRESENT CONSTRAINTS ON HEALTH POLITICS.

P.Chauvel, on behalf of the SERAG (South Europe RAdiotherapy Group).
Centre Antoine-Lacassagne, Cyclotron Biomédical 227 avenue de la Lanterne
06200 Nice France

A high-energy protontherapy facility represents an expensive investment for an institution alone, whatever could be its size, considering the particular sentence stating that «everything, concerning the medical developments, has to be realized without any extra-cost». A socio-economic study based on a critical approach of the present status must be realized and some possible solutions have therefore to be investigated.

Present status of protontherapy in Europe: The present status of protontherapy in «extended» European Community is relatively easy to summarize: six machines are presently running at low to medium energy, three for medical purpose only (Clatterbridge, Nice, Orsay), three for part-time medical applications (Villigen, Uppsala, Louvain-la-Neuve). Three of these machines could be used for higher energy applications, two facilities are involved in a reflexion on boosting possibilities, some few institutions, not yet in the field of protontherapy, are trying to join this small number.

Proposals for protontherapy machines: At present time the industrial proposals for high energy proton accelerators are relatively poor, if one compares with photontherapy. Nevertheless, some designs, predesign or feasibility studies exist. The investigated solutions cover the whole field of particles accelerators; synchrotrons, cyclotrons (room temperature or cryogenic) and linear accelerators. The mean diameter of these machines varies from 3 to 11m for cyclotrons and synchrotrons, the total length of Linacs varying from 10 to 20m. As a consequence, the sizes of the buildings and the total costs are different, possibly by a factor of 1.5. A mean cost of 9MECU could be proposed as a basis for the accelerator cost. The assumed cost for a horizontal beam treatment room is 1.5MECU and 4MECU for a gantry with sophisticated beam delivery systems. A "low-option" could encompass 2 horizontal beam + 1 gantry, the "high option" being 1 horizontal + 2 gantries.

Buildings: The main cost of the building housing such a facility is constituted by shieldings. Even if some discripancies exist between the different methods of shielding calculations and if the thickness of the concrete has to be different in the beam path and laterally, mean values of 2m for beamlines and treatment rooms, and 3m for the accelerator vault seem to be reasonable for rough estimates of the shielding volume in the different possible solutions. A cost of 1000ECU/m^3 of concrete is assumed in further calculations. The internal volume of the vault is correlated to the accelerator and can be roughly estimated to 500m^3 for a conventional cyclotron, 300m^3 for a synchrotron and 150m^3 for a supraconductive cyclotron; the shielding volumes are respectively aroud 1700, 1300 and 900m^3, numbers giving the cost in kECU. The volume of concrete for the treatment rooms depends upon the technical choice, horizontal beam or gantry, and could be estimated respectively to 550 or 800 m^3. For the beamlines, the cost also depends upon technical choices for accelerator and treatment room implantation: they could be neglected in the case of a compact installation around the first bending magnet, or estimated to 500m^3 if they run behind all the three possible treatment rooms. For a hospital-based machine, a surface of 1000m^2 has to be added for hosting the technical and medical facilities, assuming a mean cost of 1000kECU/m^2. The total cost of the buildings could be between 4.2 and 5.7MECU.

Organization: A modern protontherapy facility must be designed to treat a large number of patients per year, in order to minimize the cost of treatment towards the cost of the accelerator. Fractionation schedules are comparable to those used in conventional radiotherapy, due to the almost equal RBE. The total number of fractions will be 28 for a full course (4x2,5CGE*/week, 70CGE total dose); assuming a number of 1000 patients/year, this means 28000 fractions; if 3 treatment rooms are installed, each room must realize 9333 fractions/year. The facility could run 49 weeks, 4days/week for treatments; this gives 196 days/year. 9333 fr/ 196days=47 patients/day/room; if 3 patients are treated each hour, the facility must run 16hr/day. The 5th day is devoted to set-up of new patients. If 4 patients could be treated each hour, the total number of patients/year increases to 1344. Such a high number of patients implies that a large part of the daily repositionning of the

**CGE=Cobalt Gray Equivalent*

beam ports is realized before entering the treatment room: 2 preparation rooms/treatment room are necessary. The immobilization devices could be made in these rooms on the no-treatment day. A minimum of 2 radiographers/treatment or preparation room are required (leading to a total number of 42) and we assume that, due to the treatments complexity, a physician is needed for 150 patients/year. The treatment planning procedures are estimated to 11hrs/patient. This means that 7 physicians, 7 physicists and 7 dosimetrists are required. The other categories have also been investigated in details and the final total number appears as 111.5 people. For the operation and maintenance of the machine 2 engineers and 8 technicians are needed.
The medical equipments (X-ray, CT scan, 3-D treratment planning etc...) are estimated to 1.5MECU.

Patients accomodation: If a treatment lasts 7 weeks, simulations 1 or 1,5 weeks, the total mean stay of a patient is 9 weeks. If one assumes 10% ambulatories living in the area and 10% in-patients, 80% of the referred patients could benefit from an «alternative to hospitalisation» as hotel rooms or «low-care» hospital beds (50ECU/day); for 1000 patients/year 20 in-patients beds and 190 «out-patients beds» are permanently needed; the annual costs of out-beds is 2.5MECU. If the number of patients increases to 1350/year, the cost will be 3,4MECU. It is assumed that in-patients beds could be found in the total amount of beds of the region without any extra-cost. The mean cost/patient for transports represents 450ECU, leading to 0.4MECU for 1000 patients.

Running costs: The running costs are mainly made up of the salaries which are estimated to 4.3MECU/year and patients accomodation which represent a total amount of 2.5 to 3.4MECU/year for 1000 to 1350 patients. Transports of the patients are estimated to 0.4MECU/year; power, water, maintenance, furnitures represent around 1.5MECU and capital amortization on 20 years 1.2to 1.4MECU/year. The total for running costs is 10 to 11MECU. The cost per patients varies from 10000 to 11000ECU for 1000patients/ year to 7400 to 8150ECU for 1350 patients/year.

What choice? The choice of the accelerator and of the equipment of treatment rooms seems to be very important at a first glance when only looking at the investments for an accelerator or a gantry, but with regard to the running costs, one can see that their amortization constitutes only one tenth of the cost/year.By the way, it seems reasonable to make the best technical choice, almost whatever could the difference in price be... and to compensate by a compact design for rooms arrangement.

Comparative costs of other cancer treatments: The cost of protontherapy has to be compared to the mean cost of other cancer treatments. The following numbers are generally accepted by the experts of the European Community: - surgery: 7000 ECU, - radiotherapy: 3000ECU, - chemotherapy: 12000ECU, - bone marrow transplantation: 40000ECU. One must remember that these treatments are usually combined, surgery being followed by radiotherapy and preceded by chemotherapy. Under these conditions, the mean cost of a full treatment for a «diffficult -to-cure» tumor could be 22000ECU. Assuming a cure rate of 0.4, 60% of these patients will have a second and a third treatment with the same cost or more because of the alteration of the general status of the patient needing intensive care. The real cost of treatment (including the cost of failures) now becomes: 22000 + (44000x0.6) = 48400ECU. If we admit a mean cost of 10000ECU for a protontherapy, even combined with chemotherapy (surgery is not performed in a first intent, but as a salvage procedure), the cost of the first treatment is 22000ECU; assuming a cure rate of 65% the real cost of treatment becomes 22000 + (44000x.35) = 37400ECU . This difference for 1000 patients/year represents 11MECU saved/year, i.e. the reimbursment of the investment on 2 years and furtherly the possibility to completely cover the running costs. If the total number of patients treated increases to 1350, the facility saves 4MECU/year by comparison to the present cost of treatments and failures.

Organization of a co-operative facility: The possible number of protontherapy indications seems to be >45000/year for EC* and implies at least 20 to 30 large-scale hospital-based protontherapy facilities. At evidence these installations will have to be widely opened to national and international collaboration, in order to offer to a large number of high-level radiotherapy teams the possibility to use a few «high-tech» platforms, if one wants to avoid a rupture of the patient/physician relationship and a disregarding attitude of the groups unable to use these treatments modalities. In the same way, fundings could be raised up from inter-regional or international co-operation contracts guarantizing a real access for the patients and their physicians and physicists who thus could directly participate in the treatment. The present example of the SERAG* (South-Europe RAdiotherapy Group) demonstrates that, even if funded by an institution alone, such an organization is able to work efficiently and is susceptible of enlarging the general knowledge of radiation oncology community towards charged particles therapy.

** see other paper in the same proceedings.*

Status of the therapy project at GSI

W. Becher, D. Böhne, W. Enghardt*, T. Haberer, G. Kraft, W. Kraft-Weyrather,
M. Müller, S. Ritter I. Schall, D. Schardt, M. Scholz, H. Stelzer
GSI Darmstadt
* ZfK Rossendorf

A program for the preparation of heavy ion therapy is presently carried out at GSI. This program includes radiobiological research using light ion beams of C, O, Ne ions with energies up to several hundred MeV/u. The technical and physical part of this program consists of the development of a fast magnetic beam scanning system, of position sensitive particle counters, of beam localisation techniques using on line PET techniques, of beam fragmentation measurements in thick targets, of intensity constant extraction mode from the accelerator terminated by fast cut off from the scanning system and of the design and optimization of a dedicated medical acclerator [1].

The major advancement of heavy particle therapy compared to conventional treatment modalities is the improved dose localization due to a reduced lateral and angular scattering, the inverted depth dose profile with the intensity maximum at the end of the range in the Bragg peak, the increased biological efficiency for stopping light ions and finally, the possibilty to monitor the beam position on line in the human body with PET techniques [2]. In order to take the most possible advantage of these properties of heavy ions the beam has to be delivered target conform to the tumor and it has to be avoided that the ion beam stops in healthy tissue. This can be only reached by scanning a pencil beam with a magnetic deflection system over the target volume. For this purpose the target volume is dissected in slices of equal particle range i.e. of a different particle energies (fig.1). These slices are treated sequentially starting with the most distant slice. Because the following slices are partially preirradiated, the particle density in the following slices has to be inhomogenous in order to achieve a biological isoeffect (fig.2). For this purpose the scan pattern over each slice is first optimized to reach the desired biological effect, then the path of the beam is dissected in 16 k pixel and the particle fluence for each pixel is calculated seperatly. In the experiment the particle intensity is measured on line in a transmission counter. The beam is shifted from one pixel to the next pixel when the precalculated particle number of the first pixel is reached. Because these pixels are located very closely together the beam has not to be interrupted moving from one pixel to the next (fig.3). In order to extend this method to a 3 dimensional volume the energy of the particle beam has to be reduced from slice to slice. In a recent experiment, the heavy ion synchroton as well as the beam line to the Biomed cave was switched from one energy to the next within two seconds. The size of the beam spot as well as the location of the beam at the target location was stable enough to do raster scanning as shown in fig. 4 [3].

With these experiments all the different components for the set up of a heavy ion therapy has been tested separately. However, there is more time needed to do the therapy as a routine.

References

[1] Biophysics group GSI: Design construction and first experiments of a magnetic scanning system for therapy. Radiobiological experiments on the biological action of carbon Oxygen and Neon ions. Final report for the Eulima Collaboration, GSI report 91-18.

[2] G. Kraft: The radiobiological and physical basis for radio therapy with protons and heavier ions. Strahlentherap. Onkol. 166, 1990, 10-13.

[3] T. Haberer, W. Becker, D. Schardt: Fast Energy Variation of SIS for the Raster Scan System. GSI-Nachrichten 03-1992, 16-17.

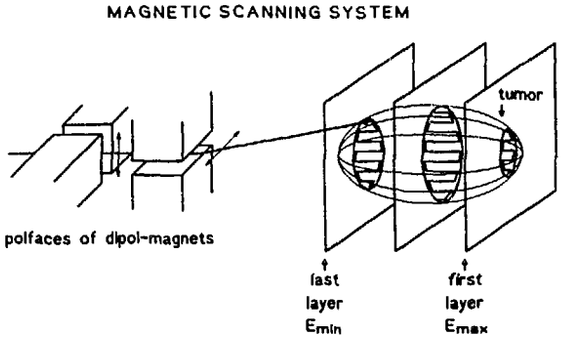

Figure 1: Schematic graph of the raster scan procedure

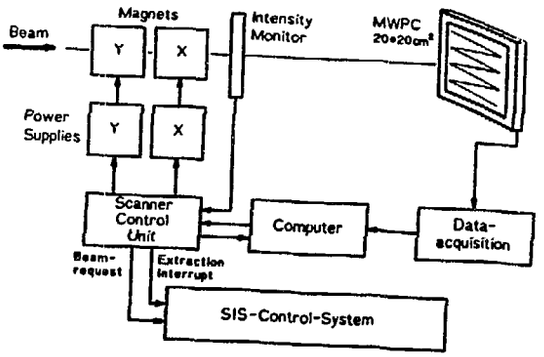

Figure 3: Block diagram of the magnetic scanning system

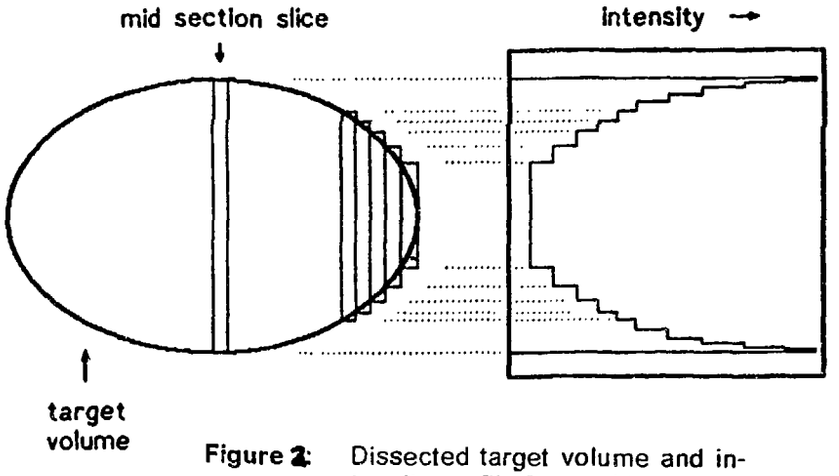

Figure 2: Dissected target volume and intensity profile for a mid section

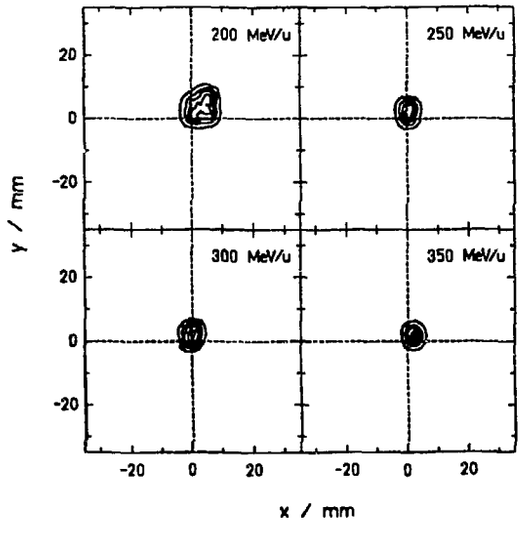

Figure 4: Four beam spots with different energies are monitored in a multi wire proportional chamber. The beam energy was switched every 2 seconds.

BARN 92 - Oct 14-15-16, 1992

List of participants

ABBE J.C., Strasbourg (CRN)
AJALTOUNI Z.,Clermont-Ferrand (LPC)
ALARD J.P., Clermont-Ferrand (LPC)
AVAN L., CNAM - Paris
AVAN P., Paris Hop Lariboisiere
AYBERGENOV T., Moscou
BARD J.J., Clermont-Ferrand
BASTID N., Clermont-Ferrand (LPC)
BECK C., Strasbourg (CRN)
BERGER L., Clermont-Ferrand (LPC)
BERTHOT J., Clermont-Ferrand (LPC)
BIMBOT R., Orsay (I.P.N.)
BLANC D., Toulouse (U.P.S.)
BOUSSANGE S., Clermont-Ferrand (LPC)
BRASSART N., Nice (CAL)
BRETEAU N., Orleans (CHRO)
CAPELANI J.C., Clermont-Ferrand (CJP)
CASTOR J., Clermont-Ferrand (LPC)
CASTRO J., Berkeley (LBL)
CHAUVEL P., Nice (CAL)
CHERUBINI R.,Legnaro (INFN)
COSTILHES J.P., Clermont-Ferrand (LPC)
COURDI A., Nice (CAL)
CUCCINOTA F., Hampton, Langley-NASA
CUGNON J., Liege (Univ)
CURTIS F., Berkeley (LBL)
DAYMARD N., Strasbourg (CRN)
DHERMAIN J., Paris (CEB/EPTA)
DHUR S., Clermont-Ferrand(LPC)
DONNARIEIX D., Clermont-Ferrand (LPC)
DUGAY M., Clermont-Ferrand
DUPIEUX P., Clermont-Ferrand (LPC)
ENGHARDT W., Rossendorf
FAIN J., Clermont-Ferrand (LPC)
FRAYSSE L., Montlucon (IUT)
FREEMANN R., Strasbourg (CRN)
GUEULETTE J., Louvain (UCL)

GUILLOT J., Orsay (IPN)
IBNOUZAHIR M.,Clermont-Ferrand (LPC)
ISABELLE D., Orleans (CERI)
JORIO M., Clermont-Ferrand (LPC)
JOUSSET J.C., Caen (CIRIL)
JUST L., Kosice
KANAI T., Chiba-Shi (NIRS)
KANTOR G., Bordeaux (Bergonie)
KOHNO T., Chiba-Shi (NIRS)
KRAFT G., Darmstadt (GSI)
KRAMER M., Darmstadt (GSI)
LARSSON B., Zurich (IMR)
LEMAIRE G., Fontenay aux Roses
MASSAUX M., Clermont-Ferrand
MEDIN J., Stockholm
MIALLIER D., Clermont-Ferrand (LPC)
MICHALIK V., Prague
MILLER J., Berkeley (LBL)
MONTAROU G., Clermont-Ferrand (LPC)
MONTBEL I., Clermont-Ferrand (LPC)
MONTRET J.C., Clermont-Ferrand (LPC)
MONTRET M., Clermont-Ferrand (LPC)
MOREL P., Clermont-Ferrand
MORIN C., Grenoble
MOSANE M., Clermont
MOTTA C., Clermont-Ferrand (CHU)
NEEF R.D., Julich
PERBAL G., Paris (Jussieu)
PIGNOL J.P., Strasbourg (CRN)
PONCY J.L., Bruyeres le Chatel
RAMILLIEN V., Clermont-Ferrand (LPC)
ROSENWALD J.C., Paris (Institut Curie)
ROZAN R., Clermont-Ferrand (CJF)
SABATIER L., Fontenay aux Roses
SANZELLE S., Clermont-Ferrand (LPC)
SAVINEL G.,Clermont-Ferrand (LPC)
SAYS L.P., Clermont-Ferrand (LPC)
SCHALL I., Darmstadt (GSI)
SCHWARTZ L., Paris (Hop Tenon)
SCHIMMERLING W., Washington (NASA)
SELTZER S., Gaithersburg (NIST)
SEVESTRE J., Paris (A.F.P.)
SOUMANA S., Clermont-Ferrand (LPC)
TAMAIN J.C., Clermont-Ferrand (LPC)

TIVERON P., Legnaro (INFN)
VETTESE F., Paris (CEB/ECTA)
VEYRE A., Clermont-Ferrand (INSERM)
VUILLAUME M., Paris (ENS)
WATT D.E., St-Andrews

Secretary and technical support:

BLISSON C., LPC
CHADELAS M., registration, LPC
DHUR S., registration, LPC
FOURNIER M., LPC
PELLET J., LPC
VIALA A., LPC

Laboratoire de Physique Corpusculaire , IN2P3/CNRS

Société Française de Physique

COMMISSARIAT A L'ÉNERGIE ATOMIQUE
IPSN/DPSHD Fontenay aux Roses

Centre Jean Perrin , Clermont-Ferrand

Ministère des Affaires Etrangères

B A R N 92 - Oct. 14-15-16 - Clermont-Ferrand